A unique mechanism generating the knee and the ankle in the local galactic zone

Antonio Codino & Francois Plouin

INFN and Dipartimento di Fisica
dell'Universita degli Studi di Perugia, Italy

Outline

- Some relevant characteristics regarding the knee and the ankle
- Basic observational facts shaping the behaviour of galactic cosmic rays
- The notion of galactic basin and its simplicity
- The computed Helium, Iron and proton knees and the related experimental data
- The computed knee of all-particle spectrum and the related experimental data
- Evidence that the knee and ankle are produced by the same mechanism
- Comments and conclusions

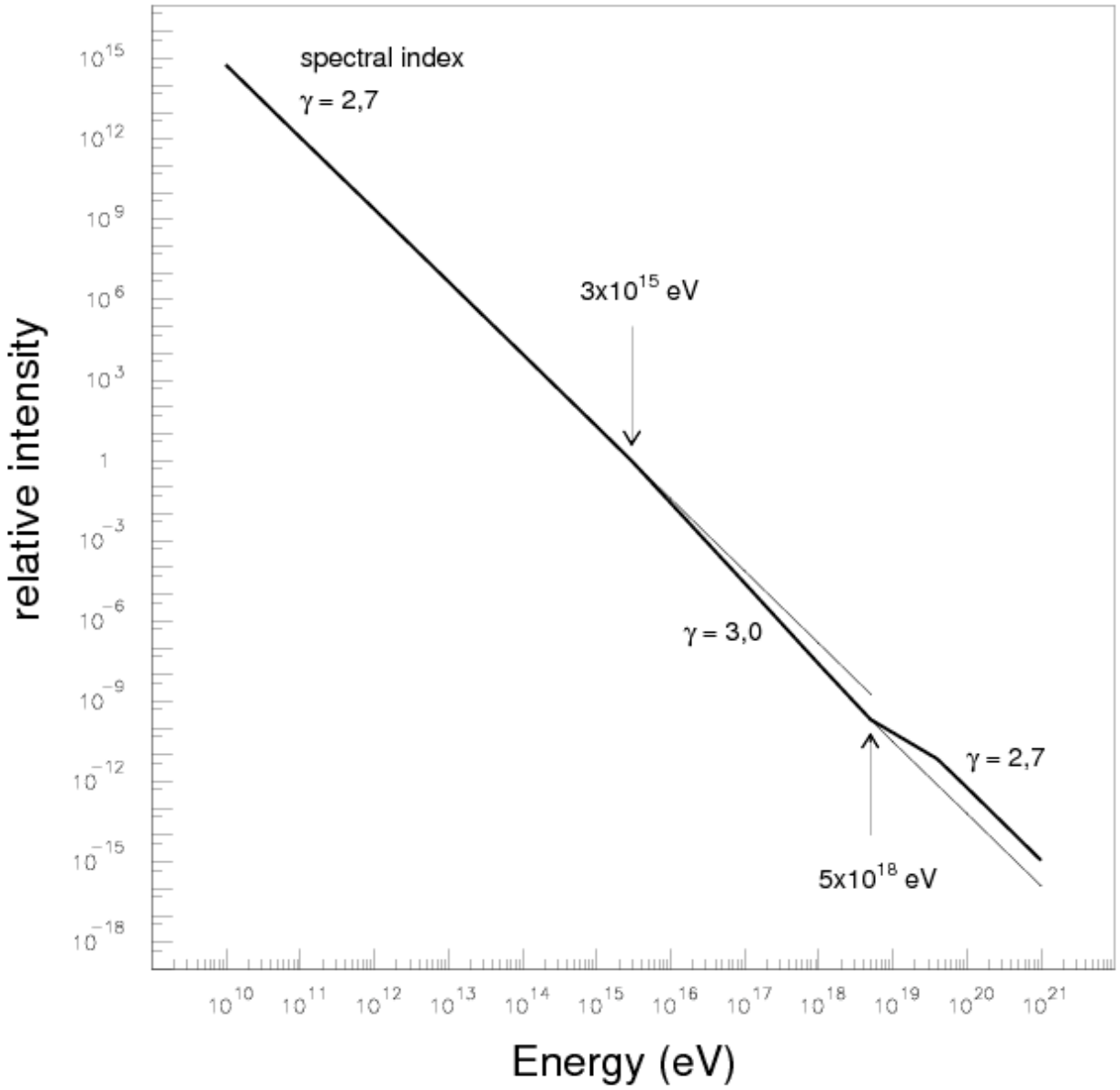
spectral index
γ = 2,7
3x10^15 eV
γ = 3,0
γ = 2,7
5x10^18 eV
relative intensity
Energy (eV)
10^15
10^12
10^9
10^6
10^3
1
10^-3
10^-6
10^-9
10^-12
10^-15
10^-18
10^10
10^11
10^12
10^13
10^14
10^15
10^16
10^17
10^18
10^19
10^20
10^21

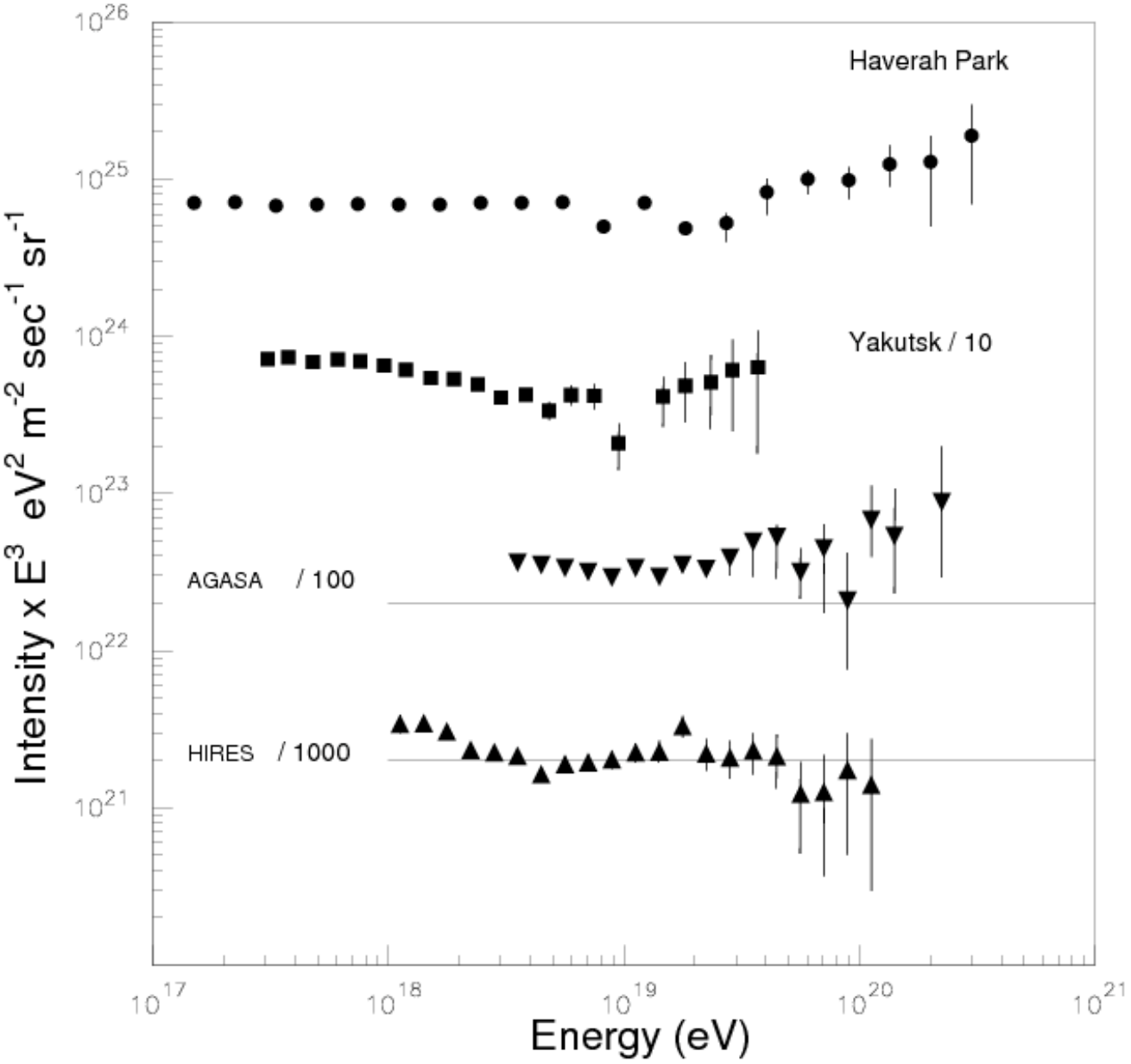
Haverah Park
Yakutsk / 10
AGASA / 100
HIRES / 1000
Intensity x E^3 eV^2 m^-2 sec^-1 sr^-1
Energy (eV)
10^26
10^25
10^24
10^23
10^22
10^21
10^17
10^18
10^19
10^20
10^21

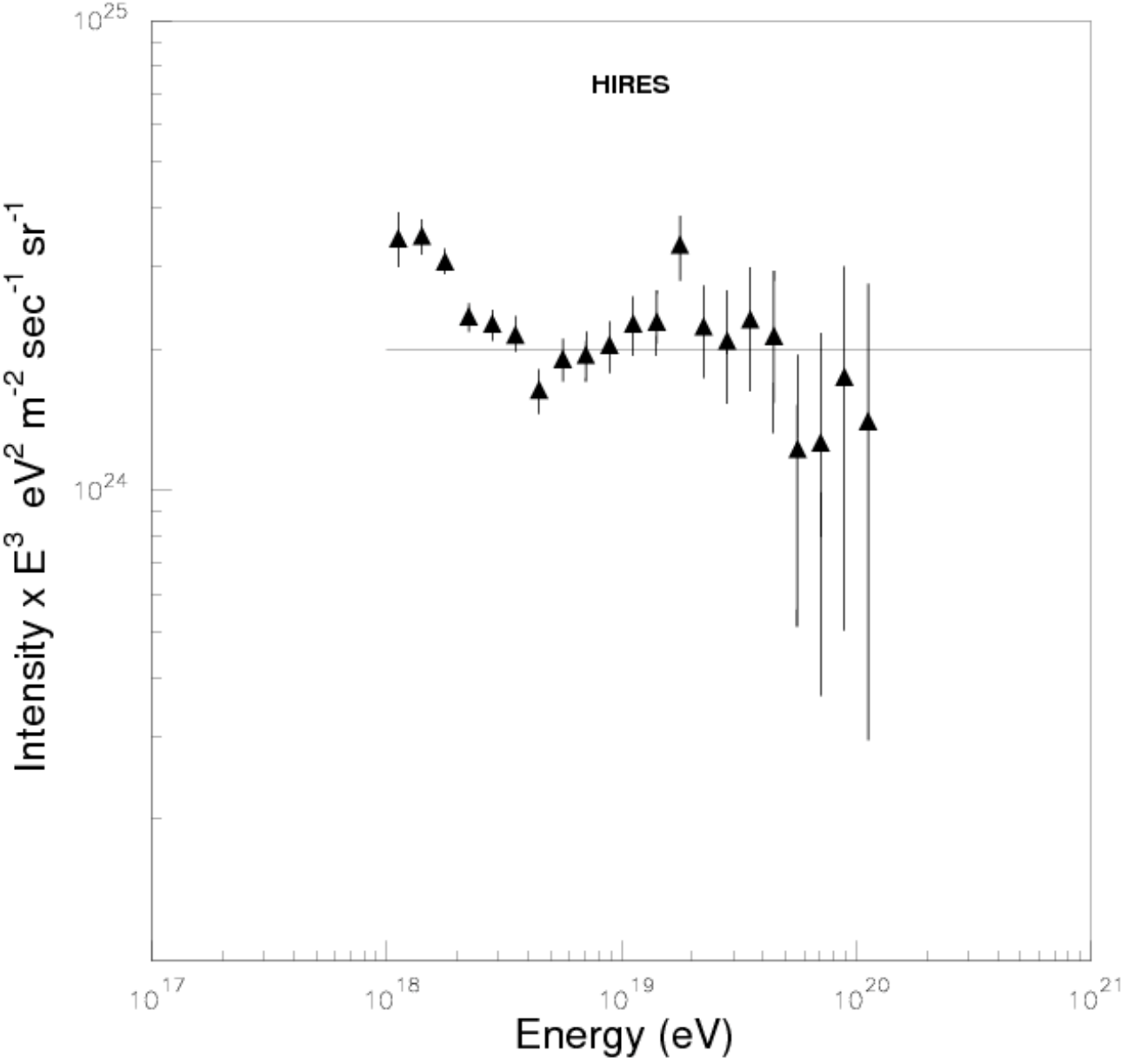
HIRES
10^{25}
10^{24}
Intensity x E^3 eV^2 m^{-2} sec^{-1} sr^{-1}
10^{17}
10^{18}
10^{19}
10^{20}
10^{21}
Energy (eV)

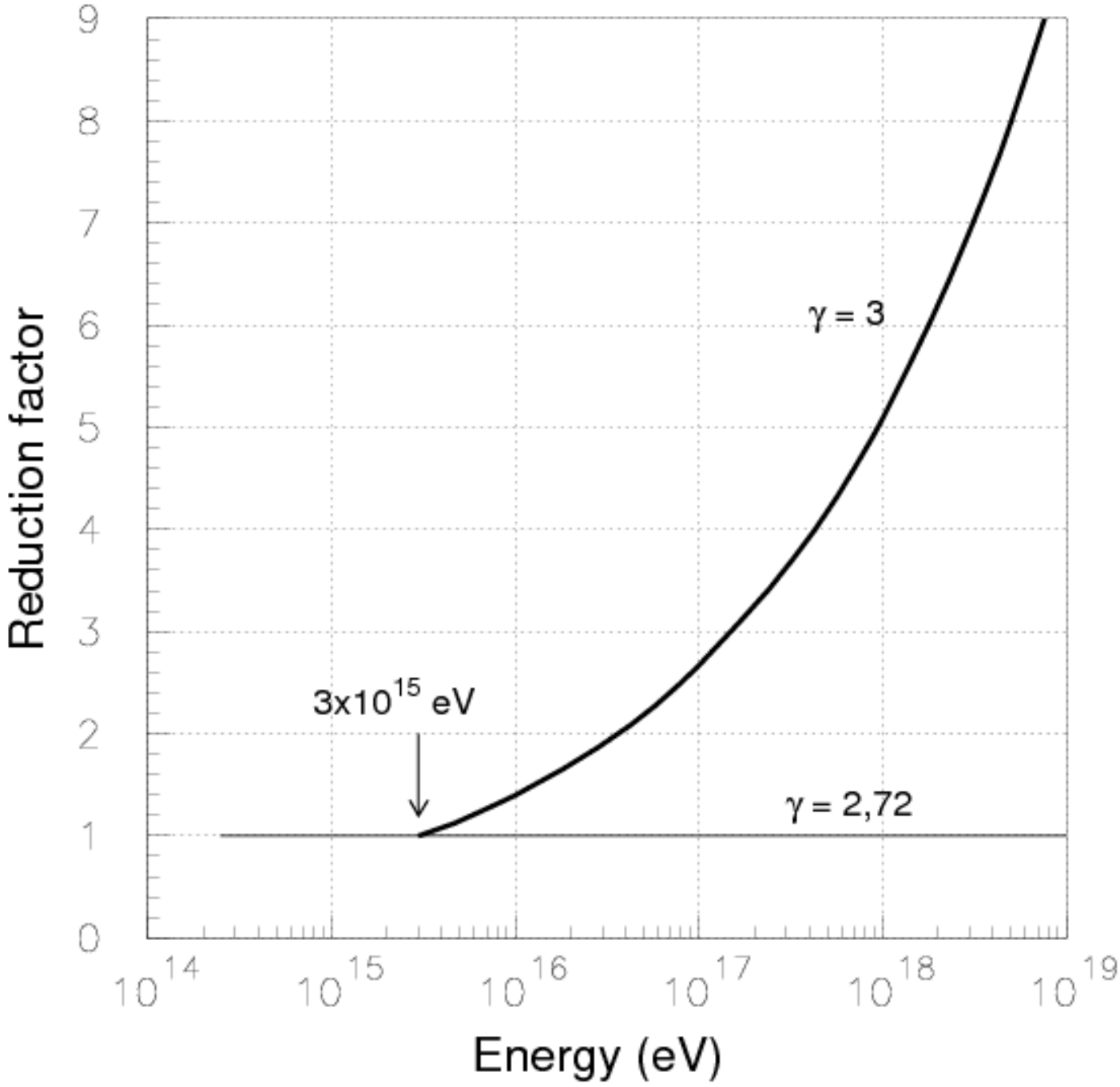
Reduction factor
9
8
7
6
5
4
3
2
1
0
γ = 3
3x10^15 eV
γ = 2,72
10^14
10^15
10^16
10^17
10^18
10^19
Energy (eV)

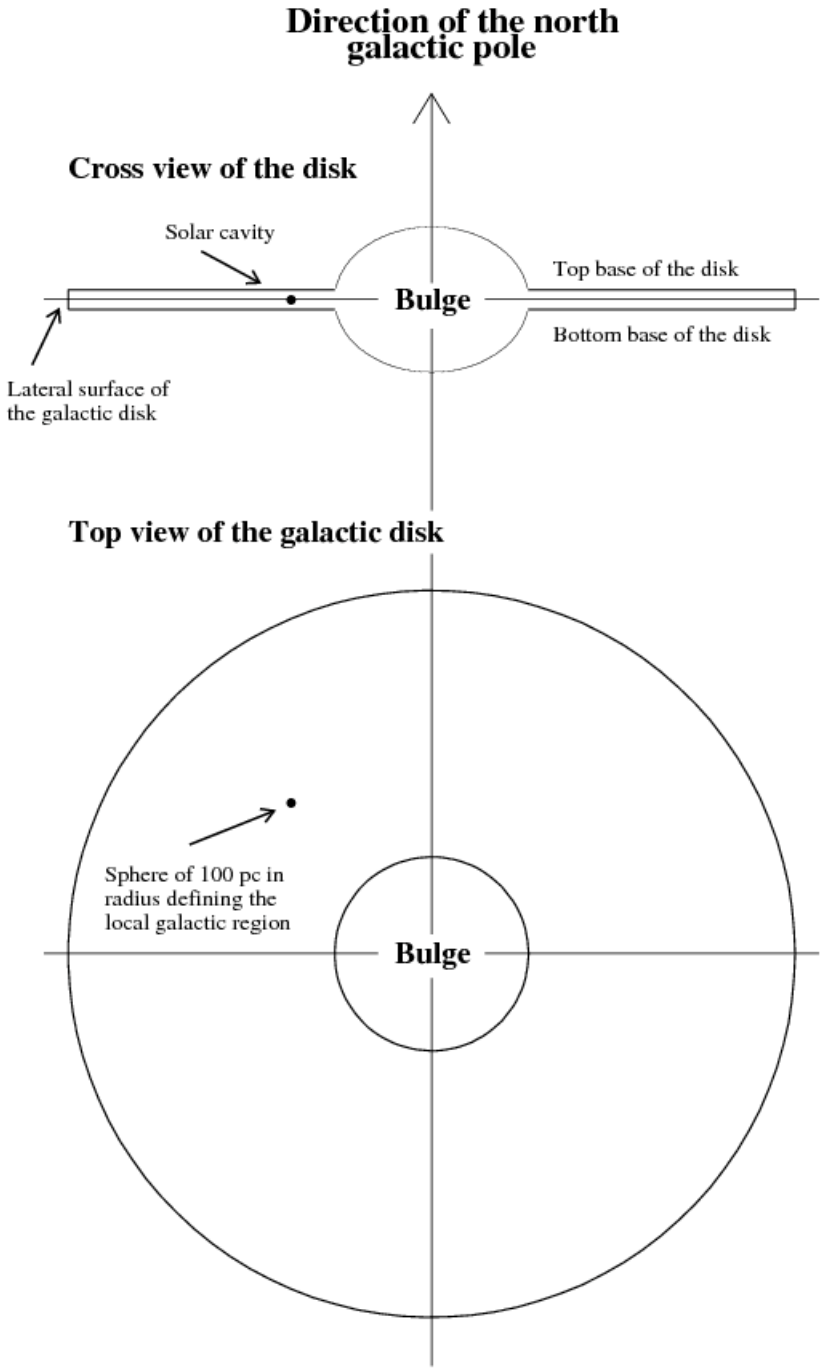
Direction of the north galactic pole
Cross view of the disk
Solar cavity
Top base of the disk
Bulge
Bottom base of the disk
Lateral surface of the galactic disk
Top view of the galactic disk
Sphere of 100 pc in radius defining the local galactic region
Bulge

Table 1: *Shapes and field strenghts of the regular magnetic fields in spiral galaxies determined by radio observations.*

Galaxy	Regular field shape	Field strenght (μG)	References
M33	spiral	3±1	Sofue et al. 1981
M51	spiral	10	Mathewson et al. 1972
NGC 6946	spiral	12±4	Klein et al. 1982
M81	spiral	8±3	Sofue et al. 1980
M83	spiral	not given	Ondrechen 1985
M31	circular	3-4	Beck 1981
IC 342	circular	7±2	Graeve et al. 1986
NGC 253	probably spiral	a few μG	Klein et al. 1983
NGC 2903	spiral	not given	Sofue et al. 1985
NGC 5055	probably spiral	not given	Sofue et al. 1985
NGC 4631	not given	a few μG	Golla et al. 1988
NGC 891	parallel to the galactic plane	a few μG	Sukumar et al. 1991
NGC 4565	parallel to the galactic plane	not given	Sukumar et al. 1991

Spiral magnetic field

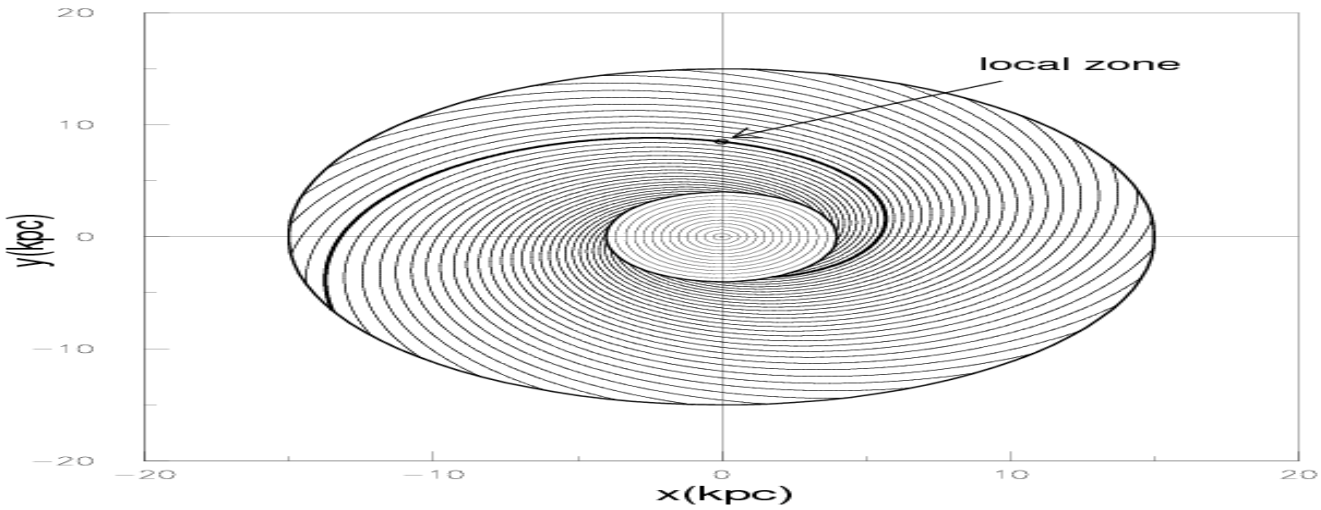

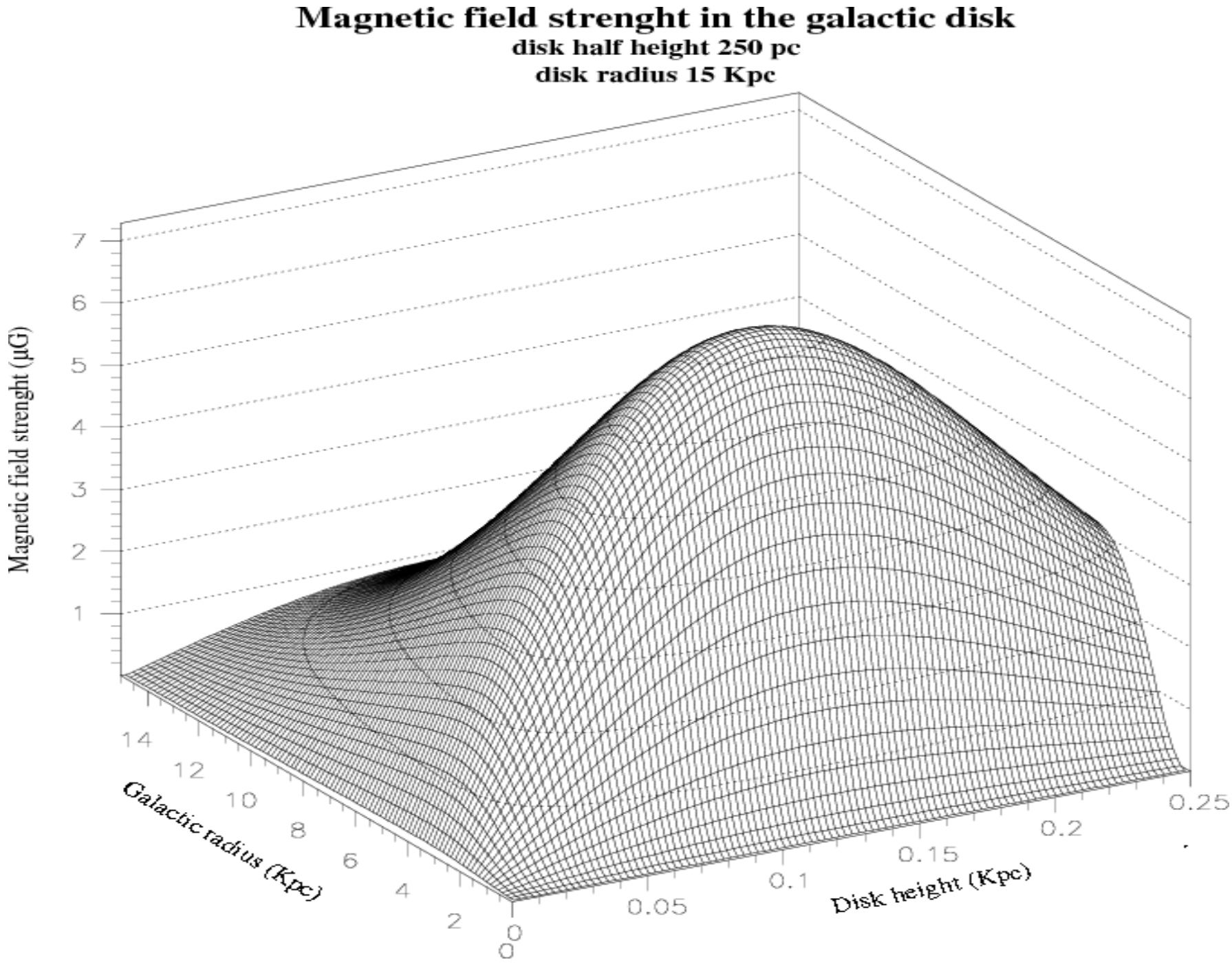
Magnetic field strenght in the galactic disk
disk half height 250 pc
disk radius 15 Kpc
Magnetic field strenght (μG)
7
6
5
4
3
2
1
Galactic radius (Kpc)
14
12
10
8
6
4
2
0
0
0.05
0.1
0.15
0.2
0.25
Disk height (Kpc)

Cosmic ray trajectories in the disk

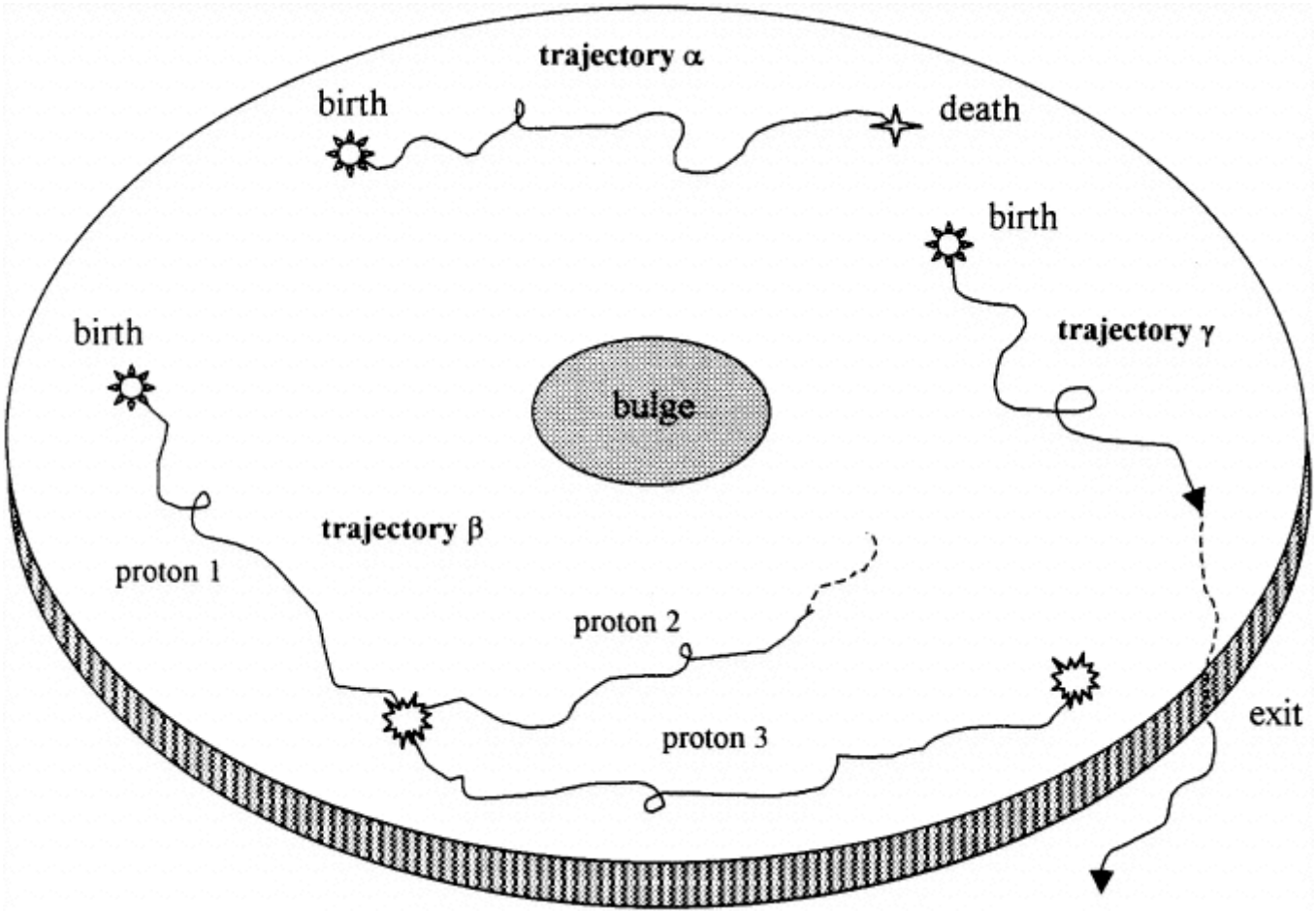

Brunetti & Codino, ApJ, 2000, 528, 789

Brunetti & Codino, ApJ, 2000, 528, 789

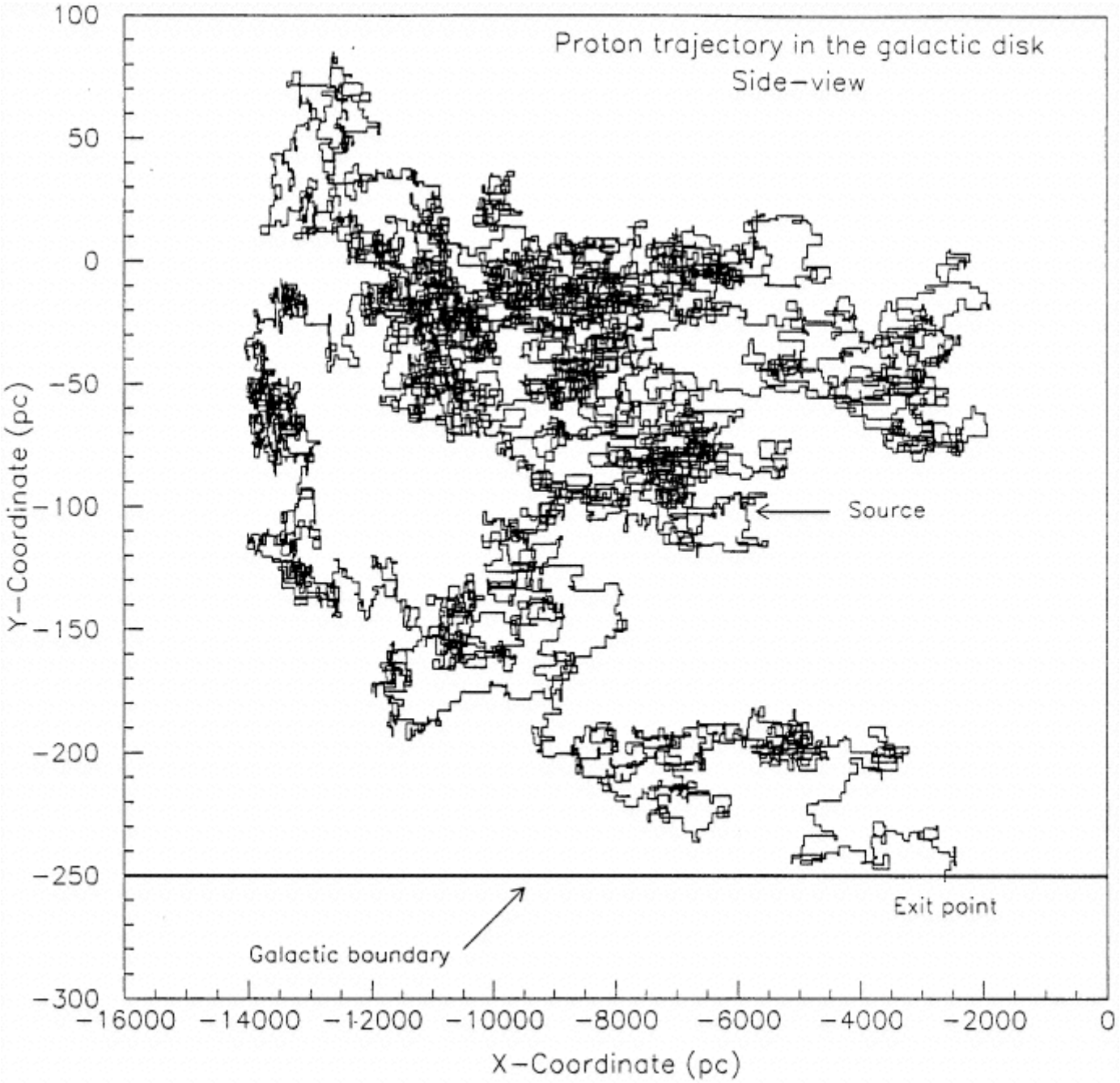

Cosmic ray trajectories in the Galaxy

Additional parameters

- Interstellar matter thickness has a mean value of one hydrogen atom / cm^3
  enhanced to 1,24 to take into account heavier elements.

- A uniform distribution of sources is represented by the equation

$$Q(r,z,l)=C\,(r-R)N(\,,z)$$

  N(,z) is the normal distribution in the z direction with a standard deviation of 80 parsec

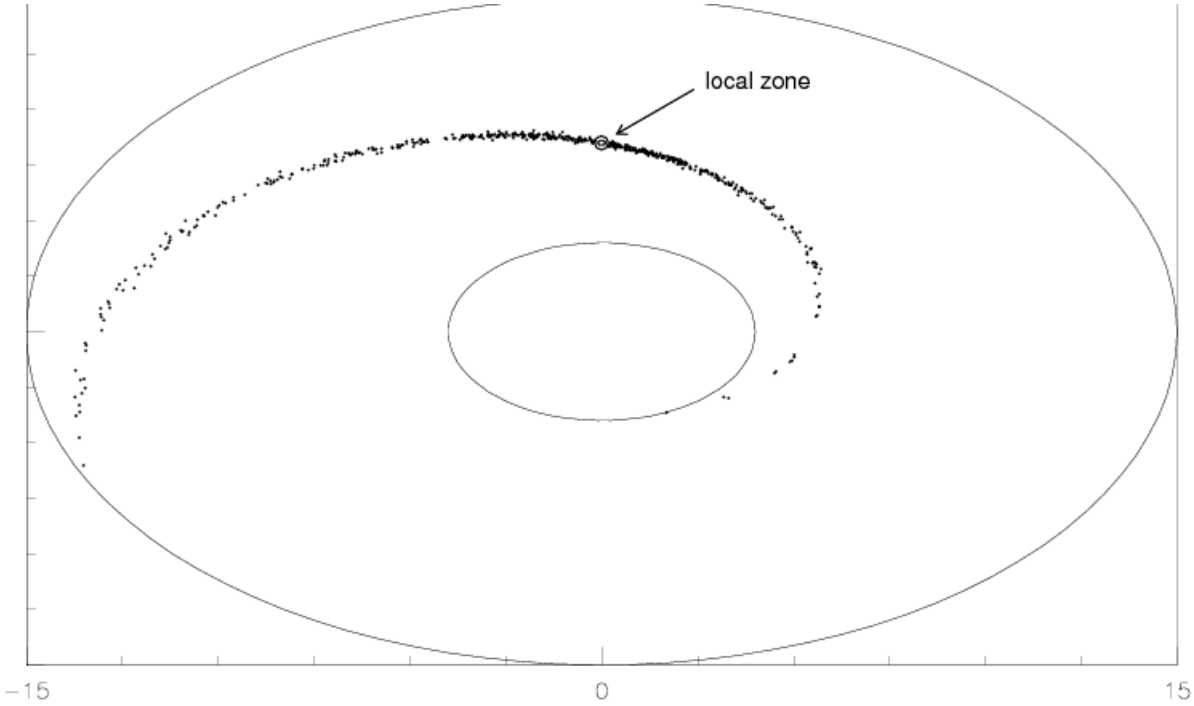

Codino & Plouin
ApJ, 2006, 639, 173

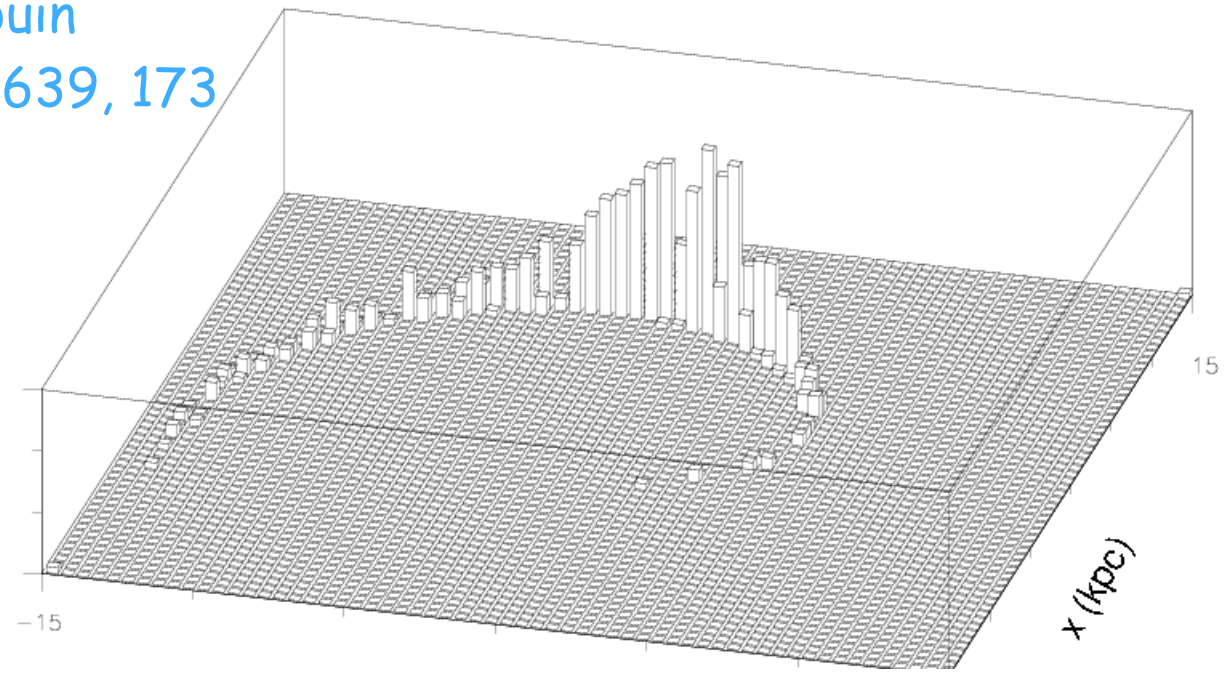

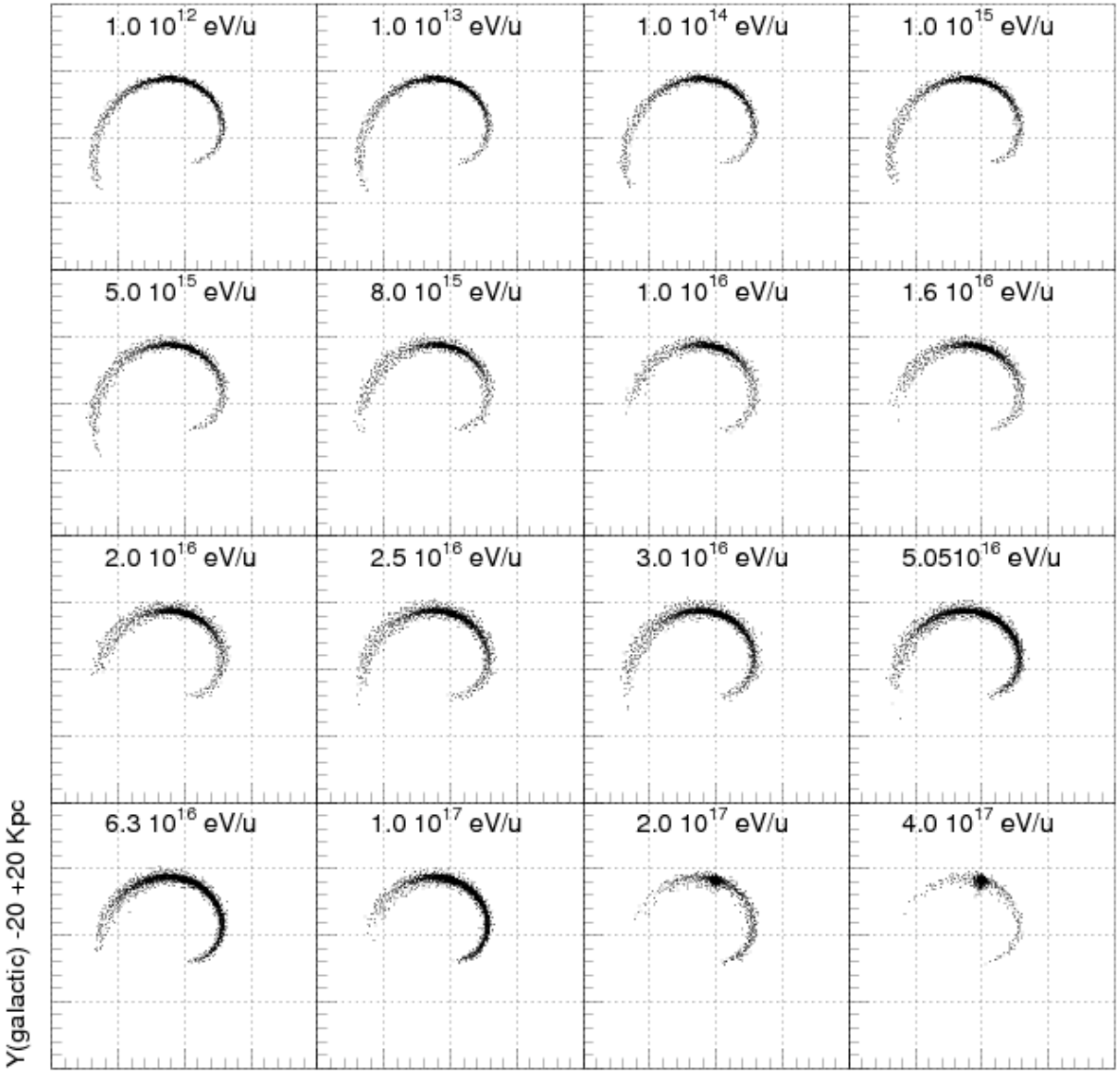
1.0 10^12 eV/u
1.0 10^13 eV/u
1.0 10^14 eV/u
1.0 10^15 eV/u
5.0 10^15 eV/u
8.0 10^15 eV/u
1.0 10^16 eV/u
1.6 10^16 eV/u
2.0 10^16 eV/u
2.5 10^16 eV/u
3.0 10^16 eV/u
5.0510^16 eV/u
6.3 10^16 eV/u
1.0 10^17 eV/u
2.0 10^17 eV/u
4.0 10^17 eV/u
Y(galactic) -20 +20 Kpc
X(galactic) -20 +20 Kpc.

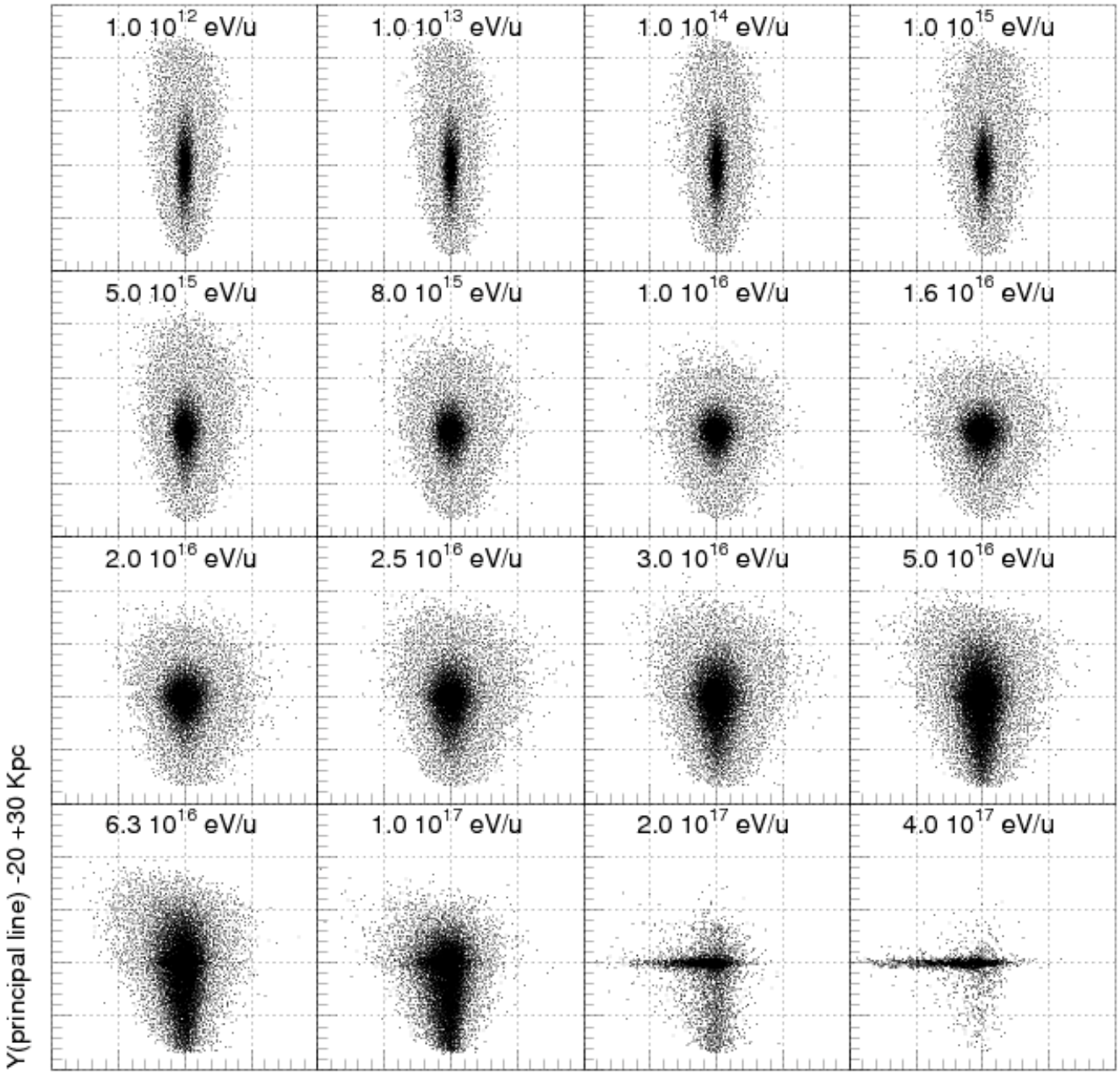
1.0 10^12 eV/u
1.0 10^13 eV/u
1.0 10^14 eV/u
1.0 10^15 eV/u
5.0 10^15 eV/u
8.0 10^15 eV/u
1.0 10^16 eV/u
1.6 10^16 eV/u
2.0 10^16 eV/u
2.5 10^16 eV/u
3.0 10^16 eV/u
5.0 10^16 eV/u
6.3 10^16 eV/u
1.0 10^17 eV/u
2.0 10^17 eV/u
4.0 10^17 eV/u
Y(principal line) -20 +30 Kpc
X(principal line) -2.0 +2.0 Kpc

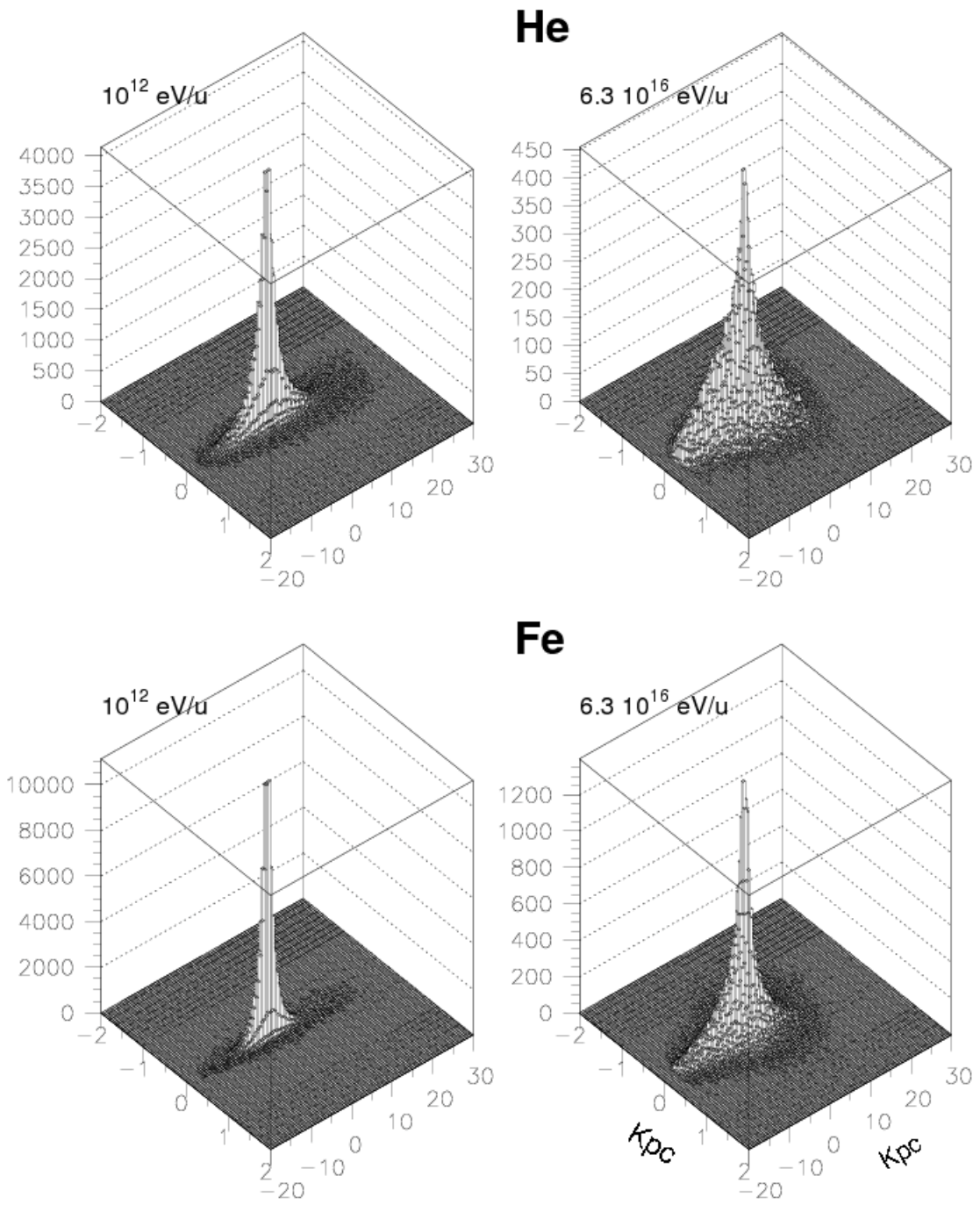
He
10^{12} eV/u
$6.3\ 10^{16}$ eV/u
Fe
10^{12} eV/u
$6.3\ 10^{16}$ eV/u
Kpc
Kpc

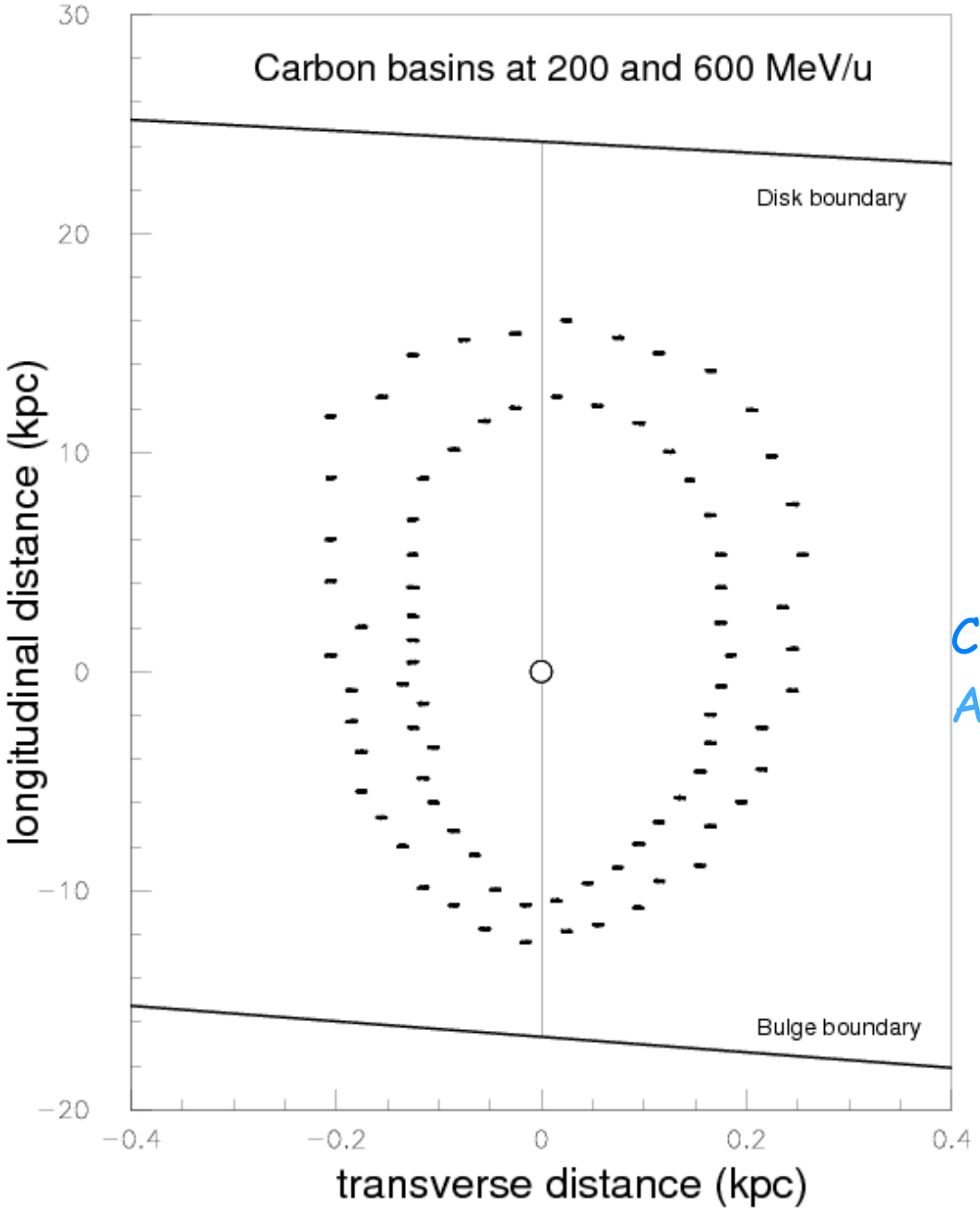

Codino & Plouin,
ApJ, 2006, 639, 173

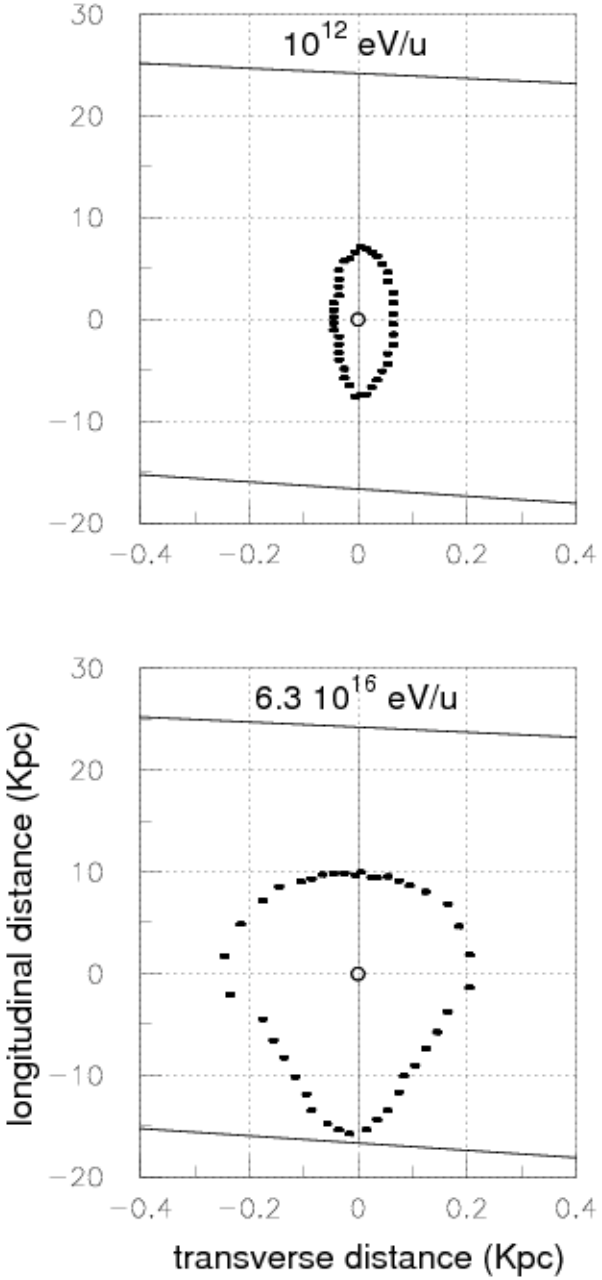
10^{12} eV/u
$6.3\ 10^{16}$ eV/u
longitudinal distance (Kpc)
transverse distance (Kpc)
30
20
10
0
−10
−20
−0.4
−0.2
0
0.2
0.4

The knees in terms of galactic basin

- As the energy increases the dimension of the galactic basins become larger and larger. When the size of a galactic basin (represented for example by the contour plots) exceeds the disk size, there is a break, a depression, in the number of cosmic rays reaching the solar cavity: this is the knee in terms of Galactic basins.
- If the size of the Galaxy (exactly, the disk thickness) would have been larger, then, the knee energy position along the energy axis would have been shifted at higher values.

- The concept of "galactic basin" is described in (Codino & Plouin, ApJ, 2006, 639, 173) but, in this paper, the explanation of the knees is not mentioned nor hinted.

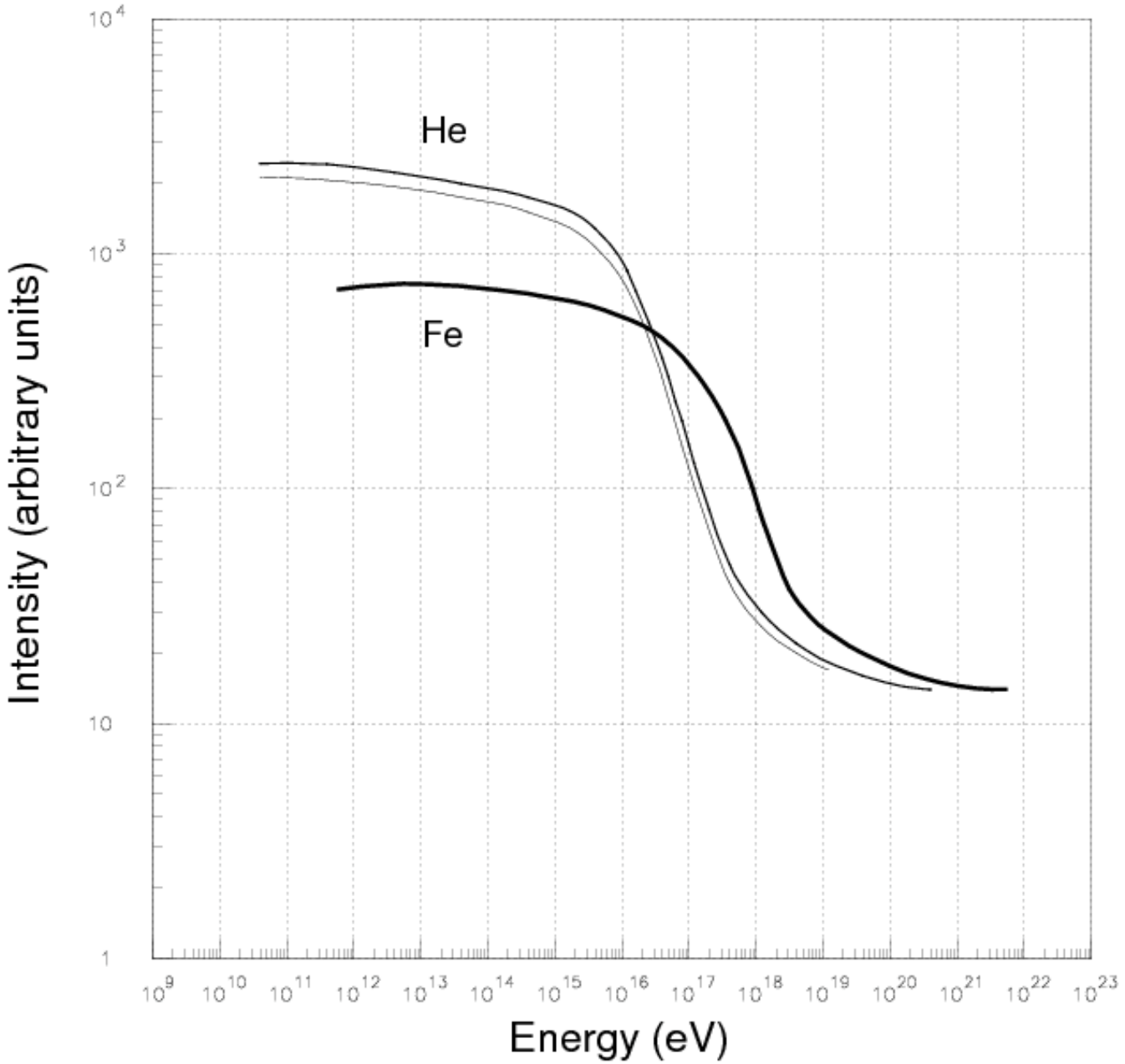
He
Fe
Intensity (arbitrary units)
Energy (eV)
10^4
10^3
10^2
10
1
10^9 10^{10} 10^{11} 10^{12} 10^{13} 10^{14} 10^{15} 10^{16} 10^{17} 10^{18} 10^{19} 10^{20} 10^{21} 10^{22} 10^{23}

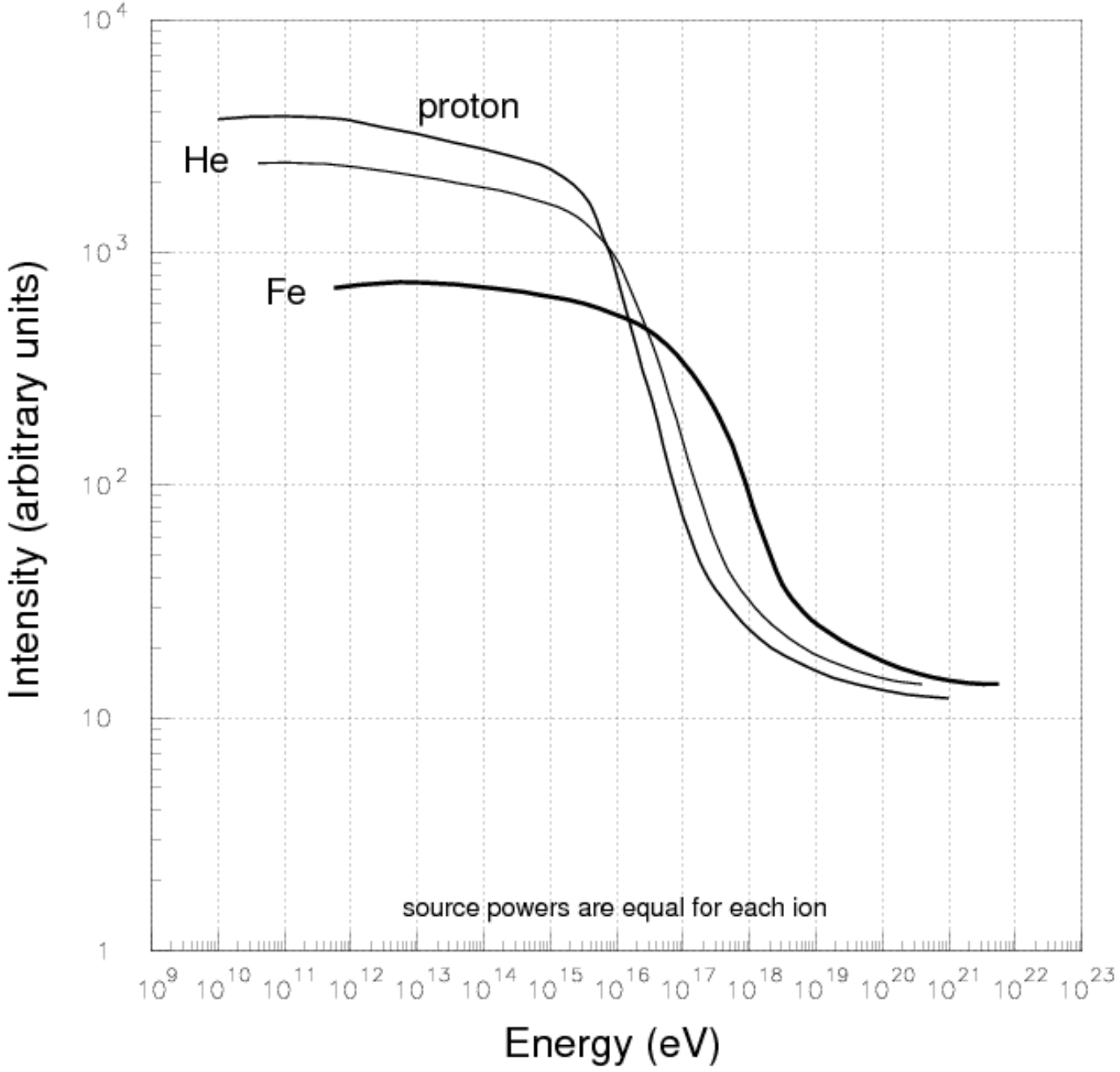
proton
He
Fe
source powers are equal for each ion
Intensity (arbitrary units)
Energy (eV)
10^4
10^3
10^2
10
1
10^9 10^10 10^11 10^12 10^13 10^14 10^15 10^16 10^17 10^18 10^19 10^20 10^21 10^22 10^23

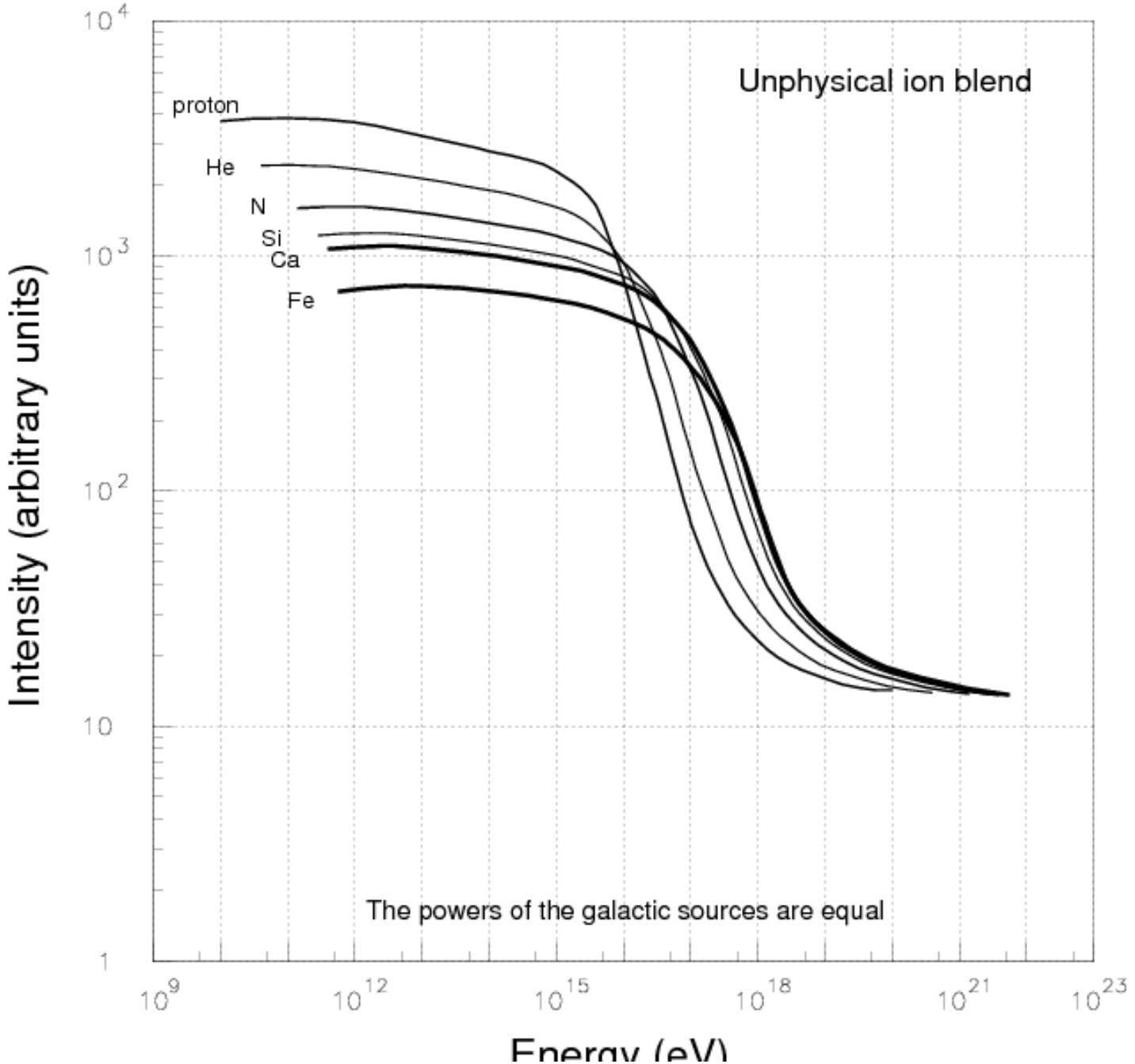
Unphysical ion blend
proton
He
N
Si
Ca
Fe
The powers of the galactic sources are equal
Intensity (arbitrary units)
Energy (eV)
10^4
10^3
10^2
10
1
10^9
10^12
10^15
10^18
10^21
10^23

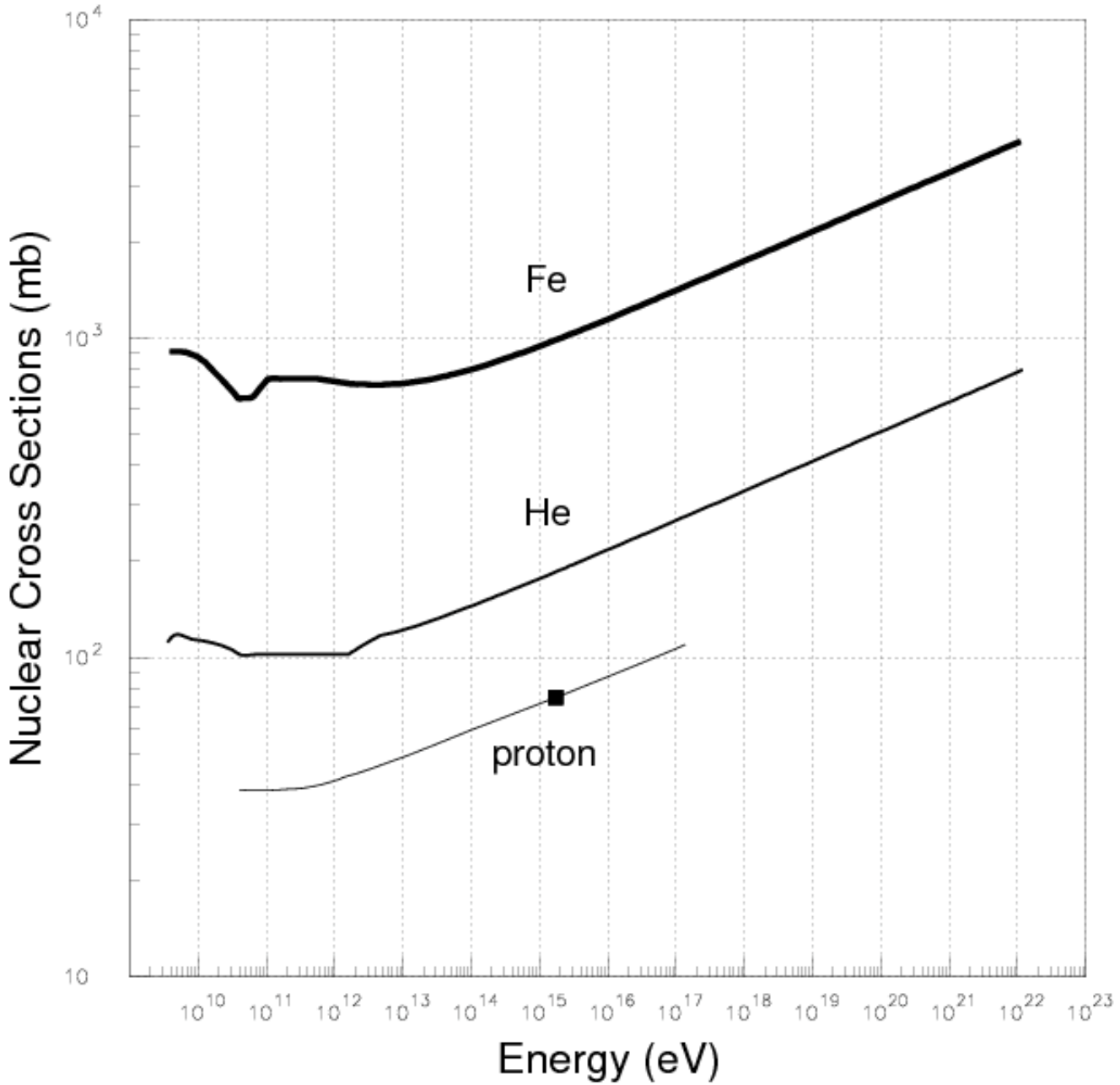
Nuclear Cross Sections (mb)
10^4
10^3
10^2
10
Fe
He
proton
10^{10} 10^{11} 10^{12} 10^{13} 10^{14} 10^{15} 10^{16} 10^{17} 10^{18} 10^{19} 10^{20} 10^{21} 10^{22} 10^{23}
Energy (eV)

Illuminating the Galaxy by an ion beam emitted from the Earth and counting the number of nuclear collisions in the disk

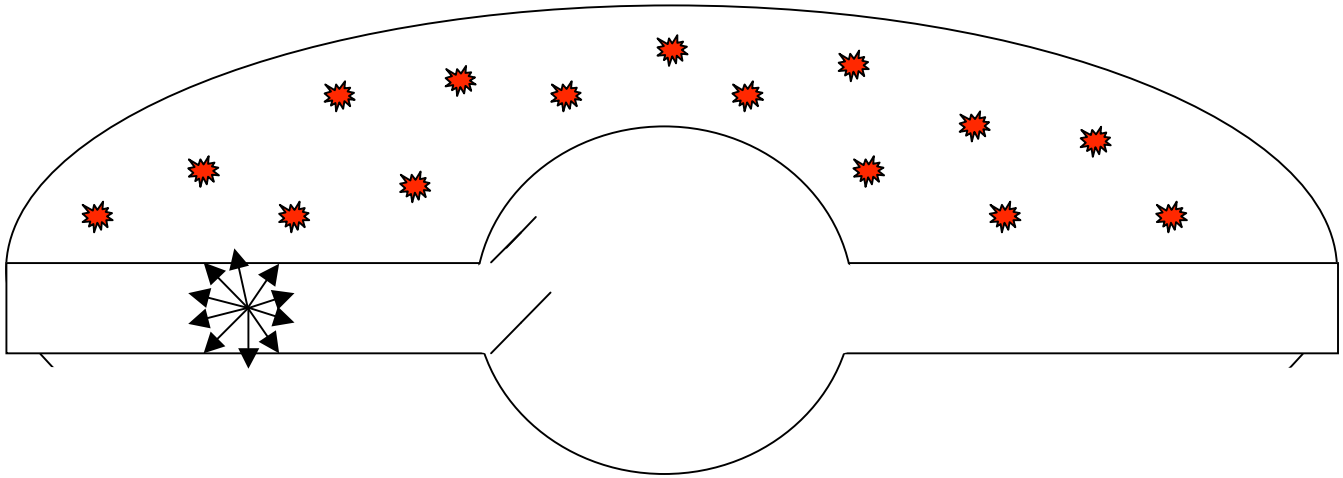

nuclear collisions

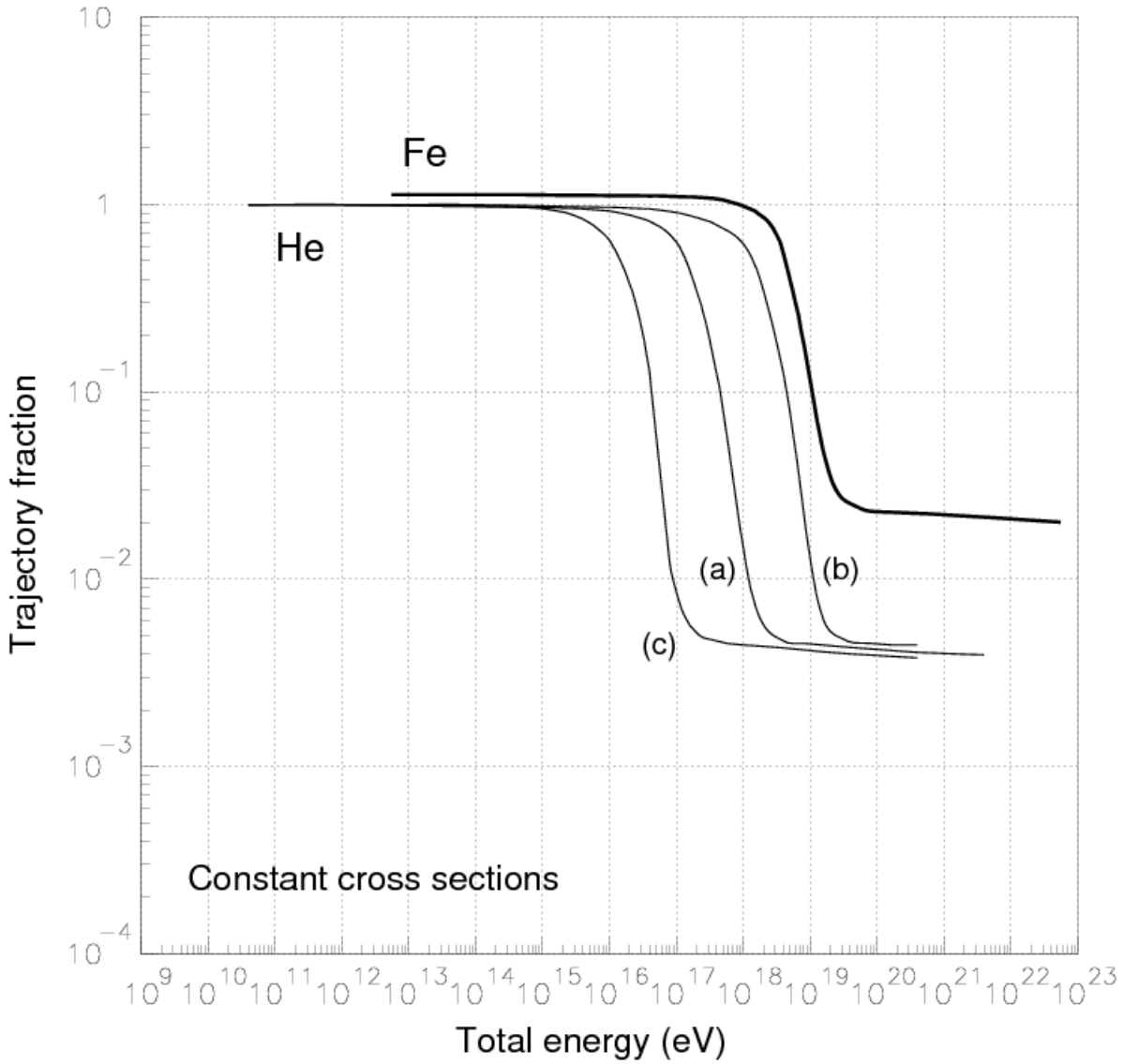
Fe
He
(a)
(b)
(c)
Constant cross sections
Trajectory fraction
Total energy (eV)
10
1
10^{-1}
10^{-2}
10^{-3}
10^{-4}
10^{9} 10^{10} 10^{11} 10^{12} 10^{13} 10^{14} 10^{15} 10^{16} 10^{17} 10^{18} 10^{19} 10^{20} 10^{21} 10^{22} 10^{23}

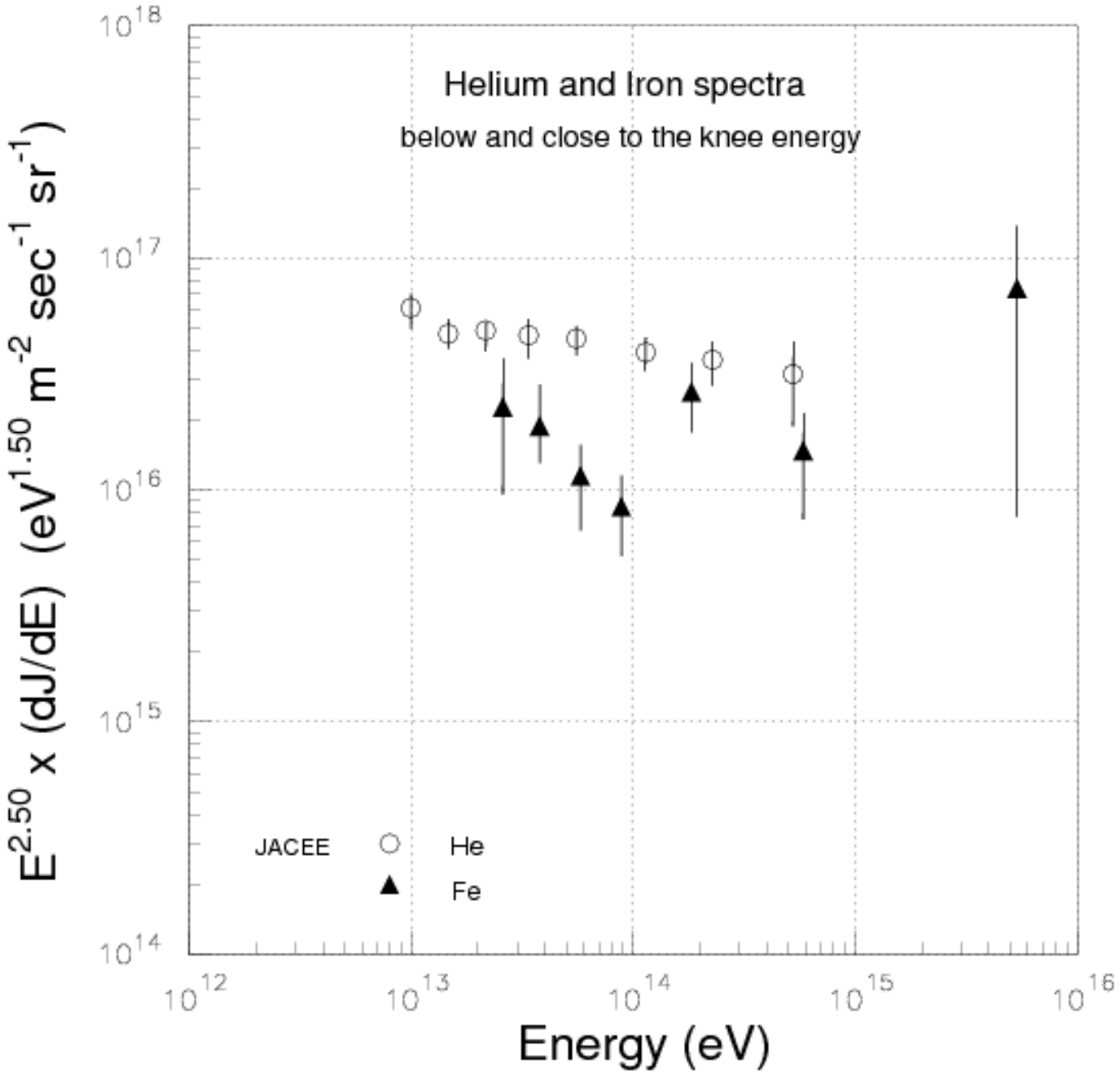
Helium and Iron spectra
below and close to the knee energy
JACEE
He
Fe
$E^{2.50}$ x (dJ/dE) ($eV^{1.50}$ m^{-2} sec^{-1} sr^{-1})
Energy (eV)
10^{18}
10^{17}
10^{16}
10^{15}
10^{14}
10^{12}
10^{13}
10^{14}
10^{15}
10^{16}

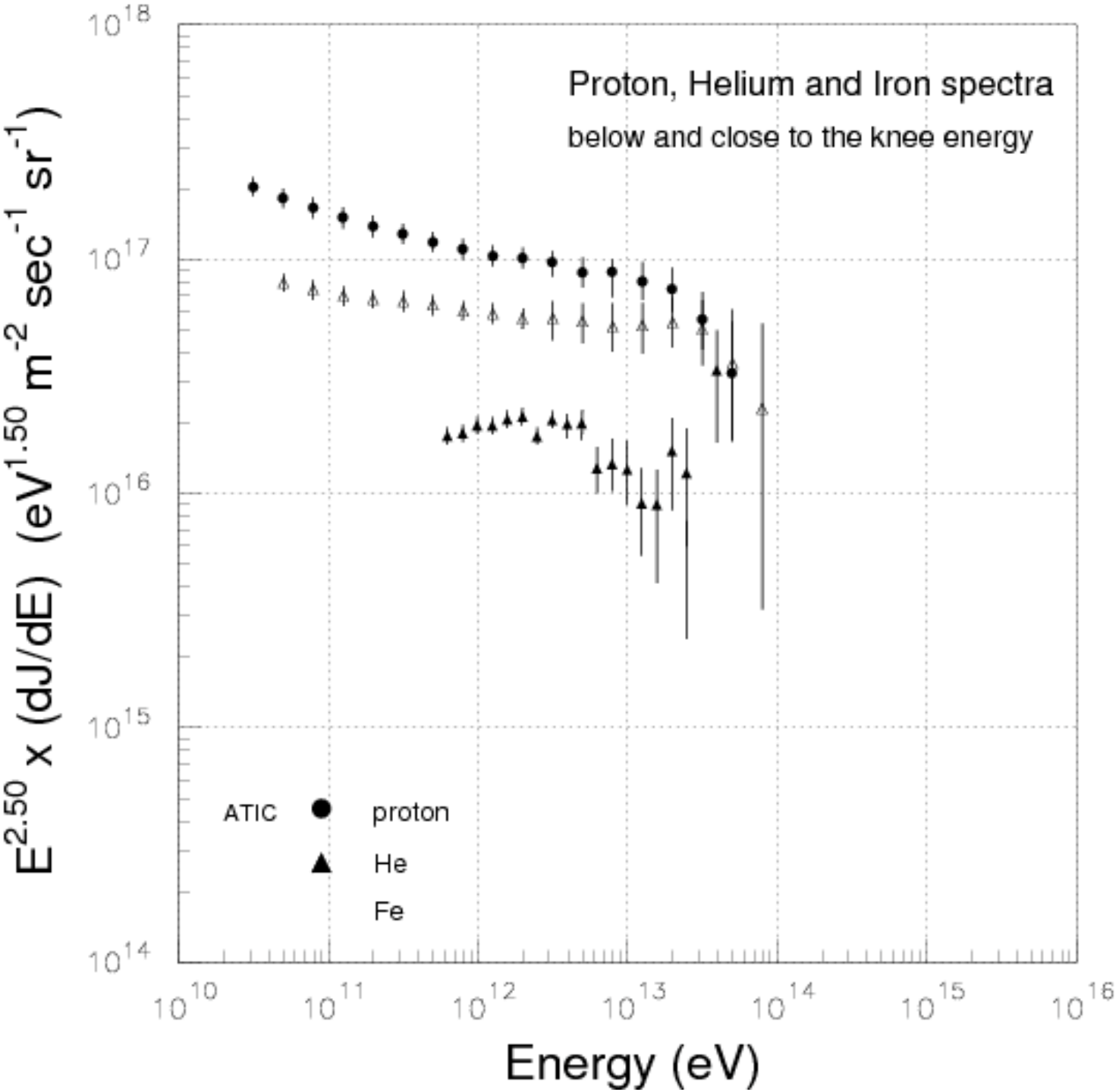
Proton, Helium and Iron spectra
below and close to the knee energy
$E^{2.50}$ x (dJ/dE) ($eV^{1.50}$ m^{-2} sec^{-1} sr^{-1})
10^{18}
10^{17}
10^{16}
10^{15}
10^{14}
10^{10}
10^{11}
10^{12}
10^{13}
10^{14}
10^{15}
10^{16}
Energy (eV)
ATIC
proton
He
Fe

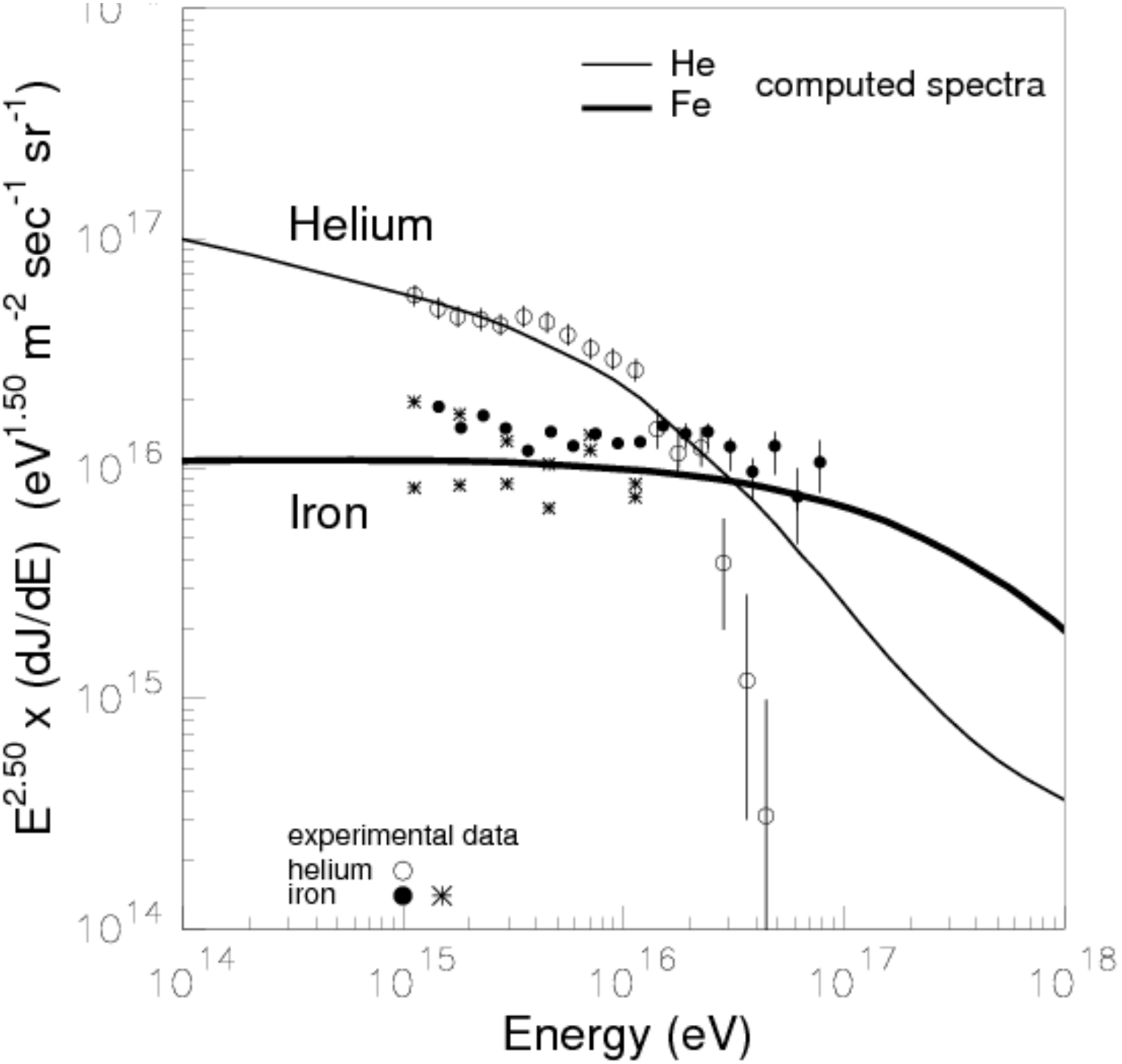
He
Fe
computed spectra
Helium
Iron
experimental data
helium
iron
$E^{2.50}$ x (dJ/dE) (eV$^{1.50}$ m^{-2} sec^{-1} sr^{-1})
Energy (eV)
10^{14}
10^{15}
10^{16}
10^{17}
10^{18}

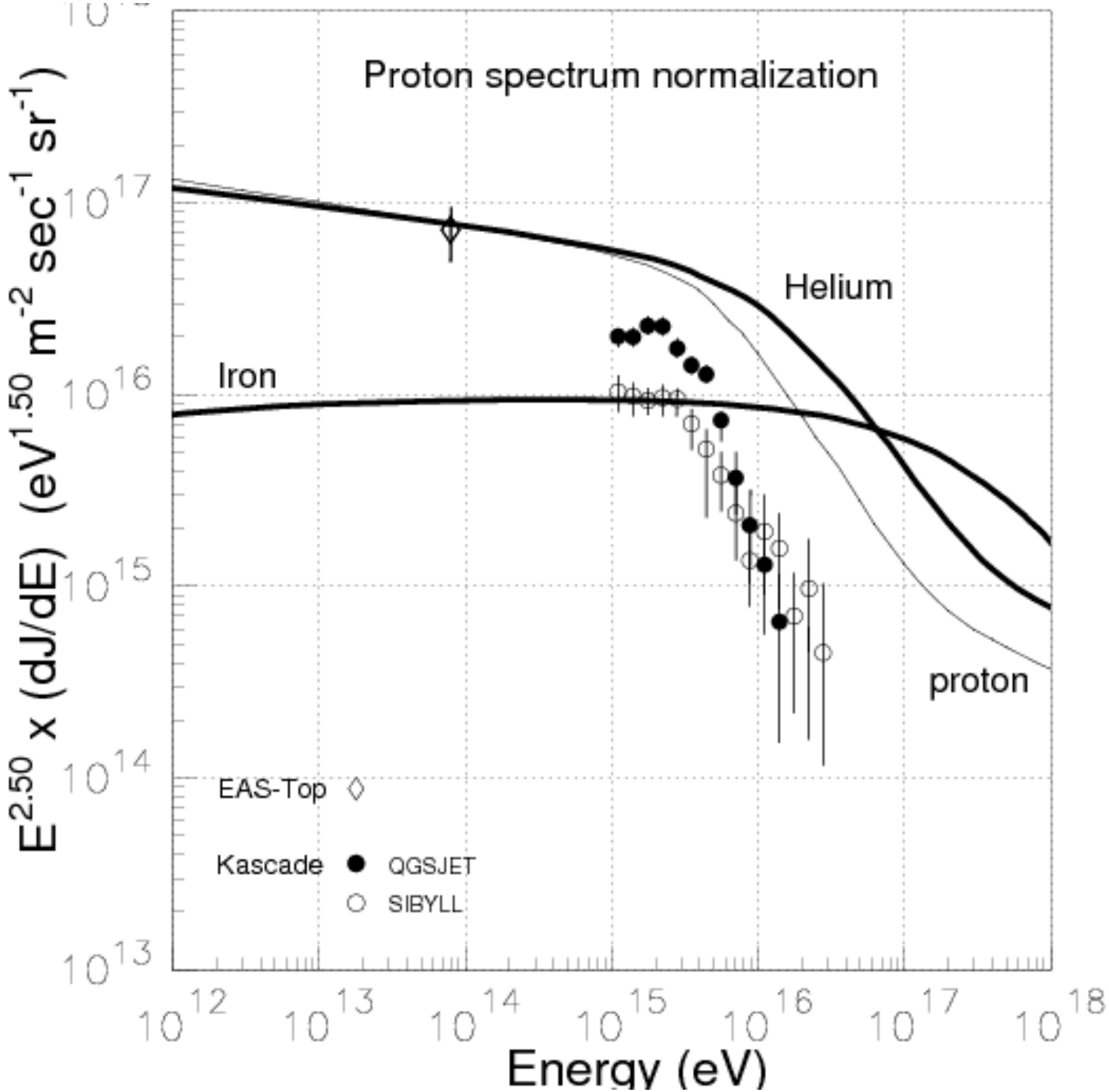
Proton spectrum normalization
Helium
Iron
proton
EAS-Top
Kascade
QGSJET
SIBYLL
$E^{2.50}$ x (dJ/dE) ($eV^{1.50}$ m^{-2} sec^{-1} sr^{-1})
Energy (eV)
10^{17}
10^{16}
10^{15}
10^{14}
10^{13}
10^{12}
10^{13}
10^{14}
10^{15}
10^{16}
10^{17}
10^{18}

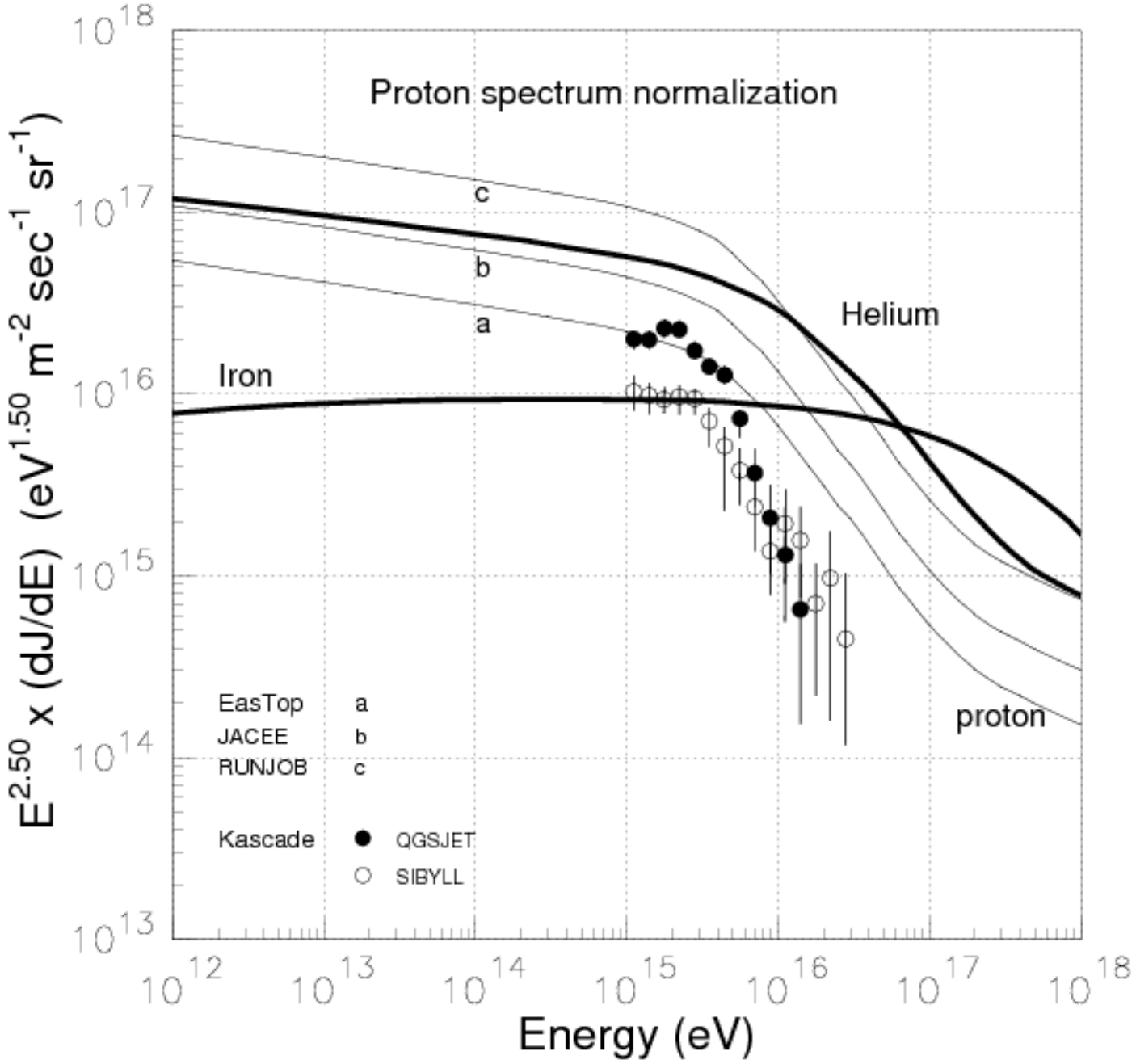
Proton spectrum normalization
c
b
a
Helium
Iron
proton
EasTop a
JACEE b
RUNJOB c
Kascade
QGSJET
SIBYLL
$E^{2.50}$ x (dJ/dE) ($eV^{1.50}$ m^{-2} sec^{-1} sr^{-1})
Energy (eV)
10^{18}
10^{17}
10^{16}
10^{15}
10^{14}
10^{13}
10^{12}
10^{13}
10^{14}
10^{15}
10^{16}
10^{17}
10^{18}

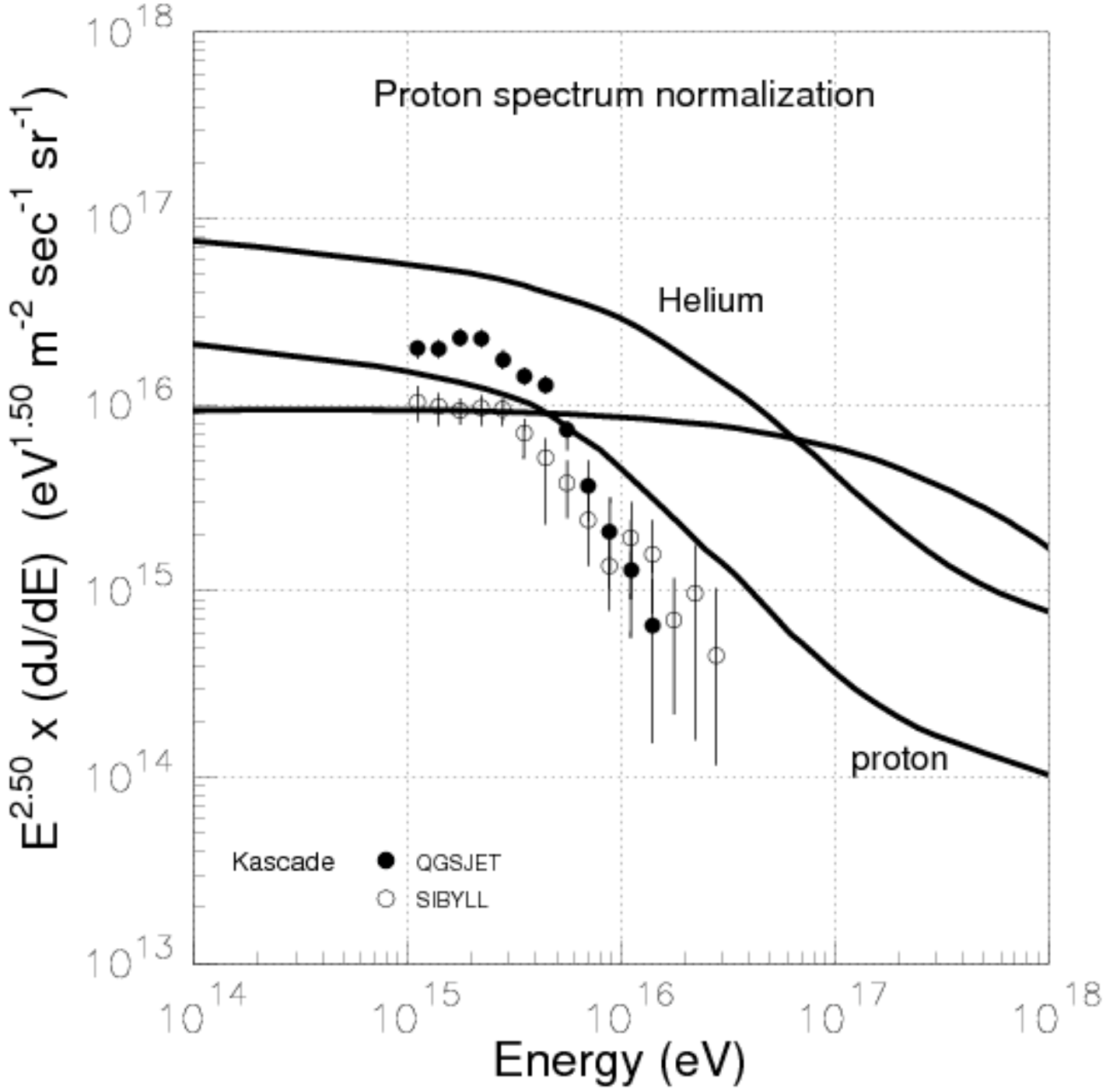
Proton spectrum normalization
Helium
proton
Kascade
QGSJET
SIBYLL
$E^{2.50}$ x (dJ/dE) ($eV^{1.50}$ m^{-2} sec^{-1} sr^{-1})
Energy (eV)
10^{18}
10^{17}
10^{16}
10^{15}
10^{14}
10^{13}
10^{14}
10^{15}
10^{16}
10^{17}
10^{18}

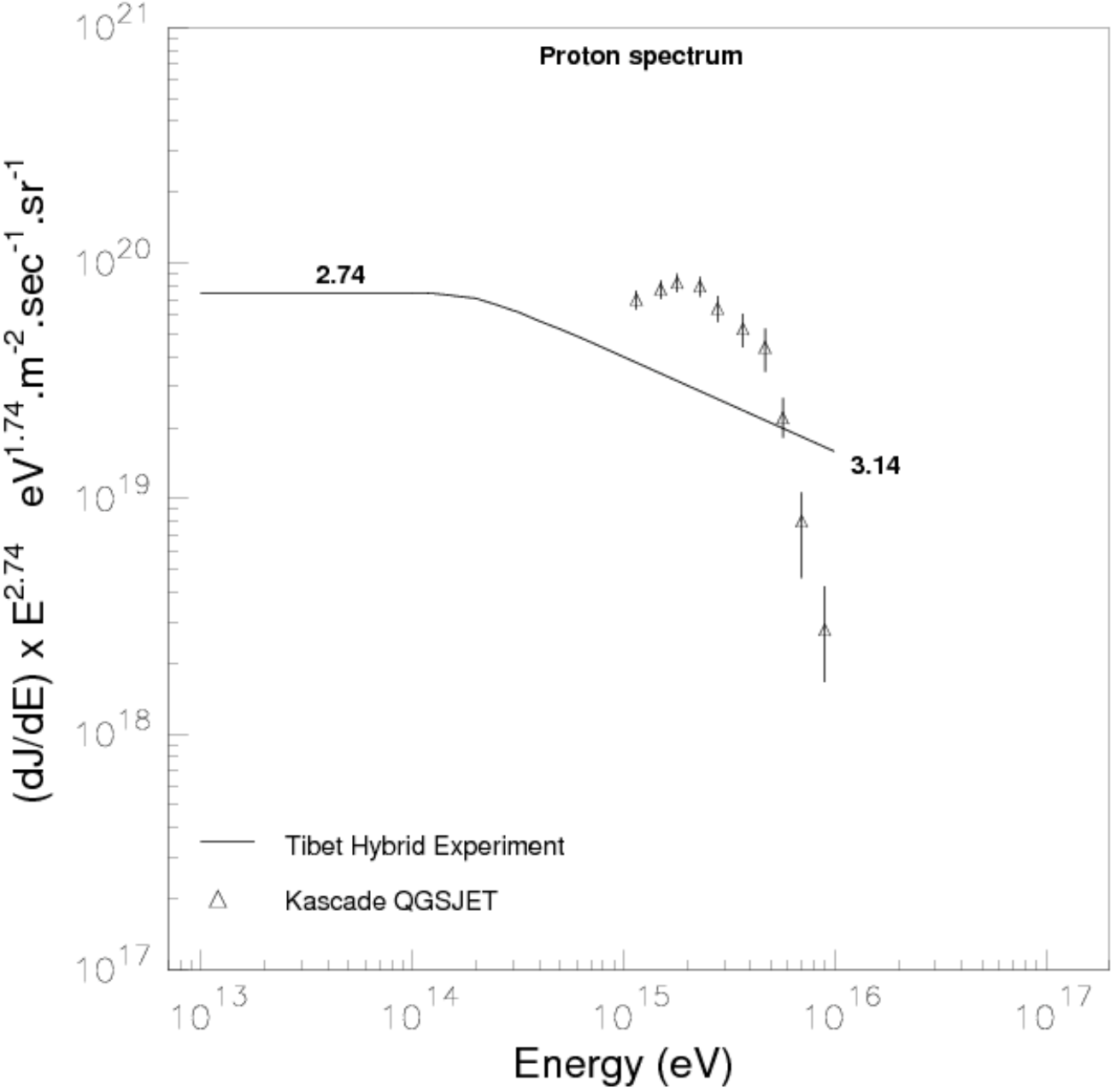
Proton spectrum
2.74
3.14
Tibet Hybrid Experiment
Kascade QGSJET
(dJ/dE) x E^2.74 eV^1.74.m^-2.sec^-1.sr^-1
Energy (eV)
10^21
10^20
10^19
10^18
10^17
10^13
10^14
10^15
10^16
10^17

Relative abundances of cosmic ions at low energies

(well below the knee energy)

BLEND 1 – Energy = 10^{12} eV

Ions	Composition (%)	Spectral index	Intensity (ions/m^2 s sr GeV)	Reference
H	41	2.75 ± 0.02	10.91 ± 0.32	Wiebel-Sooth
He	26	2.62 ± 0.02	6.60 ± 0.15	
CNO	11	2.67 ± 0.02	2.86 ± 0.06	
Ne-S	10	2.64 ± 0.03	2.43 ± 0.07	
Fe-Ni (17-26)	10	2.60 ± 0.03	2.52 ± 0.05	
Other heavy ions	0.5	2.60 ± 0.03	0.02 ± 0.02	

Relative abundances of cosmic ions at low energies

(below the knee energy)

Ion Blend (inspired by Atic)

Ion	Composition (%)	Spectral index
H	35,6	2.608
He	33,1	2.527
CNO	15,5	2.60
Ne-S	9,2	2.60
Fe (17-26)	6,2	2.50
Ca	0.1	2.60

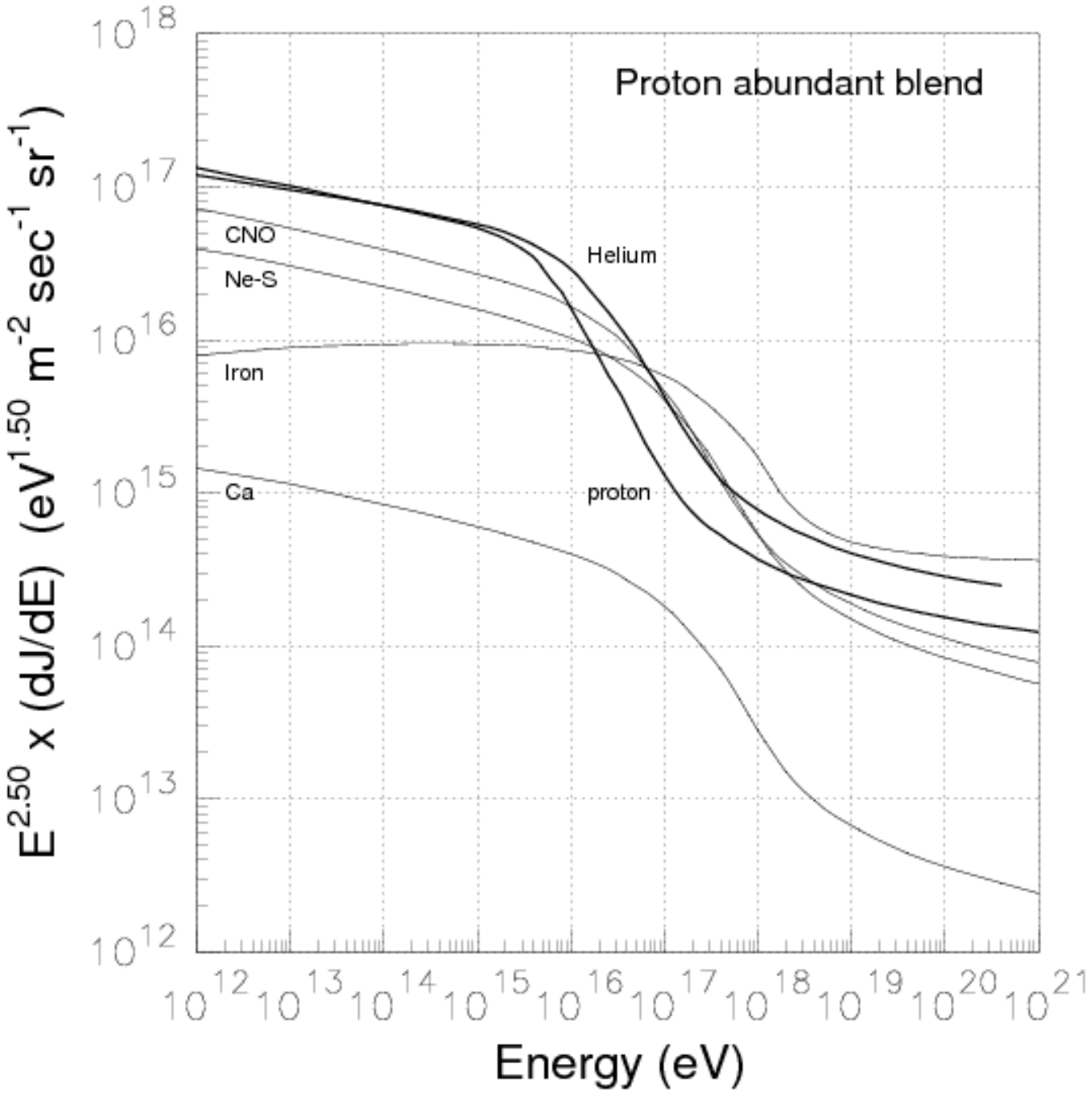
Proton abundant blend
CNO
Ne-S
Iron
Ca
Helium
proton
$E^{2.50}$ x (dJ/dE) ($eV^{1.50}$ m^{-2} sec^{-1} sr^{-1})
Energy (eV)
10^{18}
10^{17}
10^{16}
10^{15}
10^{14}
10^{13}
10^{12}
10^{12} 10^{13} 10^{14} 10^{15} 10^{16} 10^{17} 10^{18} 10^{19} 10^{20} 10^{21}

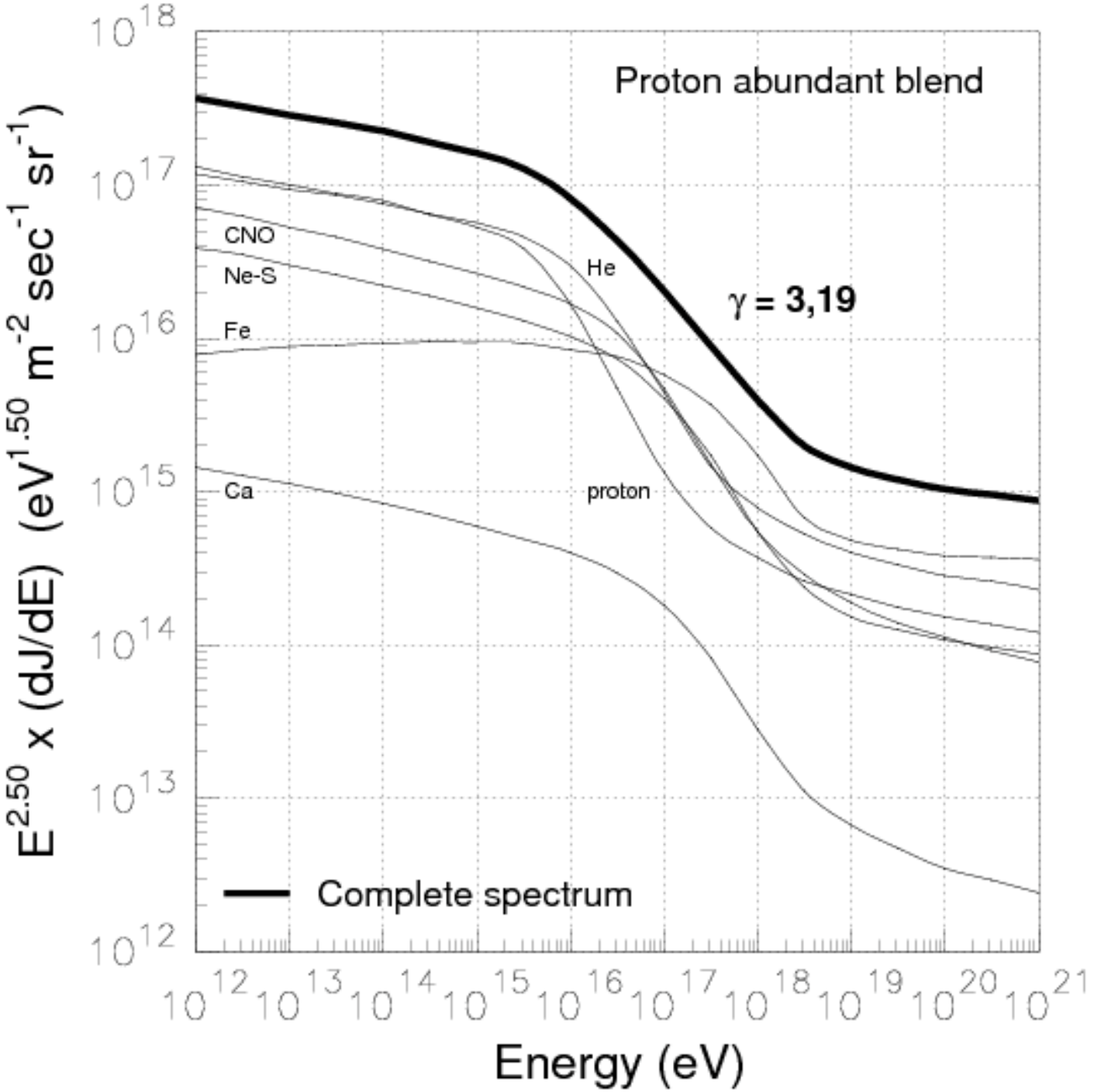
Proton abundant blend
γ = 3,19
CNO
Ne-S
Fe
Ca
He
proton
Complete spectrum
E^2.50 x (dJ/dE) (eV^1.50 m^-2 sec^-1 sr^-1)
Energy (eV)
10^18
10^17
10^16
10^15
10^14
10^13
10^12
10^12 10^13 10^14 10^15 10^16 10^17 10^18 10^19 10^20 10^21

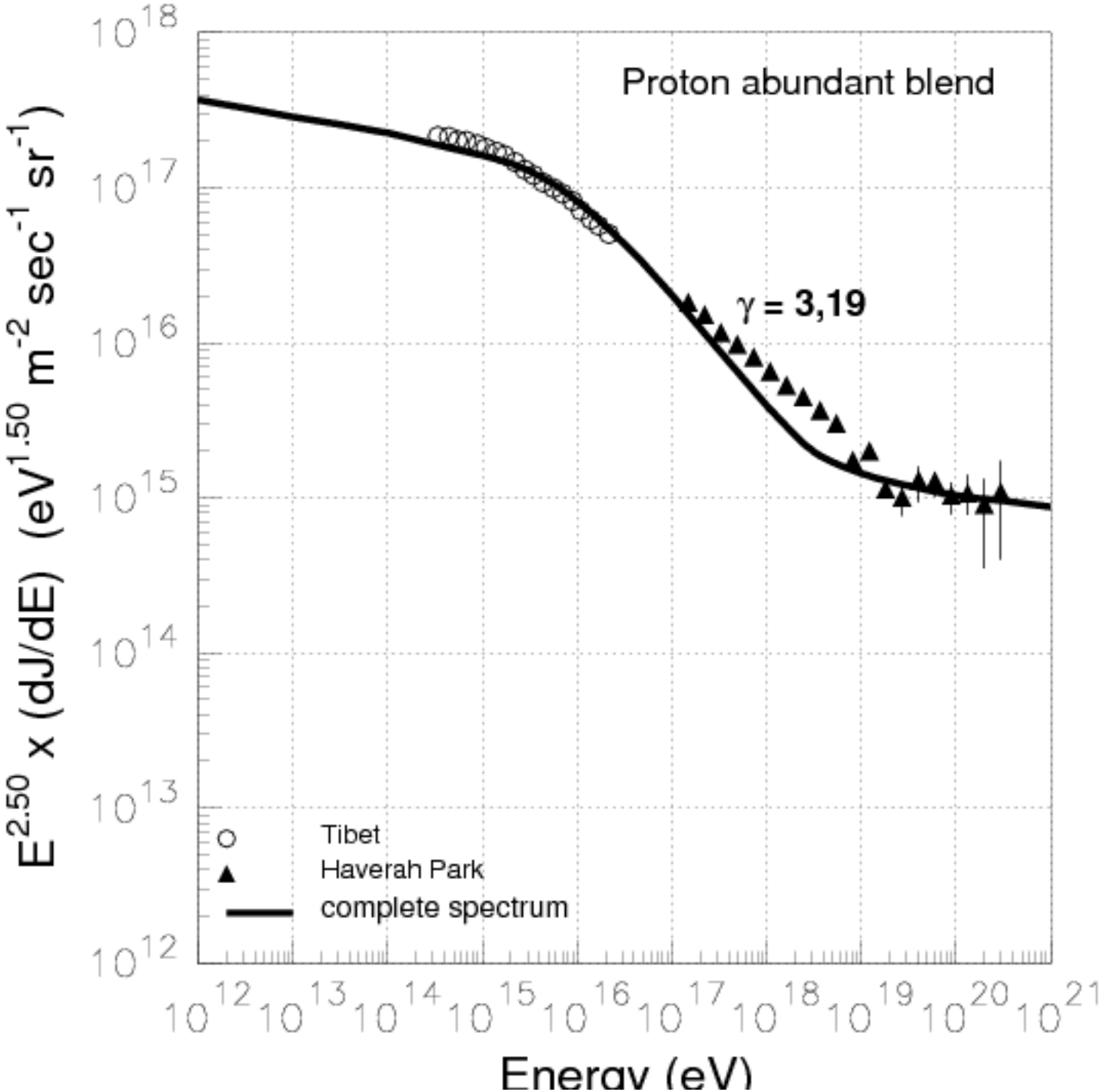
Proton abundant blend
γ = 3,19
Tibet
Haverah Park
complete spectrum
E^2.50 x (dJ/dE) (eV^1.50 m^-2 sec^-1 sr^-1)
Energy (eV)
10^18
10^17
10^16
10^15
10^14
10^13
10^12
10^12 10^13 10^14 10^15 10^16 10^17 10^18 10^19 10^20 10^21

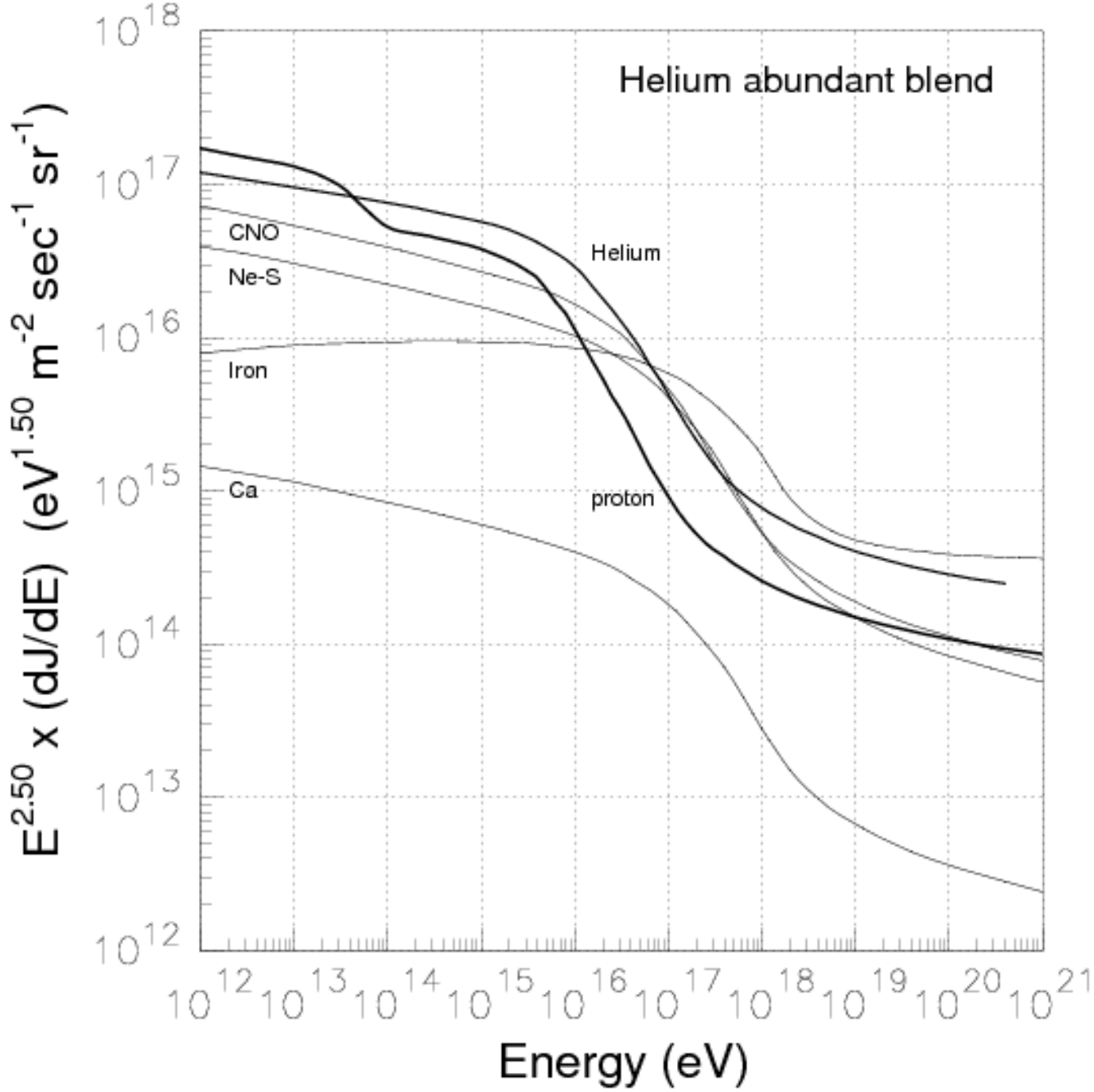
Helium abundant blend
CNO
Ne-S
Iron
Ca
Helium
proton
$E^{2.50}$ x (dJ/dE) ($eV^{1.50}$ m^{-2} sec^{-1} sr^{-1})
Energy (eV)
10^{18}
10^{17}
10^{16}
10^{15}
10^{14}
10^{13}
10^{12}
10^{12} 10^{13} 10^{14} 10^{15} 10^{16} 10^{17} 10^{18} 10^{19} 10^{20} 10^{21}

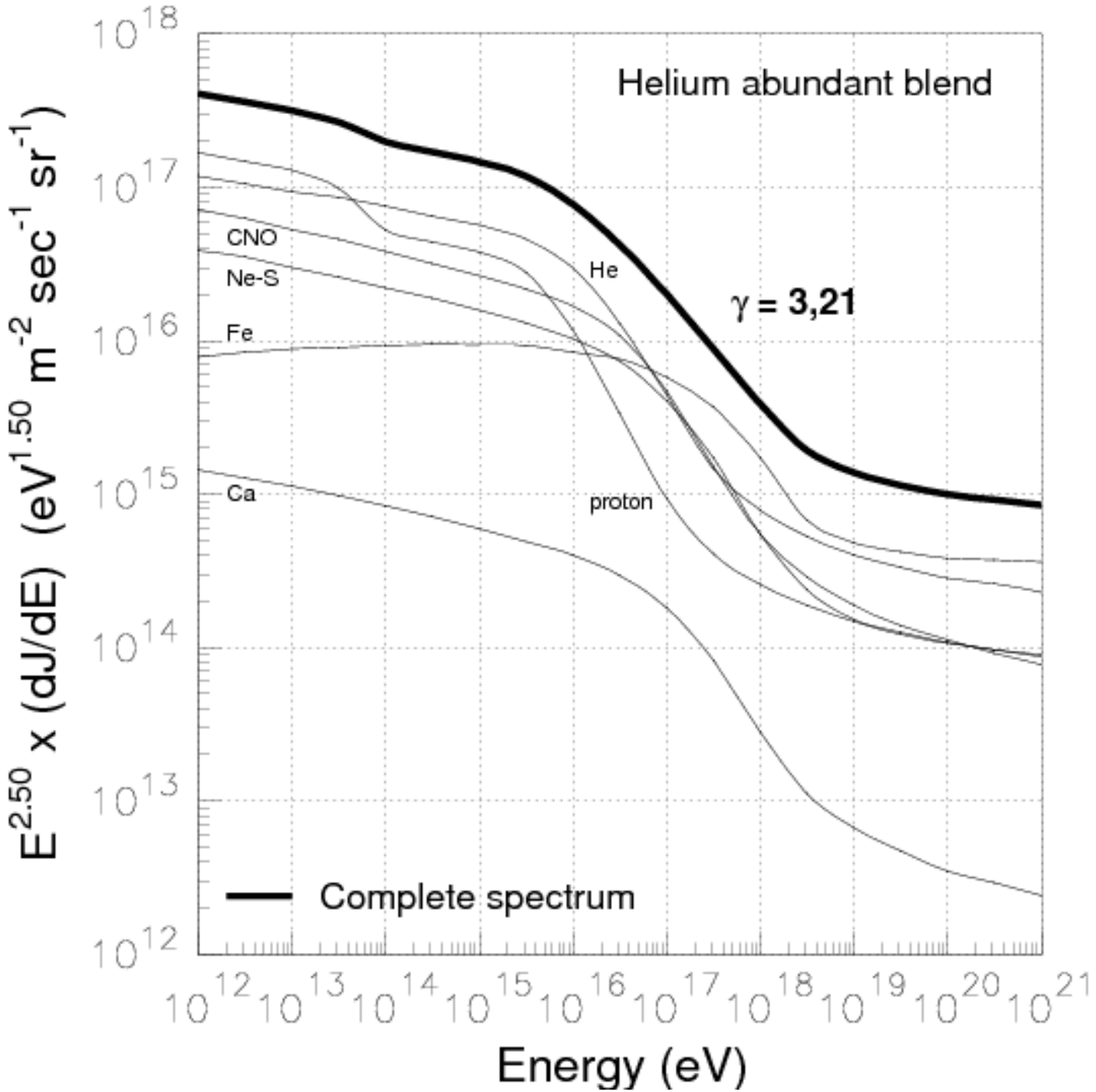
Helium abundant blend
γ = 3,21
CNO
Ne-S
Fe
Ca
He
proton
Complete spectrum
E^2.50 x (dJ/dE) (eV^1.50 m^-2 sec^-1 sr^-1)
Energy (eV)
10^18
10^17
10^16
10^15
10^14
10^13
10^12
10^12 10^13 10^14 10^15 10^16 10^17 10^18 10^19 10^20 10^21

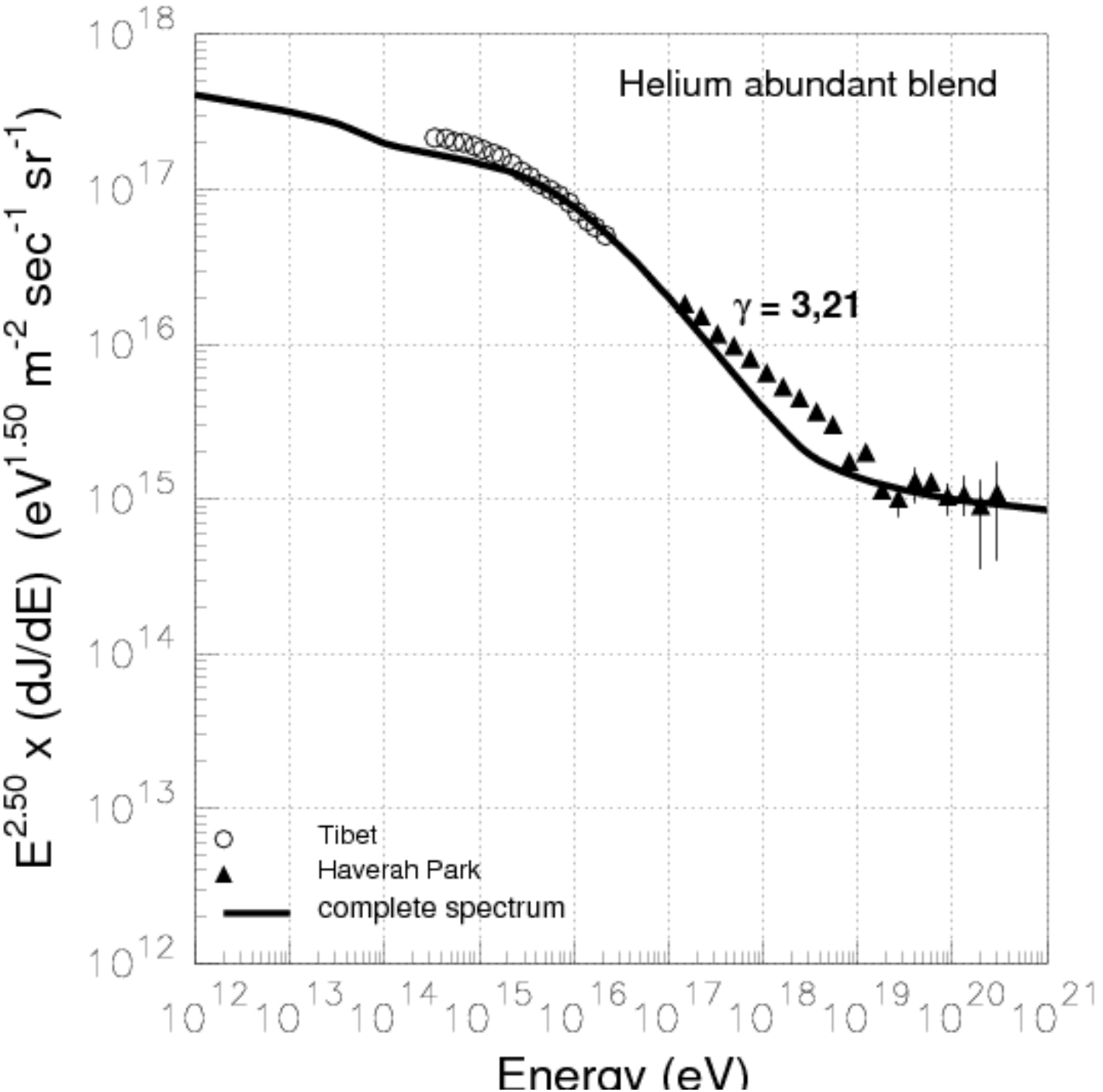
Helium abundant blend
γ = 3,21
Tibet
Haverah Park
complete spectrum
E^2.50 x (dJ/dE) (eV^1.50 m^-2 sec^-1 sr^-1)
Energy (eV)
10^18
10^17
10^16
10^15
10^14
10^13
10^12
10^12 10^13 10^14 10^15 10^16 10^17 10^18 10^19 10^20 10^21

Relative abundances of cosmic ions at low energies

(below the knee energy)

PROTON ABUNDANT BLEND (steep spectra) – Energy = 2×10^{15} eV

Ion	Composition (%)	Spectral index
H	32,8	2.72
He	29,7	2.72
CNO	11,7	2.65
Ne-S	10,0	2.65
Fe (17-26)	15,0	2.60
Ca	0.8	2.60

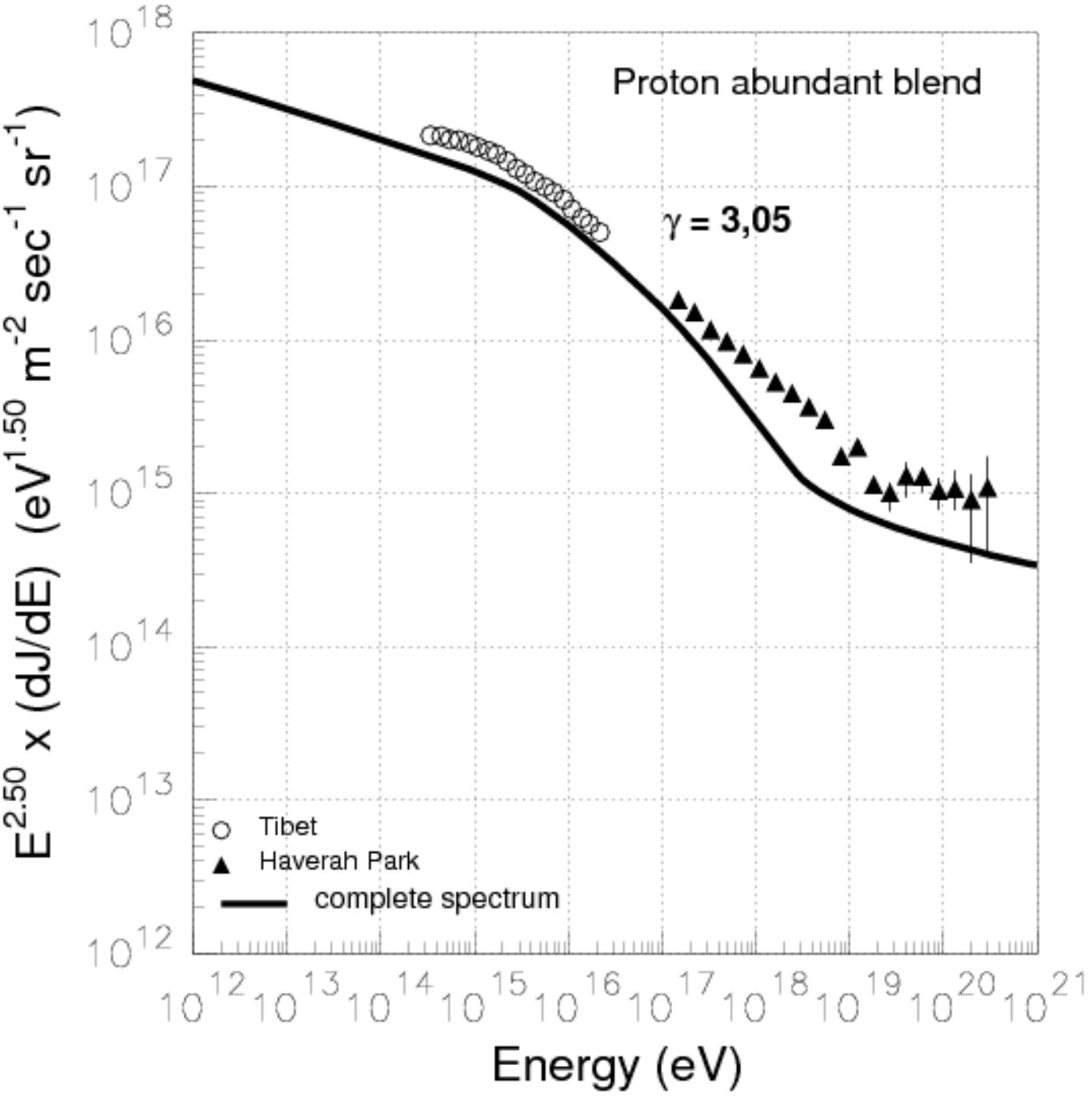
Proton abundant blend
γ = 3,05
Tibet
Haverah Park
complete spectrum
E^2.50 x (dJ/dE) (eV^1.50 m^-2 sec^-1 sr^-1)
Energy (eV)
10^18
10^17
10^16
10^15
10^14
10^13
10^12
10^12 10^13 10^14 10^15 10^16 10^17 10^18 10^19 10^20 10^21

Relative abundances of cosmic ions at low energies

(below the knee energy)

PROTON superABUNDANT BLEND – Energy = 2×10^{15} eV

Ion	Composition (%)	Spectral index
H	41,0	2.72
He	25,5	2.72
CNO	10,0	2.65
Ne-S	8,60	2.65
Fe (17-26)	12,8	2.60
Ca	0.74	2.60

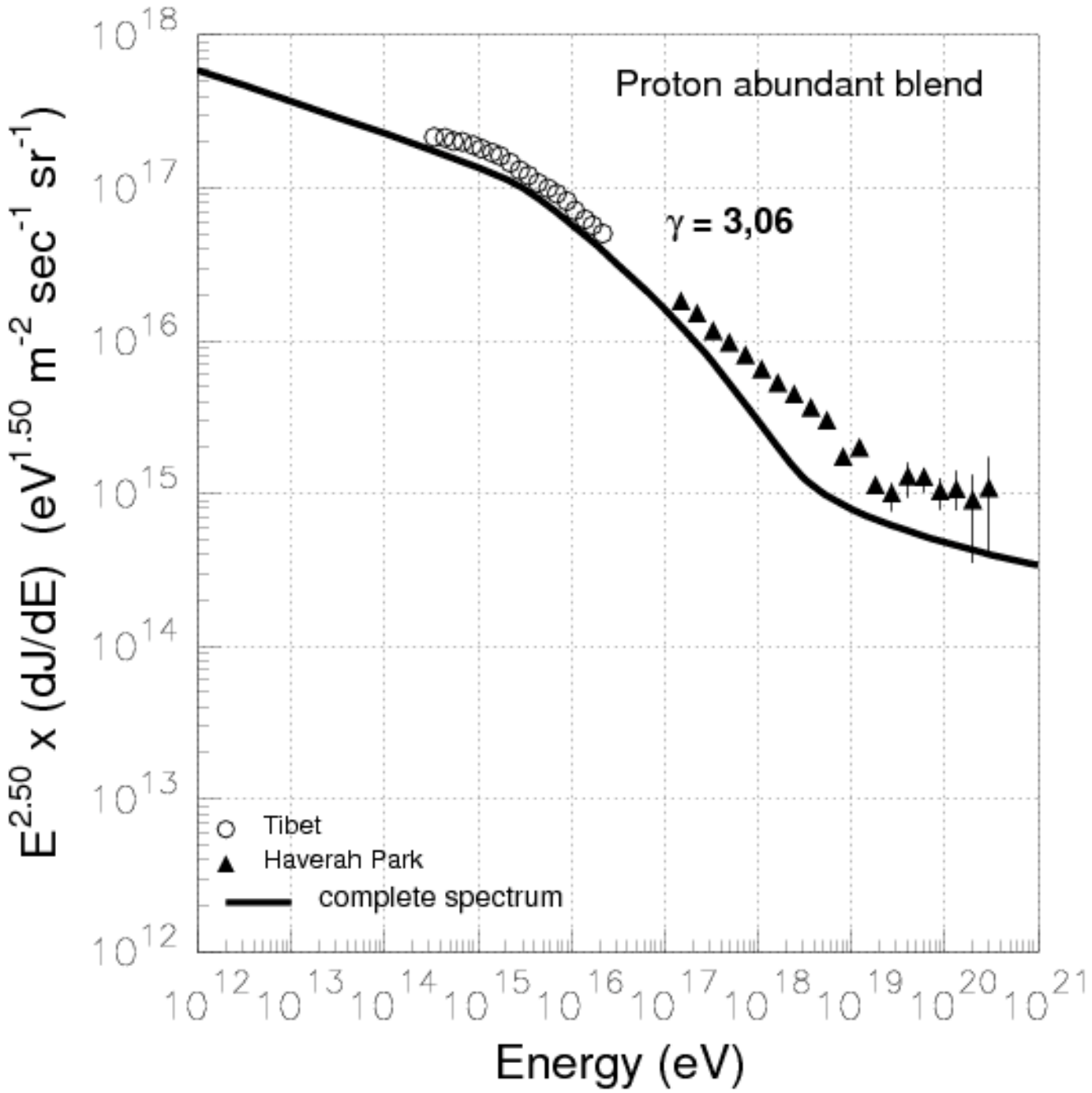
Proton abundant blend
γ = 3,06
Tibet
Haverah Park
complete spectrum
E^2.50 x (dJ/dE) (eV^1.50 m^-2 sec^-1 sr^-1)
Energy (eV)
10^18
10^17
10^16
10^15
10^14
10^13
10^12
10^12 10^13 10^14 10^15 10^16 10^17 10^18 10^19 10^20 10^21

Relative abundances of cosmic ions at low energies

(below the knee energy)

He Abundant BLEND - Energy = 2×10^{15} eV

Ion	Composition (%)	Spectral index
H	19,6	2.72
He	35,5	2.72
CNO	14,0	2.65
Ne-S	12,0	2.65
Fe (17-26)	17,8	2.50
Ca	0.1	2.60

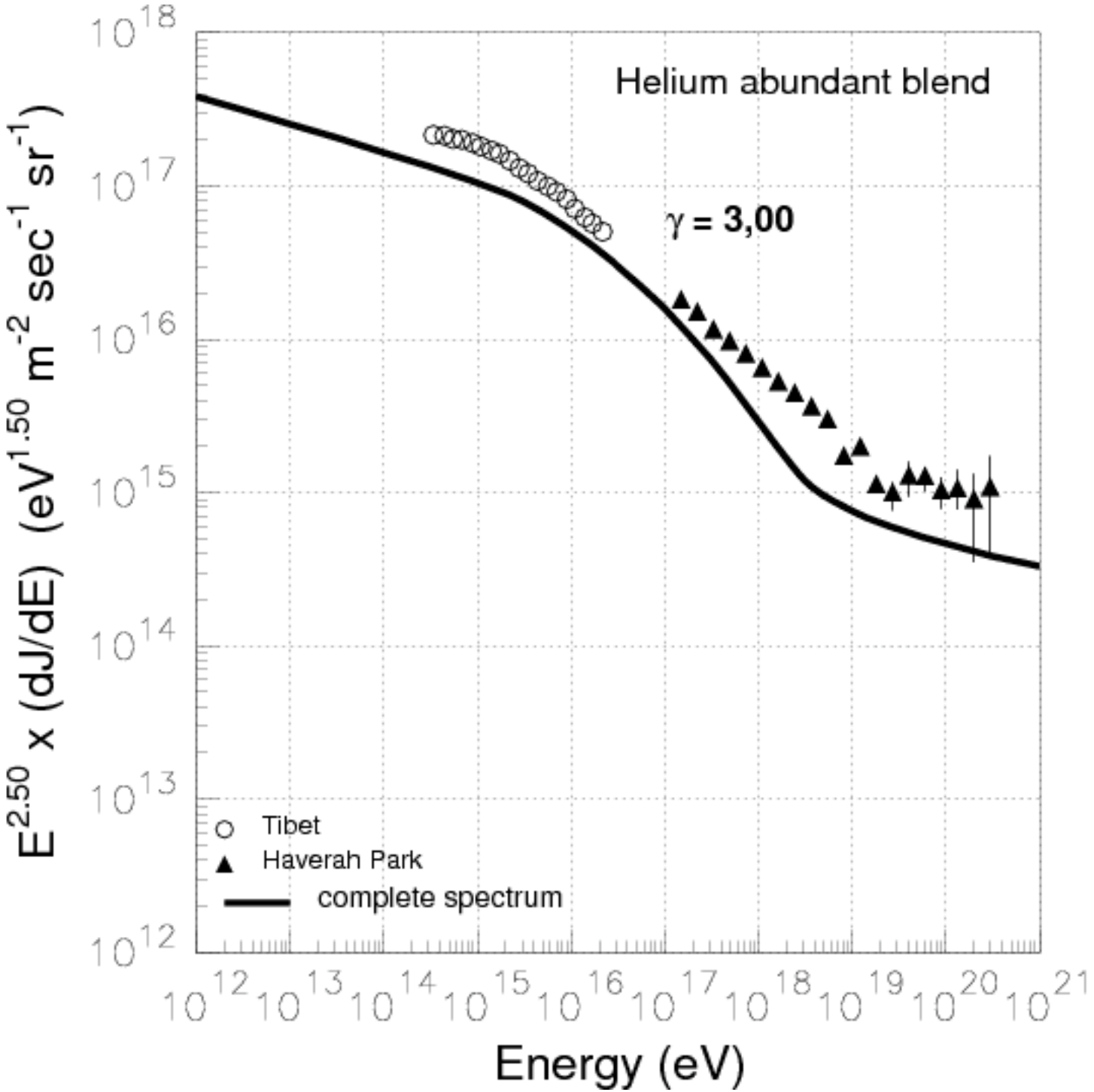
Helium abundant blend
γ = 3,00
Tibet
Haverah Park
complete spectrum
E^2.50 x (dJ/dE) (eV^1.50 m^-2 sec^-1 sr^-1)
Energy (eV)
10^18
10^17
10^16
10^15
10^14
10^13
10^12
10^12 10^13 10^14 10^15 10^16 10^17 10^18 10^19 10^20 10^21

The ankle

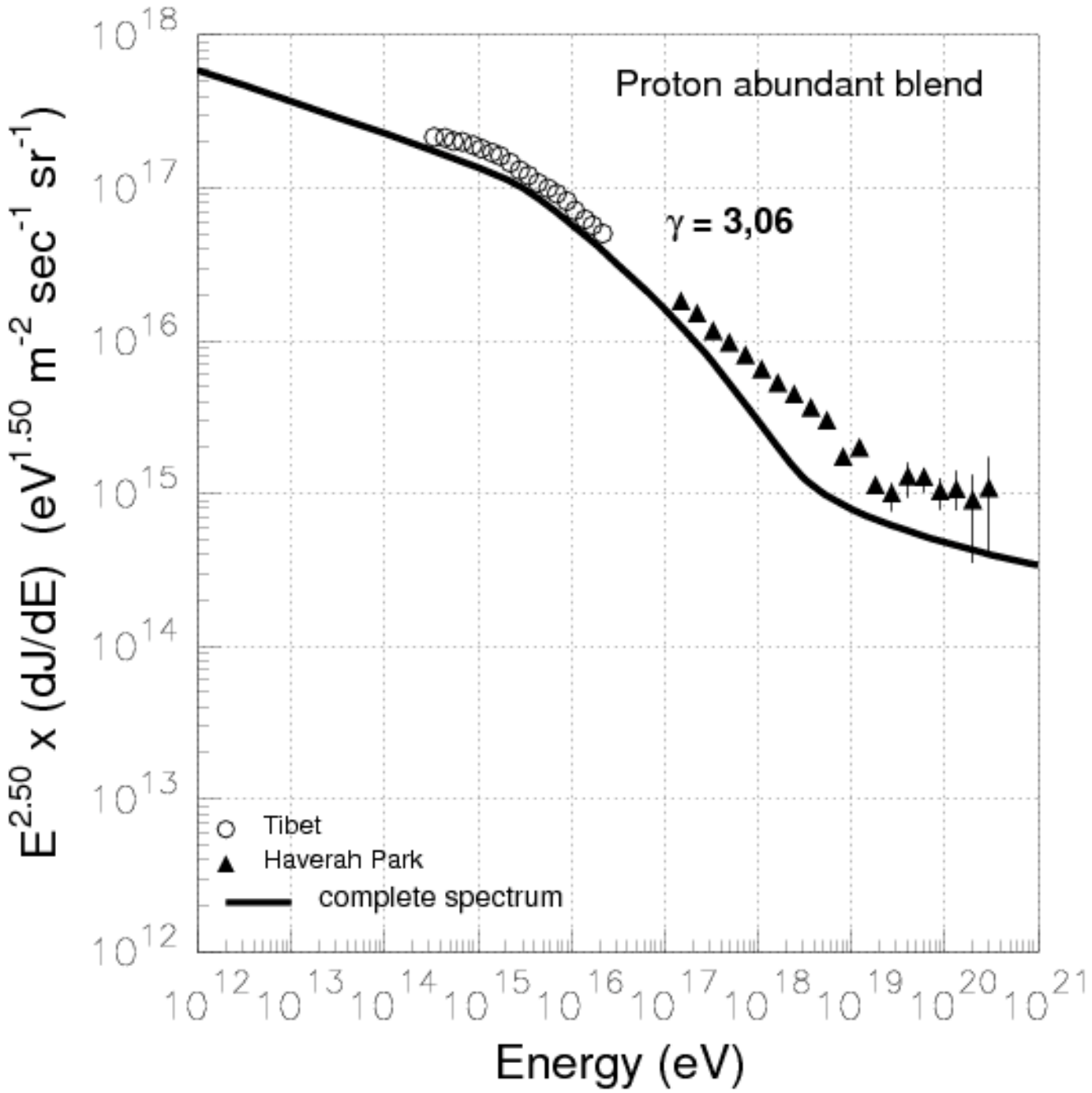
Proton abundant blend
γ = 3,06
Tibet
Haverah Park
complete spectrum
E^2.50 x (dJ/dE) (eV^1.50 m^-2 sec^-1 sr^-1)
Energy (eV)
10^18
10^17
10^16
10^15
10^14
10^13
10^12
10^12 10^13 10^14 10^15 10^16 10^17 10^18 10^19 10^20 10^21

The extragalactic component

Cosmic ray overflowing the Galaxy

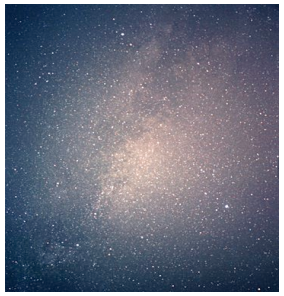

Cosmic rays entering the Milky Way

Assume that a significant amount of the extragalactic component of cosmic rays reach the local galactic zone, at some energy. Let us suppose that :

- the relative abundances of the extragalactic cosmic ions in the intergalactic space are similar to those overflowing from the Milky Way Galaxy ;

- the extragalactic cosmic rays entering the Milky Way Galaxy encounter the same structures of magnetic fields and interstellar matter as do galactic cosmic rays.

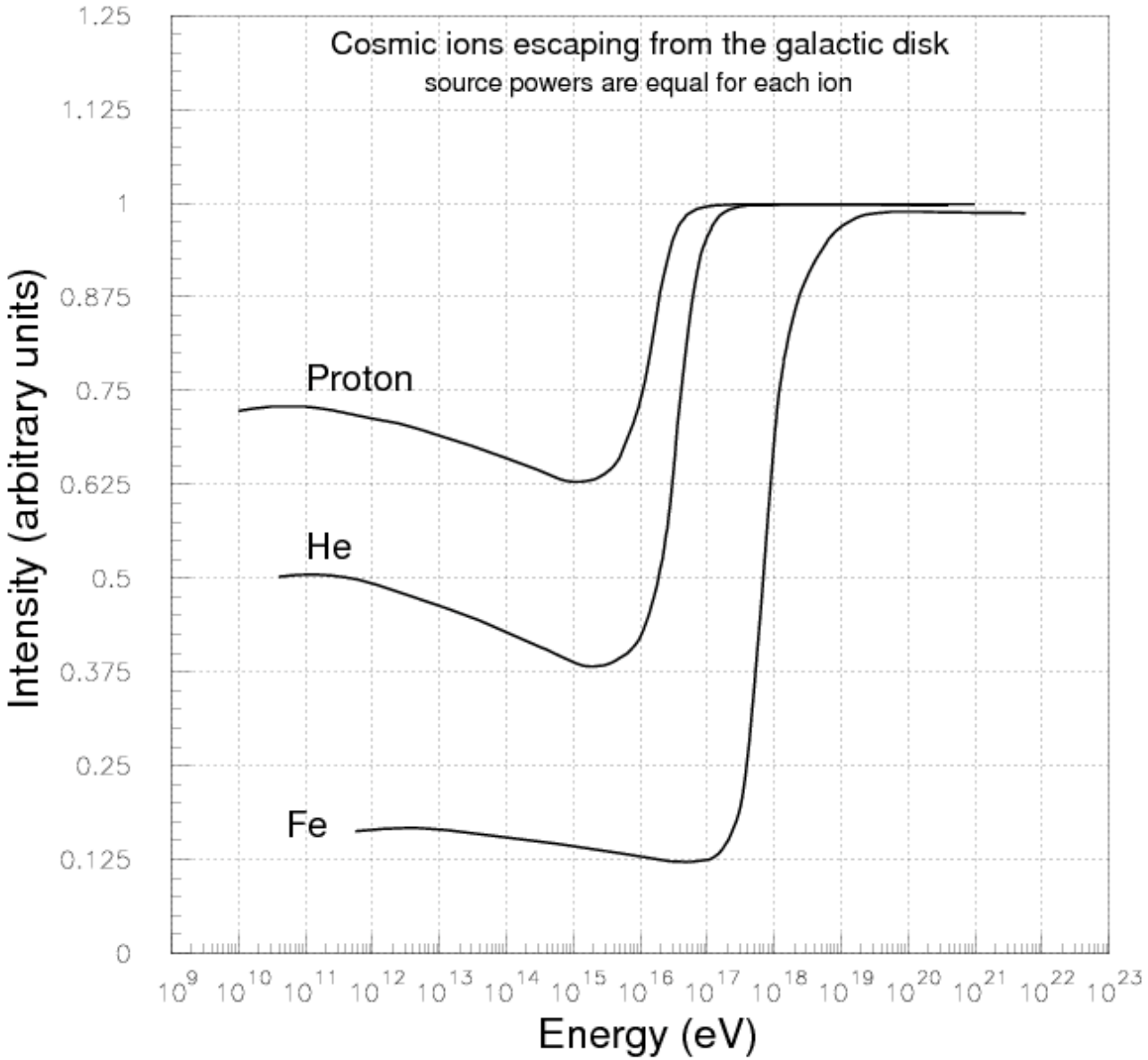
Cosmic ions escaping from the galactic disk
source powers are equal for each ion
Proton
He
Fe
Intensity (arbitrary units)
Energy (eV)
1.25
1.125
1
0.875
0.75
0.625
0.5
0.375
0.25
0.125
0
10^{9} 10^{10} 10^{11} 10^{12} 10^{13} 10^{14} 10^{15} 10^{16} 10^{17} 10^{18} 10^{19} 10^{20} 10^{21} 10^{22} 10^{23}

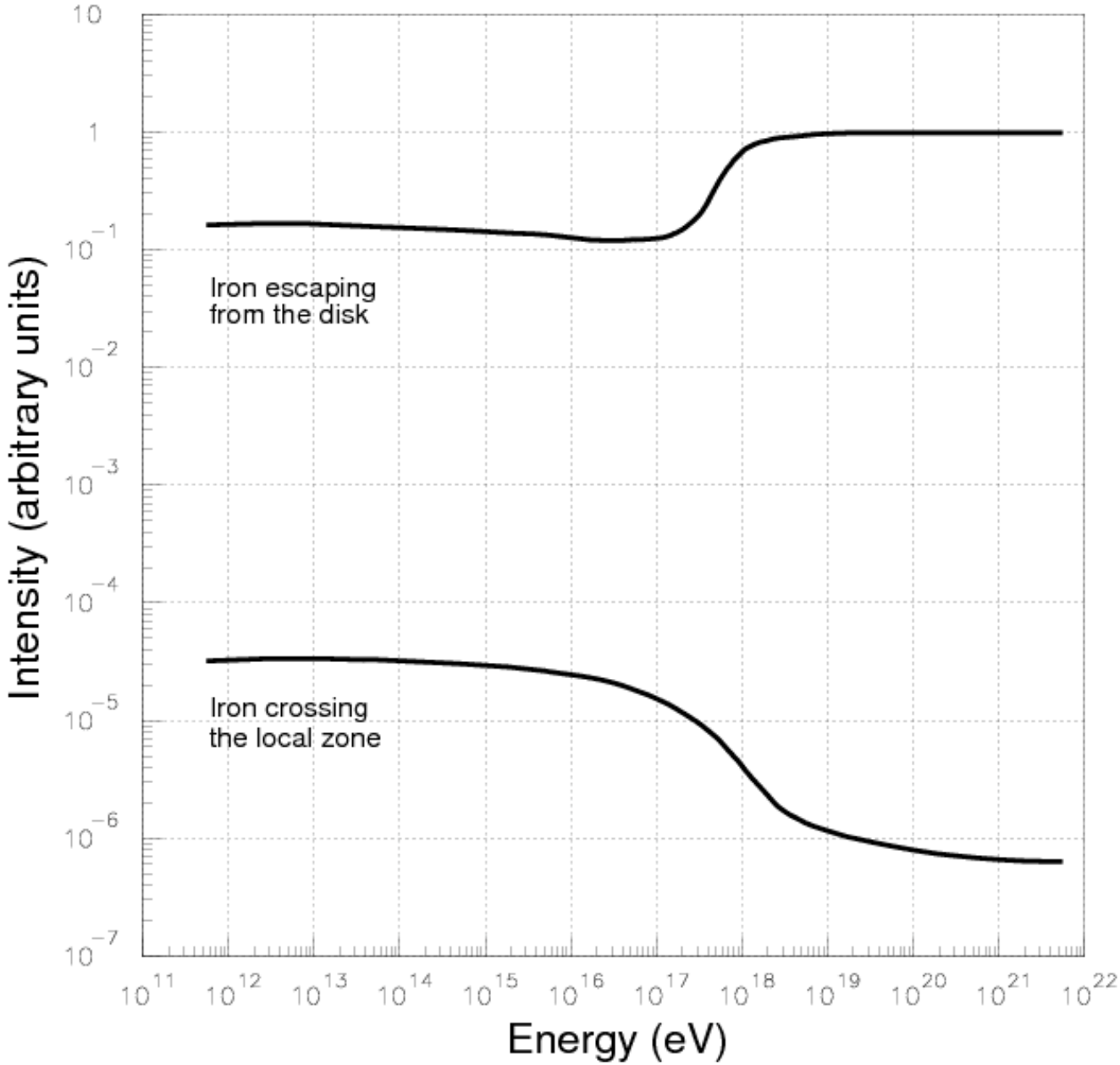
Intensity (arbitrary units)
10
1
10^{-1}
10^{-2}
10^{-3}
10^{-4}
10^{-5}
10^{-6}
10^{-7}
Iron escaping
from the disk
Iron crossing
the local zone
10^{11} 10^{12} 10^{13} 10^{14} 10^{15} 10^{16} 10^{17} 10^{18} 10^{19} 10^{20} 10^{21} 10^{22}
Energy (eV)

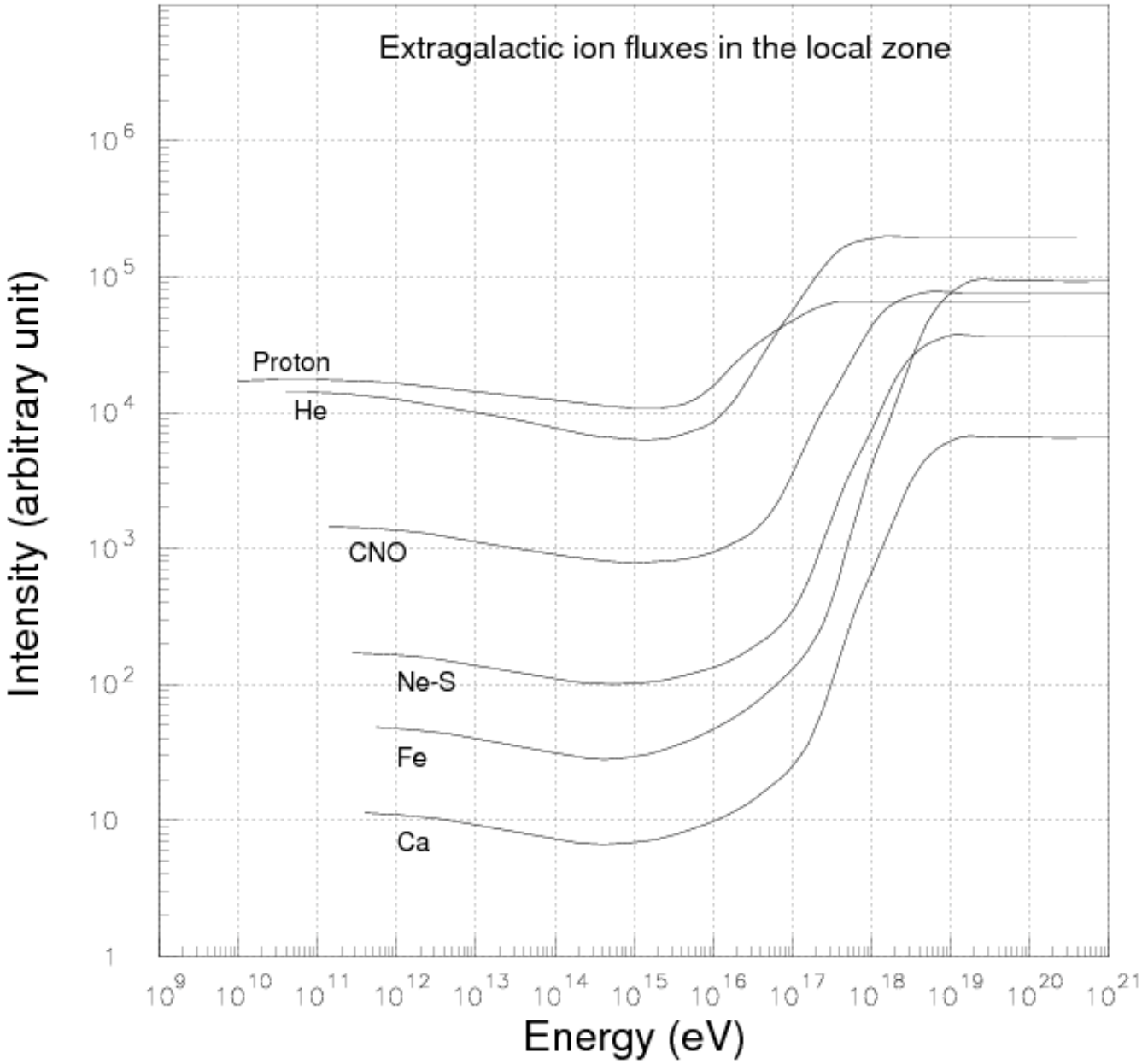
Extragalactic ion fluxes in the local zone
Intensity (arbitrary unit)
Energy (eV)
Proton
He
CNO
Ne-S
Fe
Ca
10^6
10^5
10^4
10^3
10^2
10
1
10^9
10^{10}
10^{11}
10^{12}
10^{13}
10^{14}
10^{15}
10^{16}
10^{17}
10^{18}
10^{19}
10^{20}
10^{21}

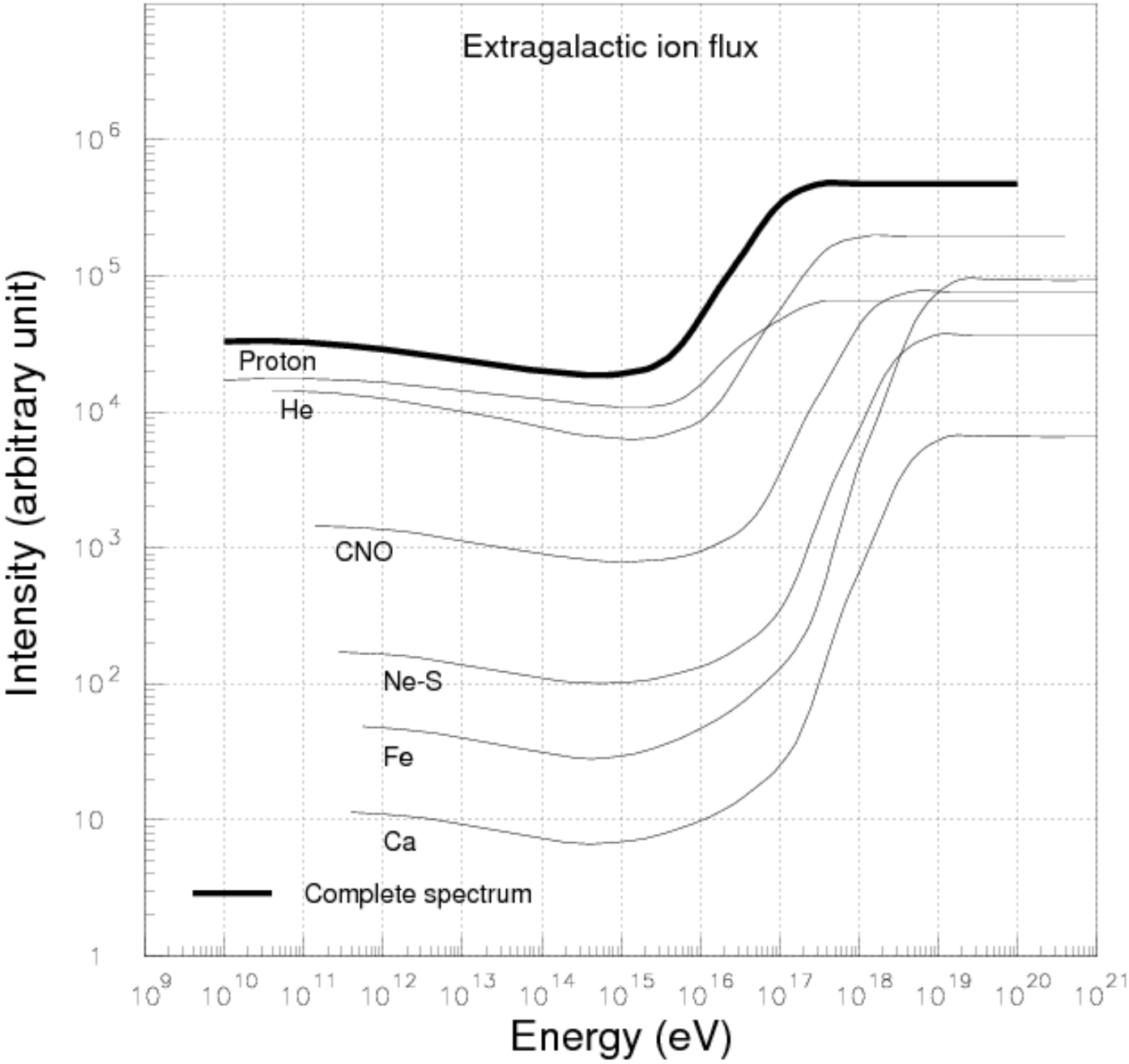
Extragalactic ion flux
Intensity (arbitrary unit)
10^6
10^5
10^4
10^3
10^2
10
1
Proton
He
CNO
Ne-S
Fe
Ca
Complete spectrum
10^9 10^{10} 10^{11} 10^{12} 10^{13} 10^{14} 10^{15} 10^{16} 10^{17} 10^{18} 10^{19} 10^{20} 10^{21}
Energy (eV)

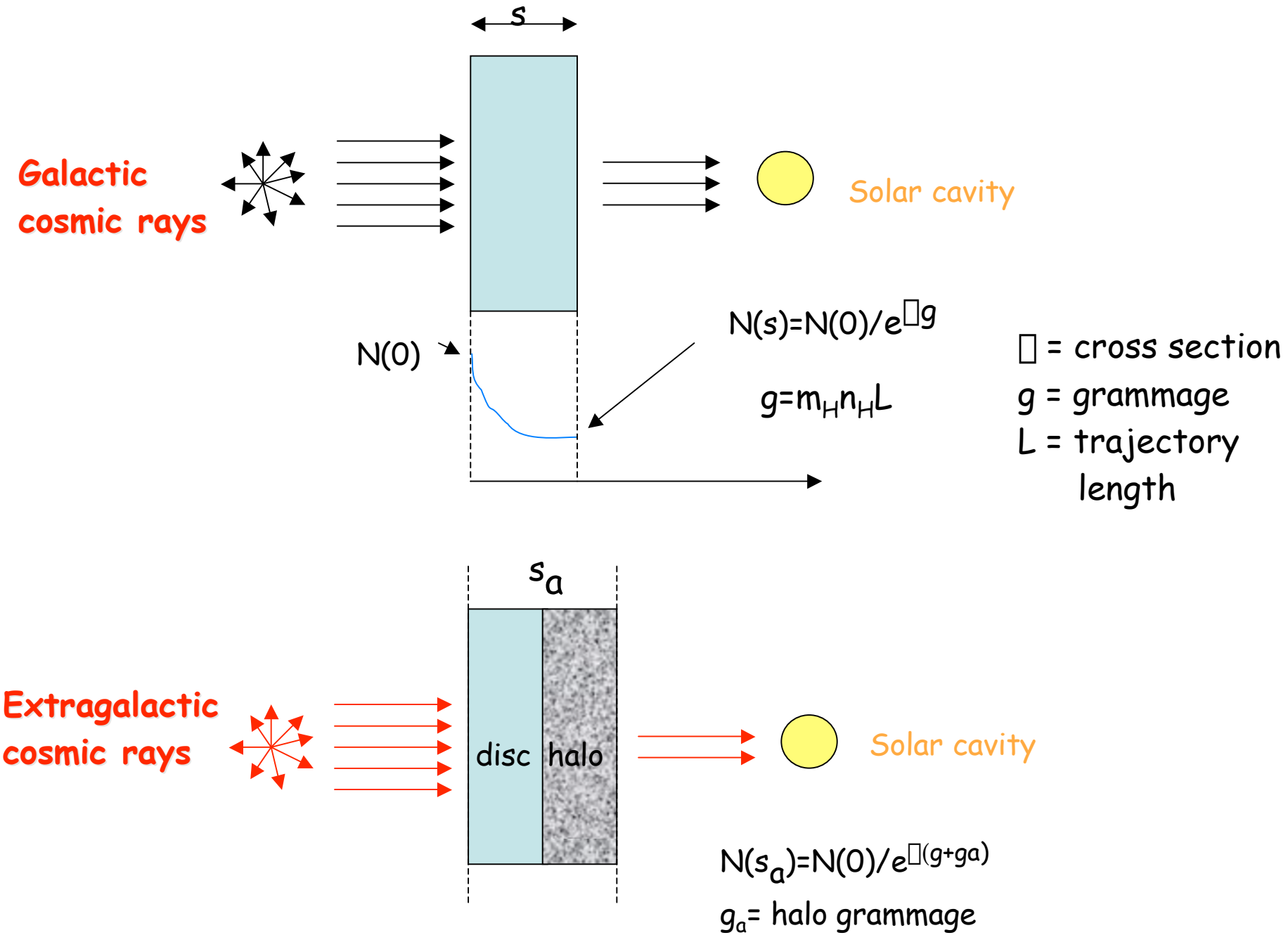
s
Galactic
cosmic rays
Solar cavity
N(0)
N(s)=N(0)/e^σg
g=m_H n_H L
σ = cross section
g = grammage
L = trajectory
length
s_a
Extragalactic
cosmic rays
disc
halo
Solar cavity
N(s_a)=N(0)/e^σ(g+g_a)
g_a= halo grammage

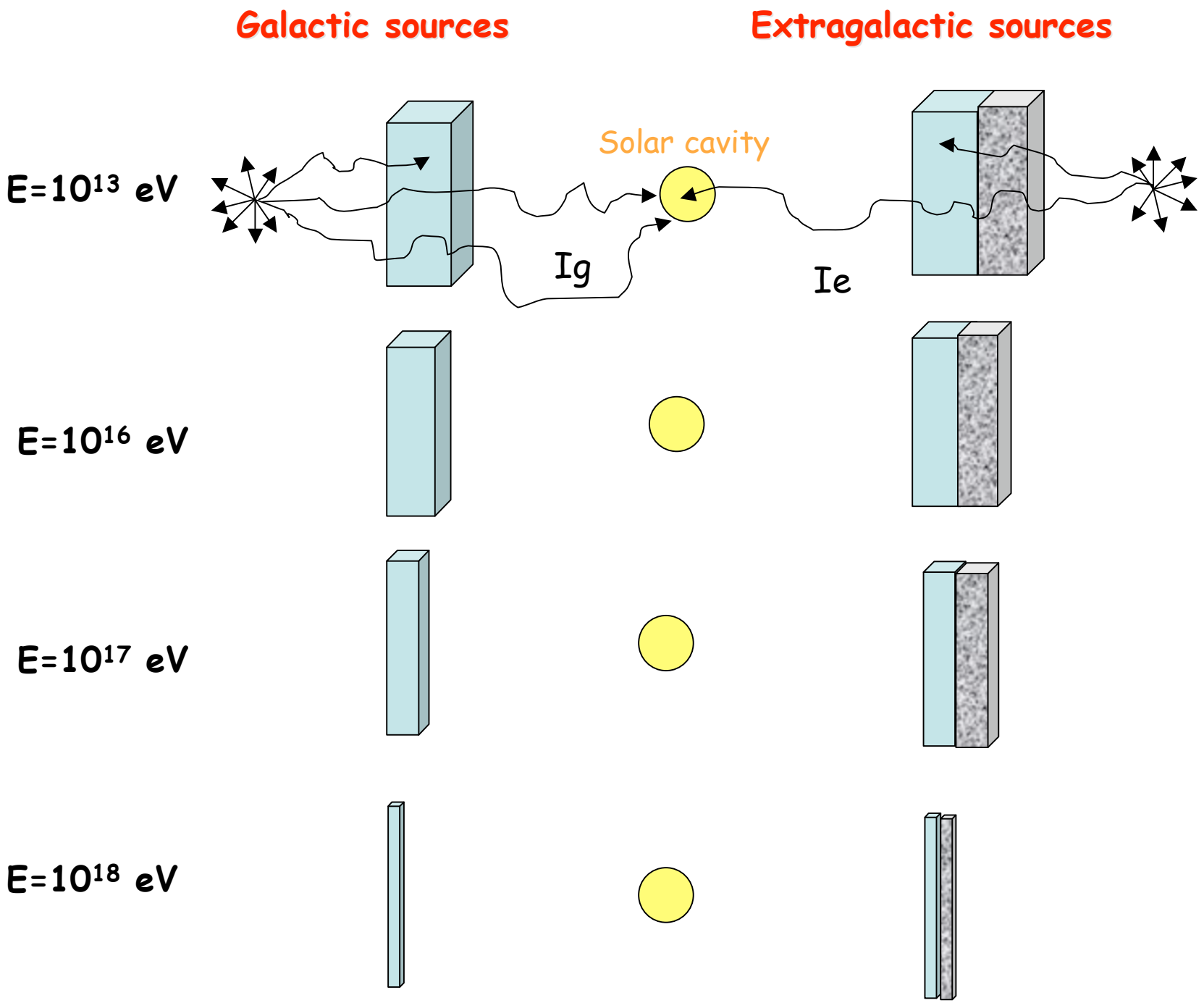
Galactic sources
Extragalactic sources
Solar cavity
E=10¹³ eV
Ig
Ie
E=10¹⁶ eV
E=10¹⁷ eV
E=10¹⁸ eV

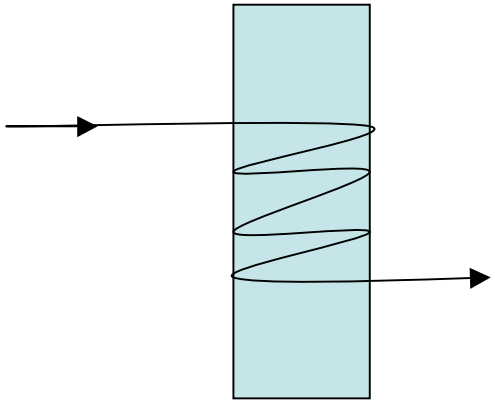

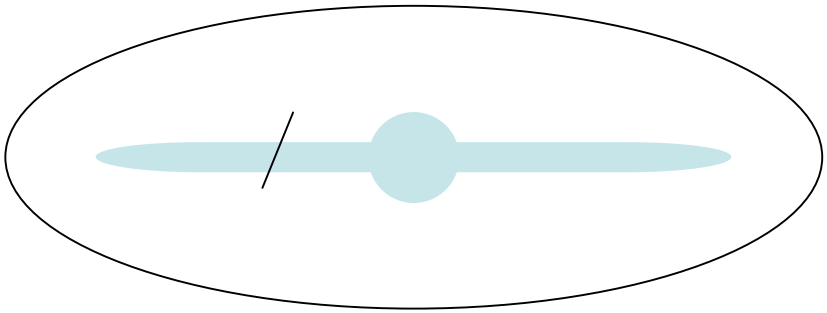

g grammage g/cm^2

Gas column swept out
by the cosmic ray

$g=m_H n_H v_d s_d$

v_d number of inversions of motion in the disk
s_d equivalent thikness in the disk
(mean distance source-observer)

The same variables are used in the halo :

$g_a=m_H n_H v_a s_a$

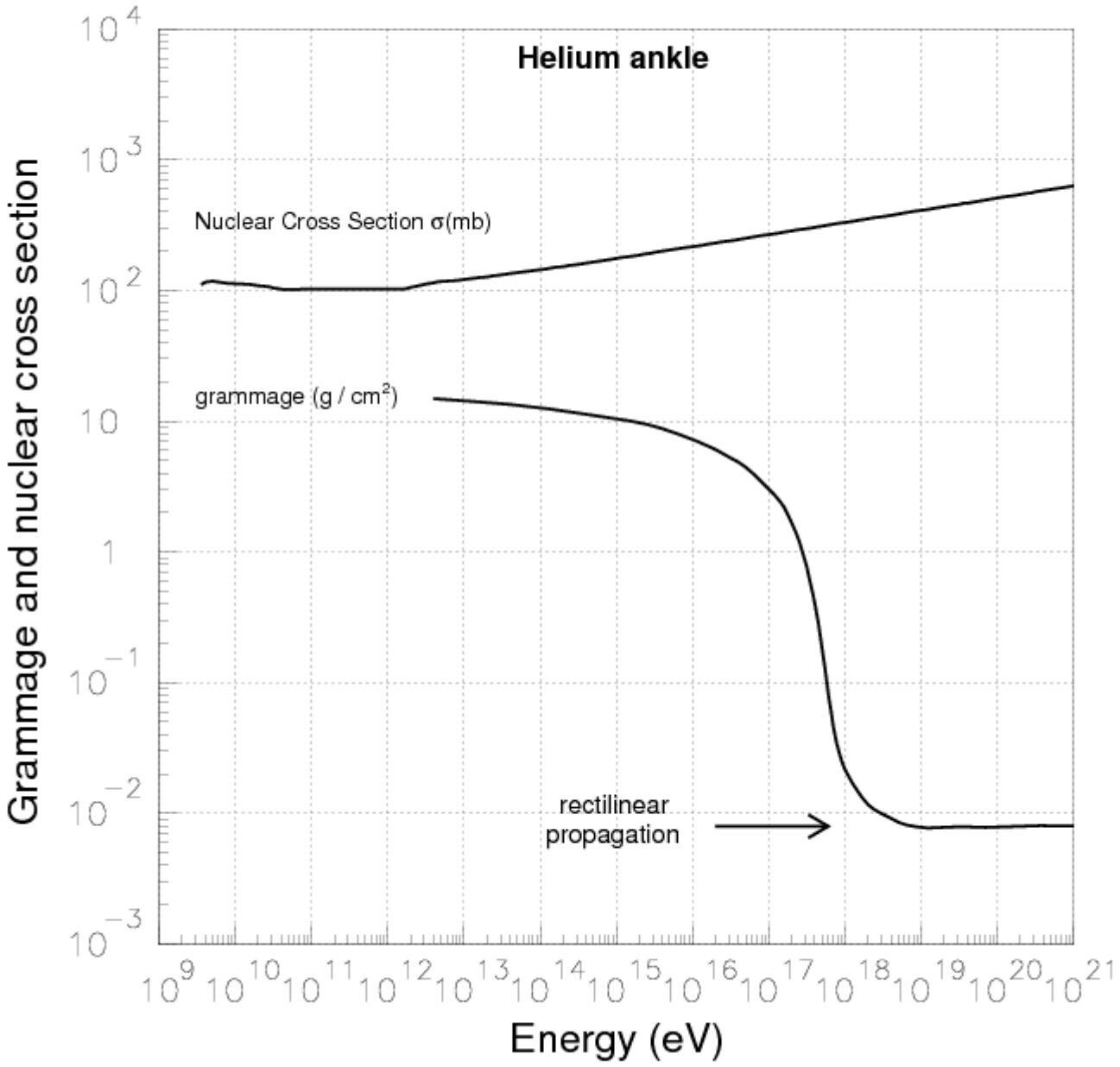
Helium ankle
Nuclear Cross Section σ(mb)
grammage (g / cm²)
rectilinear
propagation
Grammage and nuclear cross section
Energy (eV)
10⁴
10³
10²
10
1
10⁻¹
10⁻²
10⁻³
10⁹ 10¹⁰ 10¹¹ 10¹² 10¹³ 10¹⁴ 10¹⁵ 10¹⁶ 10¹⁷ 10¹⁸ 10¹⁹ 10²⁰ 10²¹

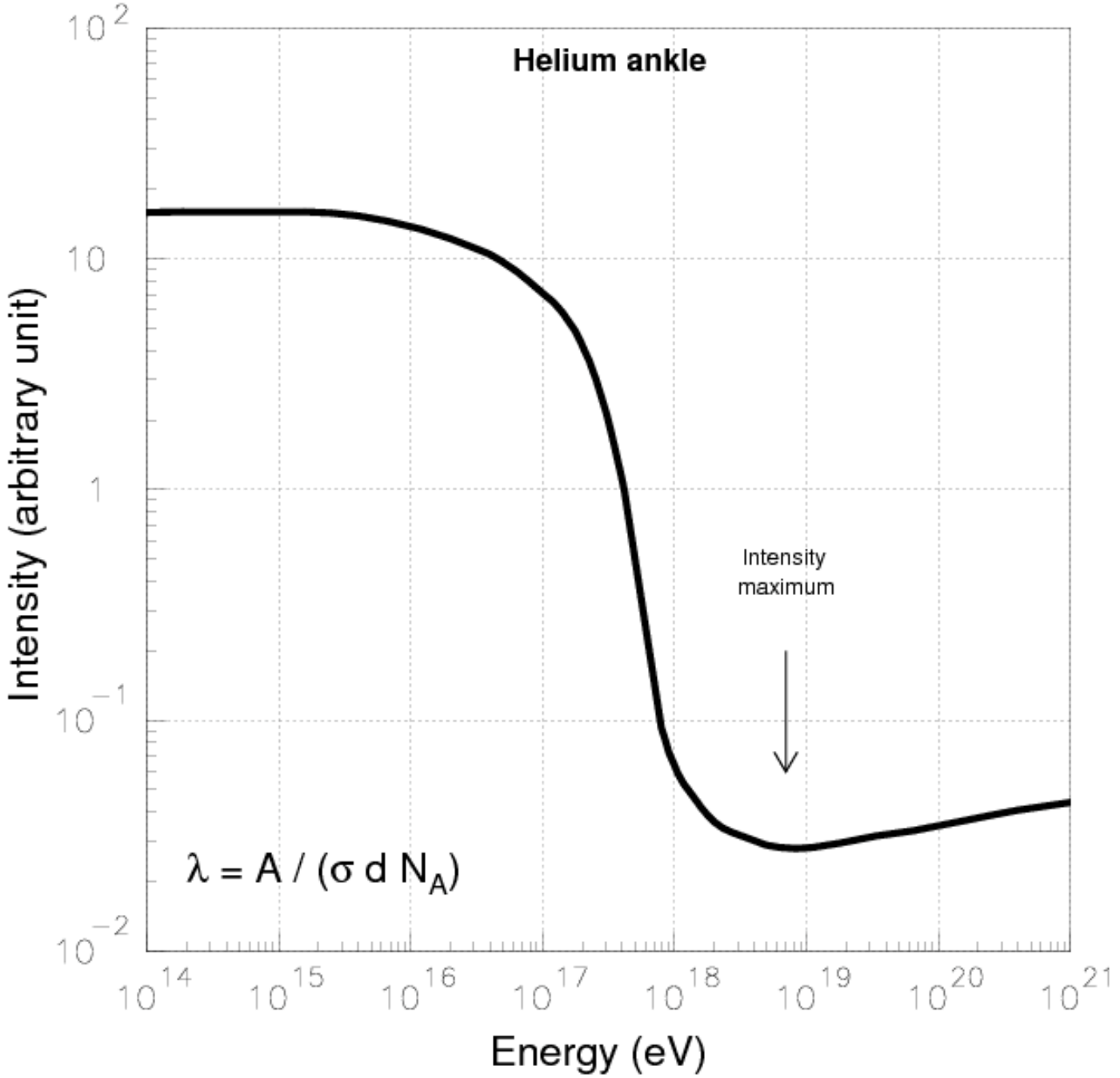
Helium ankle
Intensity (arbitrary unit)
10^2
10
1
10^{-1}
10^{-2}
Intensity
maximum
$\lambda = A / (\sigma d N_A)$
10^{14}
10^{15}
10^{16}
10^{17}
10^{18}
10^{19}
10^{20}
10^{21}
Energy (eV)

Rectilinear propagation

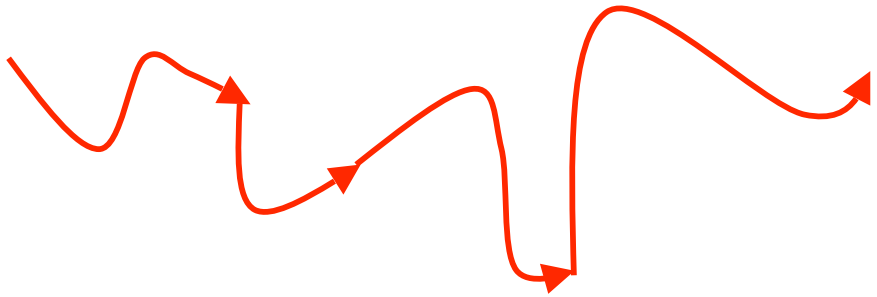

Cosmic rays, in the rectilinear propagation, penetrate the insterstellar medium in straight line segments.

The energy at which the rectilinear propagation sets on is an unmistakeable, clear reference for the ankle generation, because the average field strength in the disk is known.

For Helium this energy is 4×10^{18} eV and for Iron 3×10^{19} eV .

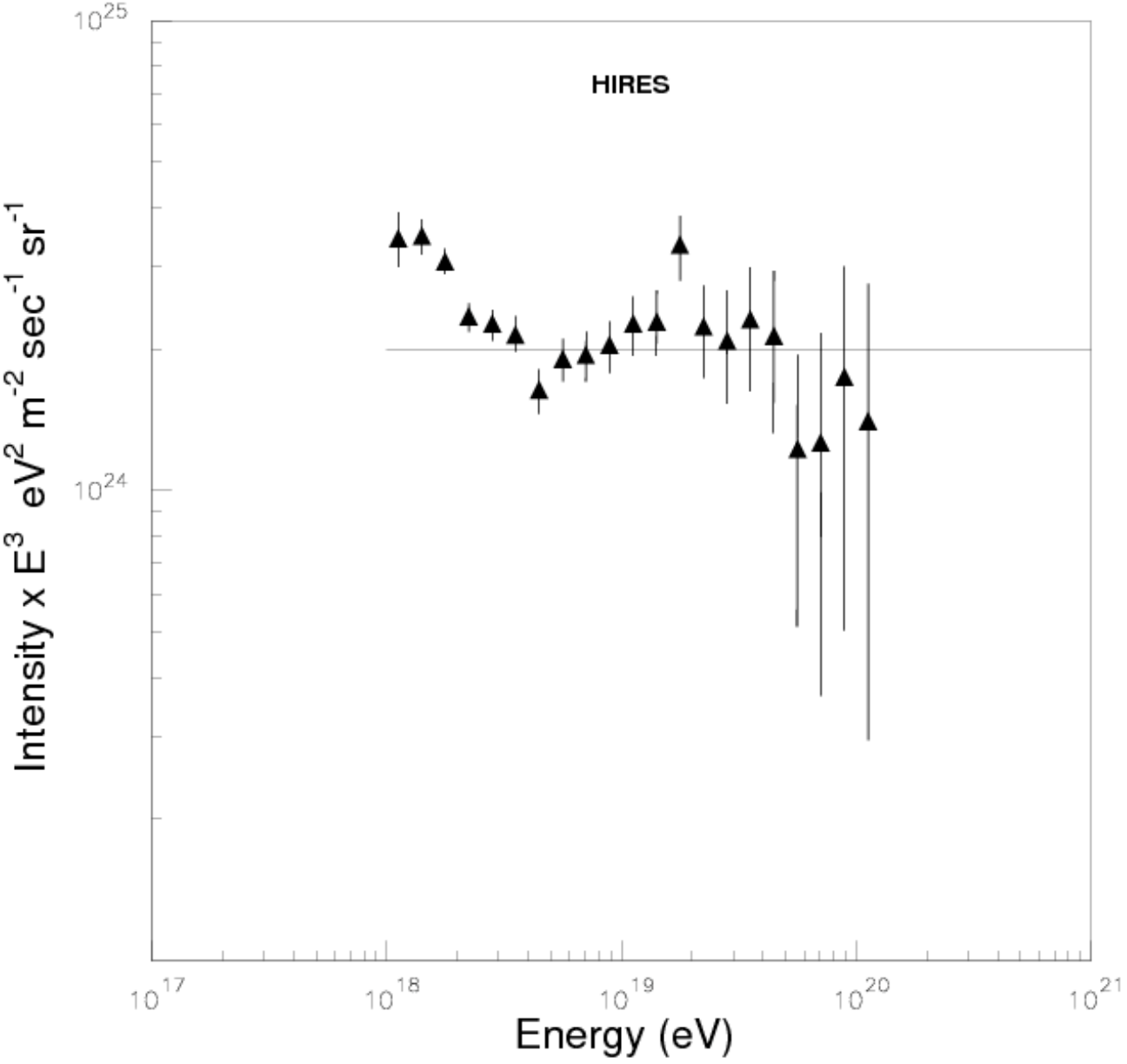
HIRES
10^{25}
10^{24}
Intensity x E^3 eV^2 m^{-2} sec^{-1} sr^{-1}
10^{17}
10^{18}
10^{19}
10^{20}
10^{21}
Energy (eV)

Silent assumptions of this study

The spectral indices of single cosmic rays measured by the experiments below 10^{15} eV and ion abundances as well, are the major inputs in the evaluation of the energy spectra above 10^{15} eV.

The values of the spectral indices used in the calculation of the ion spectra are constant from a few GeV up to 10^{21} eV (i.e. no ad hoc adjustement, no arbitrariness).

No distinction is made between spectral indices of the sources and those observed at Earth.

Conclusions (1)

The computed spectra of individual ions (Protons, Helium and Iron) are in good agreement with the experimental data (only the shapes of the spectra) of the Kaskade experiment.

Regardless of the particular ion blend, the computed position along the energy axis of the knee of the all-particle spectrum also matches the results of the experiments.

With the above inputs the all-particle energy spectrum between the knee and the ankle is calculated showing a spectral index of 3.05 for a proton abundant blend and 3.06 for an helium abundant blend i.e the spectral index is close to the observed value of 3 in the range 10^{15} and 10^{17} eV.

This agreement is particularly meaningful since the energy spectra of individual ions have slopes of 3.38 (Helium) and 3.34 (Fe) in the same energy range. The computed indices of 3.05 and 3.06 between 10^{15}-10^{17} eV are the result of the sum of all the ion spectra as indicated in the figure.

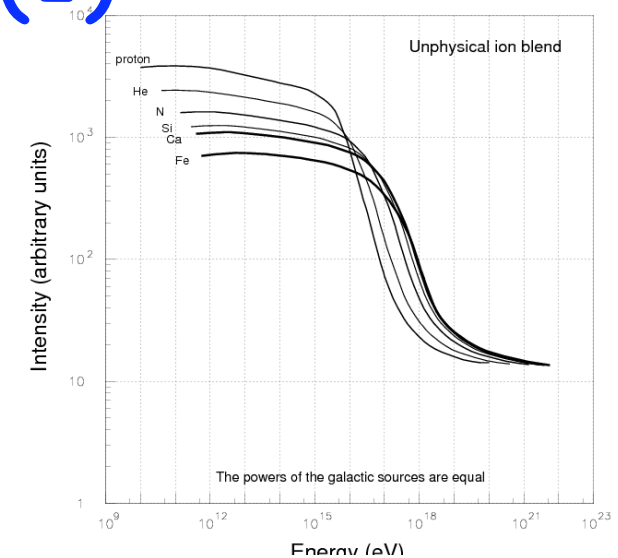

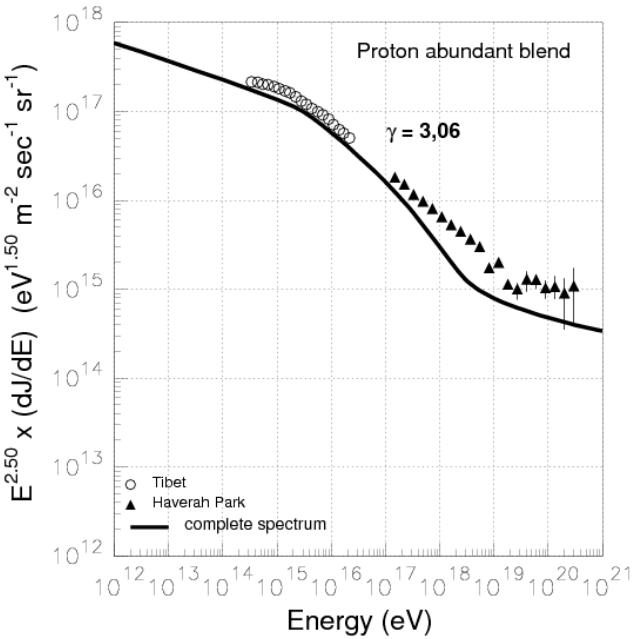

Conclusions (2)

Assuming the existence of an extragalactic component in the intergalactic space surrounding the Milky Way, it is interesting to determine its intensity at Earth.

This extragalactic component might be conceived in a variety of forms like :

(a) Debris from normal galaxies in the cosmic vicinity (e.g. 40 Mpc)
(b) Debris from powerful galaxies
(c) Reentrant particles overflowed from the Milky Way
(d) Cosmic ray populations re-accelerated in the intergalactic space.

Whatever may be the ion abundances populating the intergalactic space (within the plausible limits bound to the experimental data at Earth), there exists a unique point along the energy axis where the extragactic component must have a maximum of intensity. This characteristic is almost independent from the ion blend and the spectral indices of individual ions.

This unique energy point is of capital importance because its position, along the energy axis, is determined only by a physical phenomena

Conclusions (3)

The positions of the ankles and the knees along the energy axis are distinctively and uniquely interconnected by the average field strength which forges the grammage, and by the rate at which inelastic cross sections rise with energy, as shown in the plot aside.

This fundamental conclusion corroborate the explanation

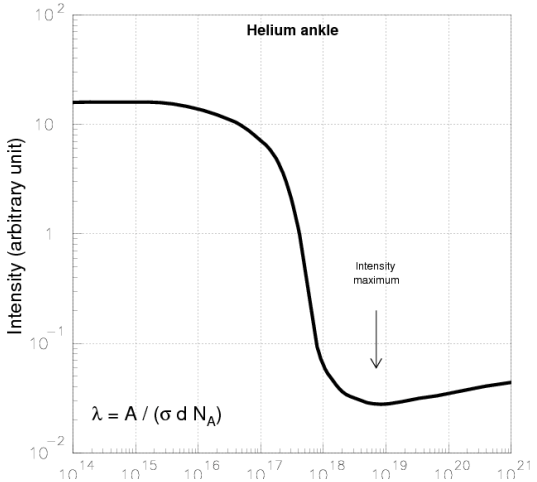

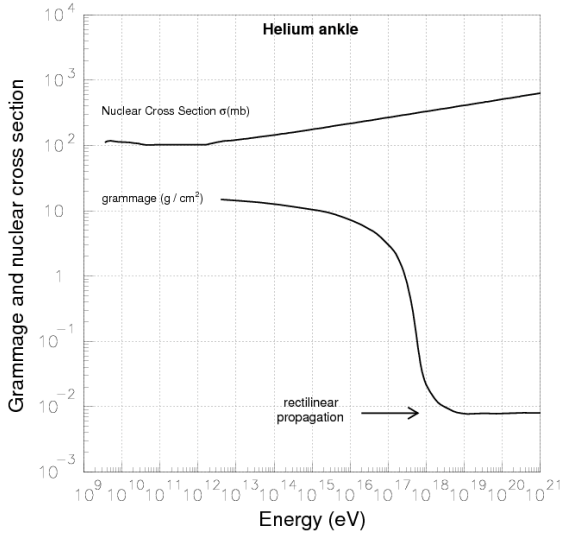

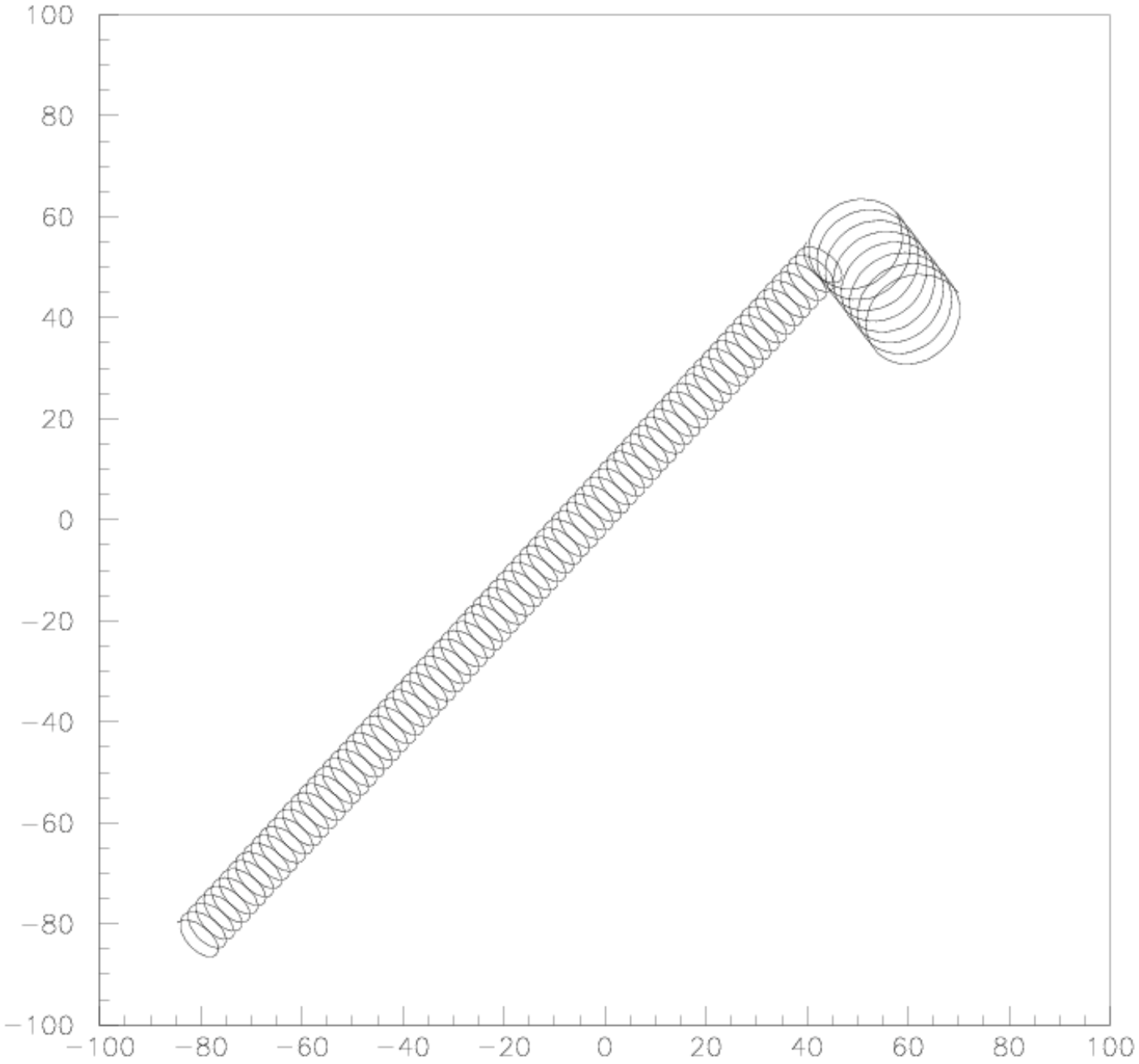
100
80
60
40
20
0
−20
−40
−60
−80
−100
−100
−80
−60
−40
−20
0
20
40
60
80
100

Conclusions (3)

The intensity of cosmic ions generated in the disk obeys to a constant spectral index as This fall of intensity cannot continue indefinitely with increasing energy.

The rate of nuclear collisions is determined by inelastic cross sections and by the grammage experienced by the cosmic rays.

At a particular distinctive energy, cosmic ions traverse the Galaxy in straight line segments. This particular energy is determined by the field strenght in the disk and only by the magnetic field.

This energy is 5×10^{18} eV for Helium and 6×10^{19} eV for Iron. For protons, it is expected to be lower than that of Helium.

For galactic cosmic ions beyond the ankle region, the spectral index should reverse to the same value before the knee energy region.

For the extragalactic cosmic rays, a maximum of intensity is an enhancement of

The positions of the ankles and the knees along the energy axis are uniquely

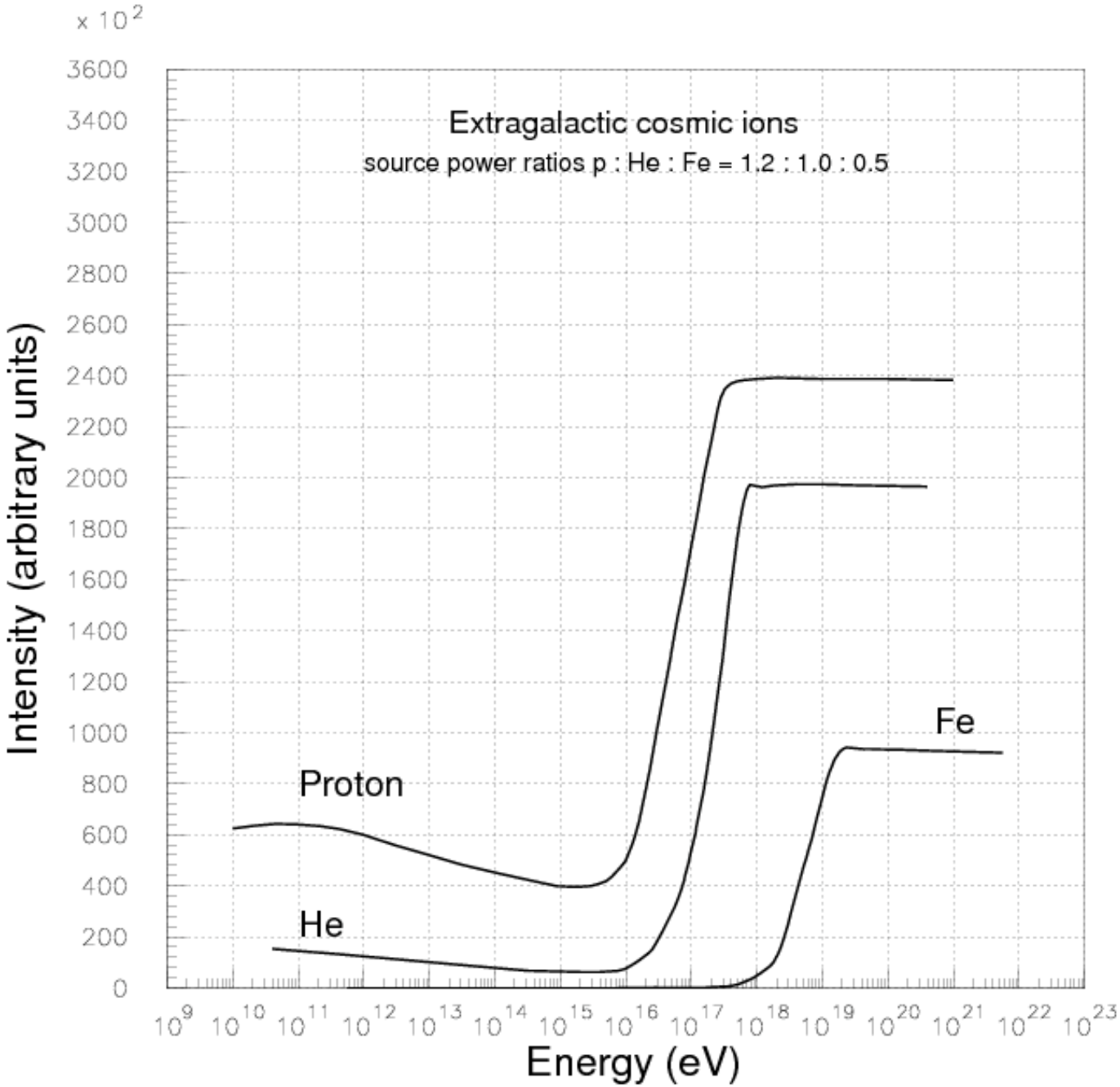
x 10^2
3600
3400
3200
3000
2800
2600
2400
2200
2000
1800
1600
1400
1200
1000
800
600
400
200
0
Intensity (arbitrary units)
Extragalactic cosmic ions
source power ratios p : He : Fe = 1.2 : 1.0 : 0.5
Proton
He
Fe
10^9 10^10 10^11 10^12 10^13 10^14 10^15 10^16 10^17 10^18 10^19 10^20 10^21 10^22 10^23
Energy (eV)

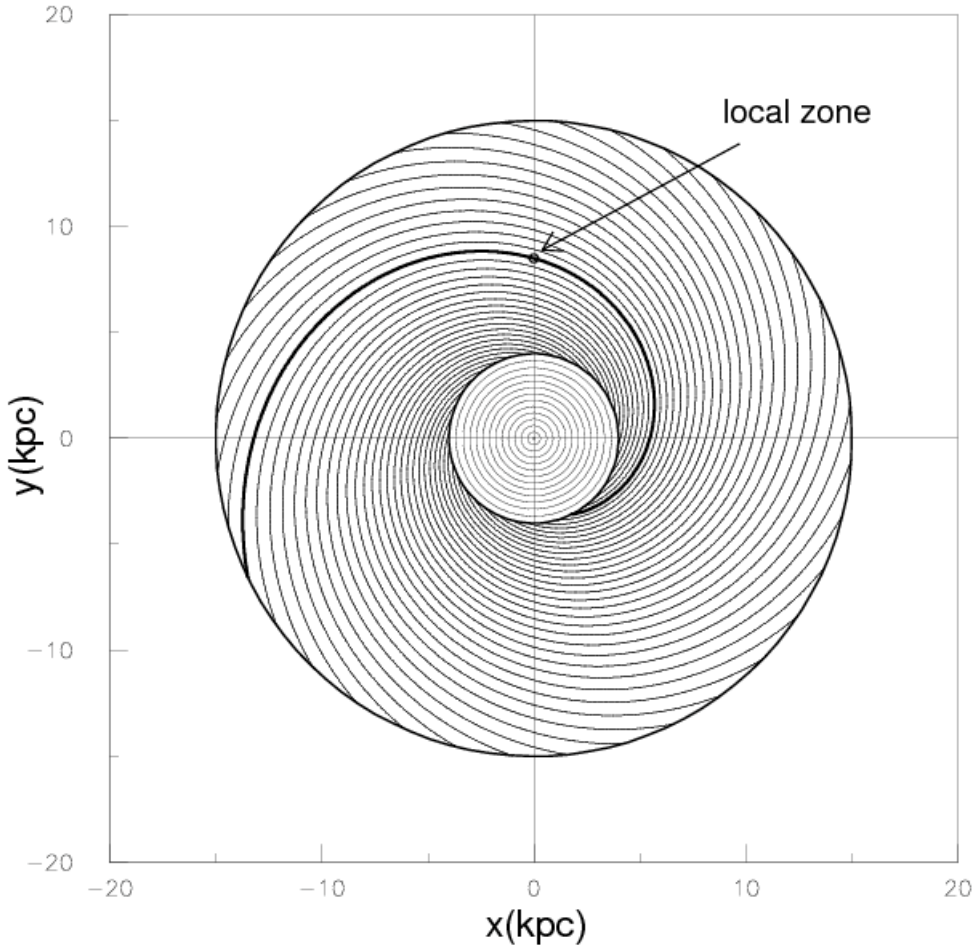
local zone
20
10
0
−10
−20
y(kpc)
−20
−10
0
10
20
x(kpc)

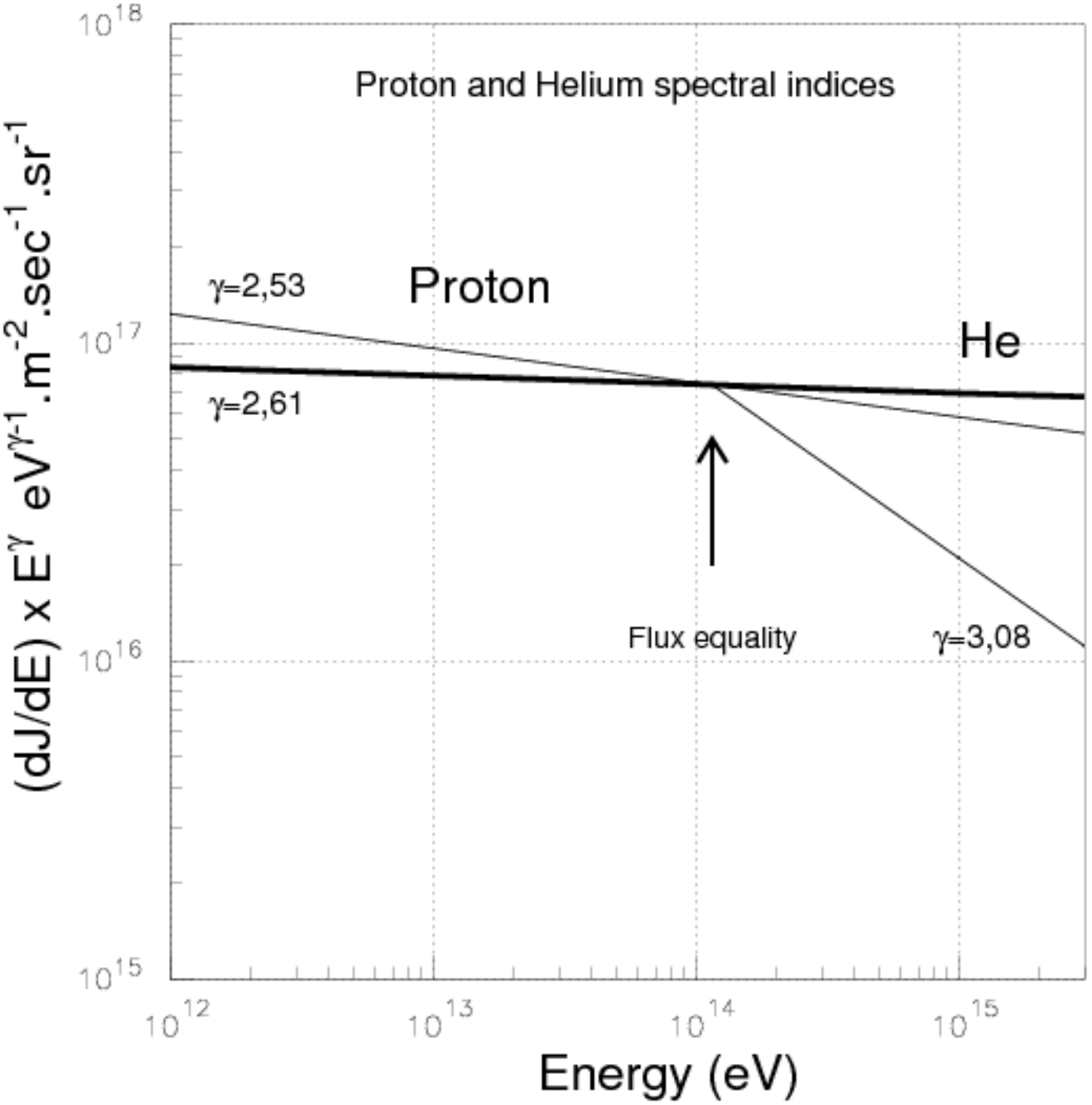
Proton and Helium spectral indices
Proton
He
γ=2,53
γ=2,61
γ=3,08
Flux equality
(dJ/dE) x E^γ eV^γ-1.m^-2.sec^-1.sr^-1
Energy (eV)
10^18
10^17
10^16
10^15
10^12
10^13
10^14
10^15

Contour levels for helium, carbon, aluminium and iron illustrating the distribution of cosmic ray sources feeding the local galactic zone

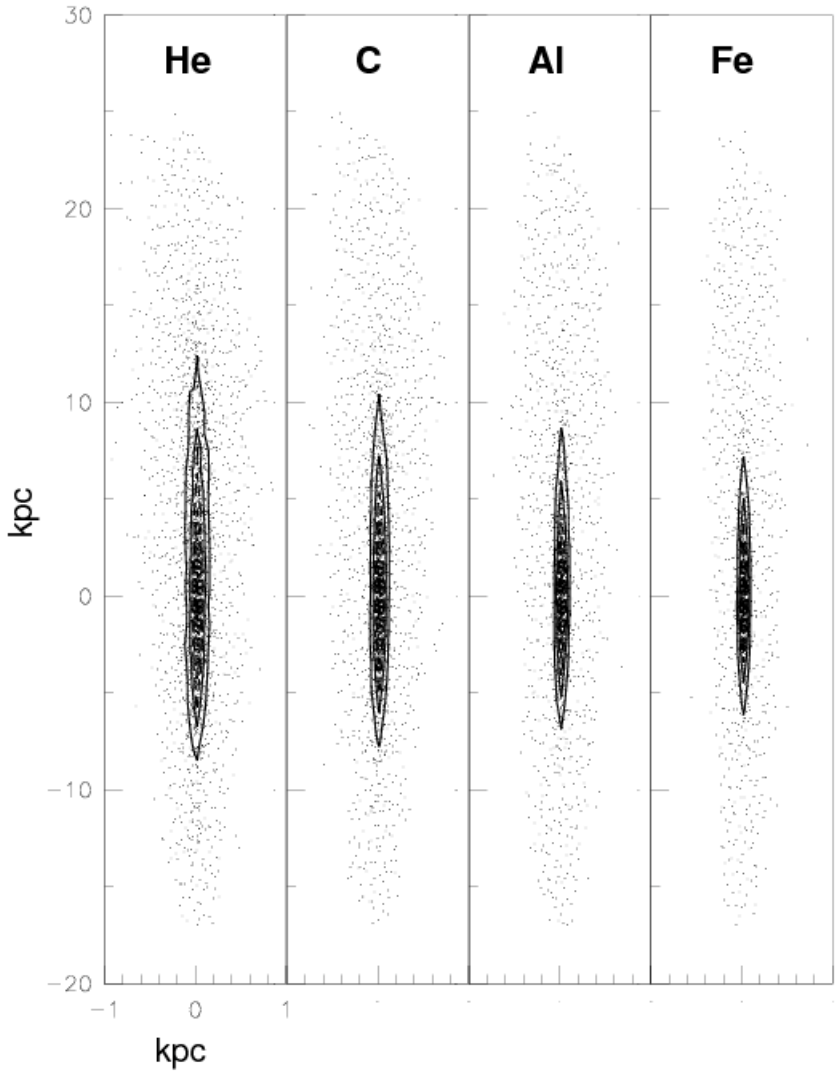

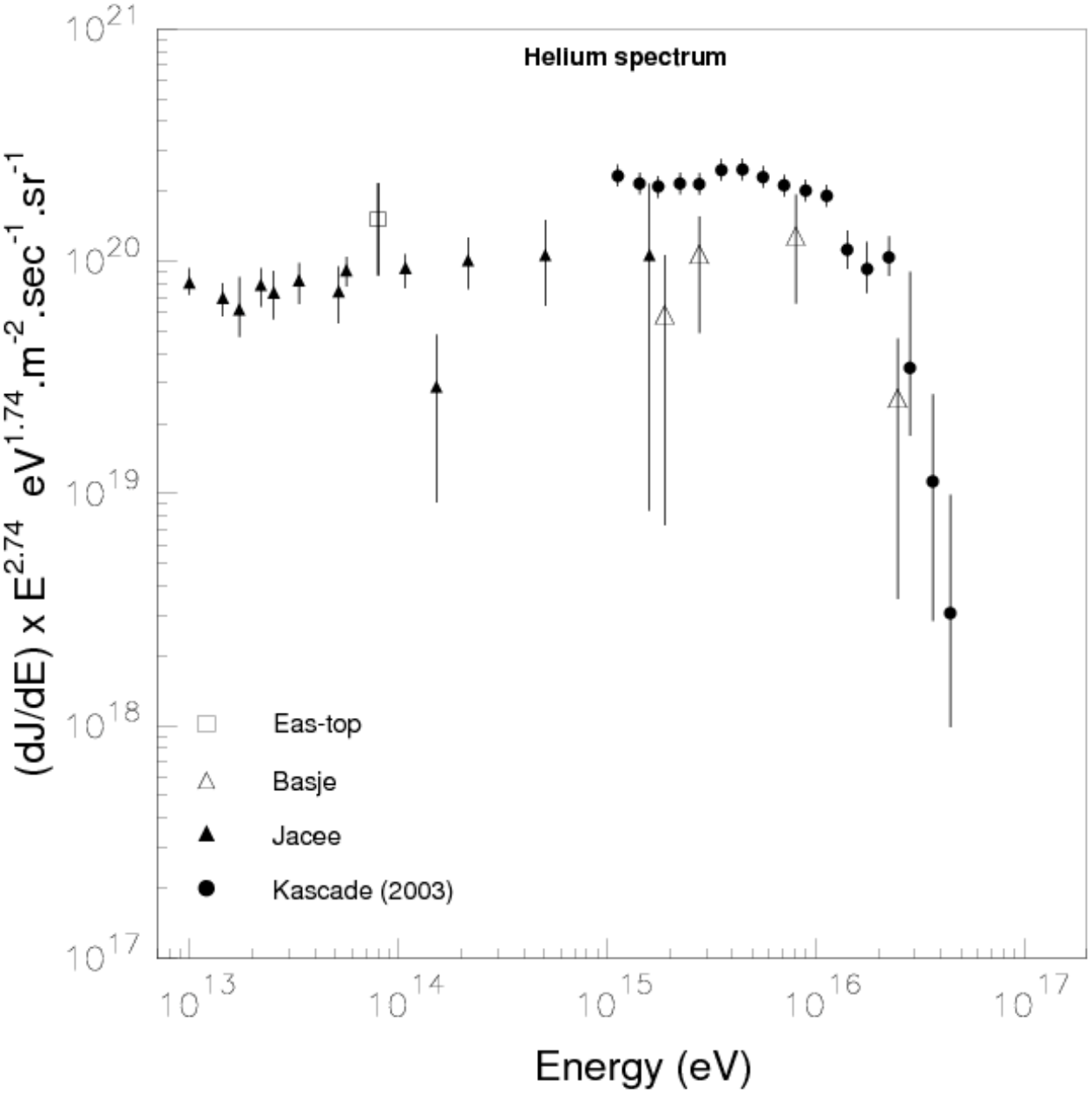
Helium spectrum
(dJ/dE) x E^2.74 eV^1.74.m^-2.sec^-1.sr^-1
10^21
10^20
10^19
10^18
10^17
10^13
10^14
10^15
10^16
10^17
Energy (eV)
Eas-top
Basje
Jacee
Kascade (2003)

La componente extragalattica

Cosmici in uscita

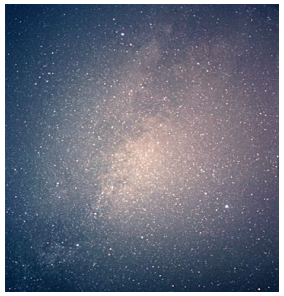

Cosmici in entrata alla Via Lattea

Ammettiamo per semplicità che esista una componente extragalattica della radiazione cosmica che raggiunga la zona locale. Quindi supponiamo che:

- le abbondanze relative degli ioni cosmici extragalattici siano le stesse dei raggi cosmici in uscita dalla Via Lattea

- la componente extragalattica in ingresso alla Via Lattea incontri la medesima struttura di campi magnetici e di materia interstellare intercettate dai raggi cosmici galattici.

The origin of the ankle

Antonio Codino

INFN and Dipartimento di Fisica
dell'Universita degli Studi di Perugia, Italy

Outline of the presentation

- Why there is a change of the spectral index from 2,74 to 3 in the energy region 10^{15}-10^{20} eV
- Summing up the energy spectra of individual ions in the energy interval 10^{15}-10^{20} eV
- Why there is a minimum in the cosmic ray intensity around 10^{19} eV
- Extragalactic cosmic rays and reentrant cosmic rays
- The origin of the ankle

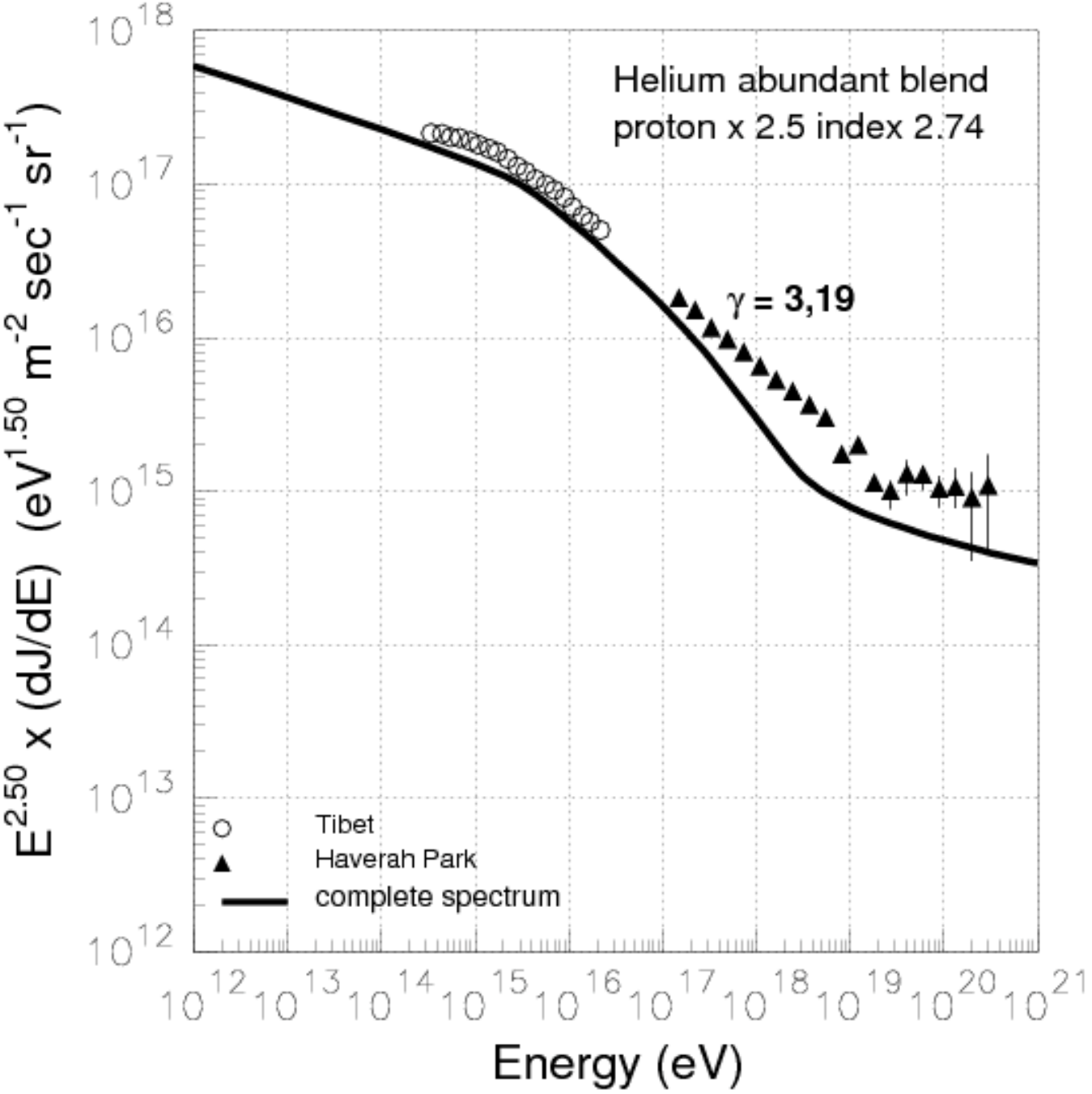
Helium abundant blend
proton x 2.5 index 2.74
γ = 3,19
Tibet
Haverah Park
complete spectrum
E^2.50 x (dJ/dE) (eV^1.50 m^-2 sec^-1 sr^-1)
Energy (eV)
10^18
10^17
10^16
10^15
10^14
10^13
10^12
10^12 10^13 10^14 10^15 10^16 10^17 10^18 10^19 10^20 10^21

A unique mechanism generating the knee and the ankle in the local galactic zone

Antonio Codino

INFN and Dipartimento di Fisica
dell'Universita degli Studi di Perugia, Italy

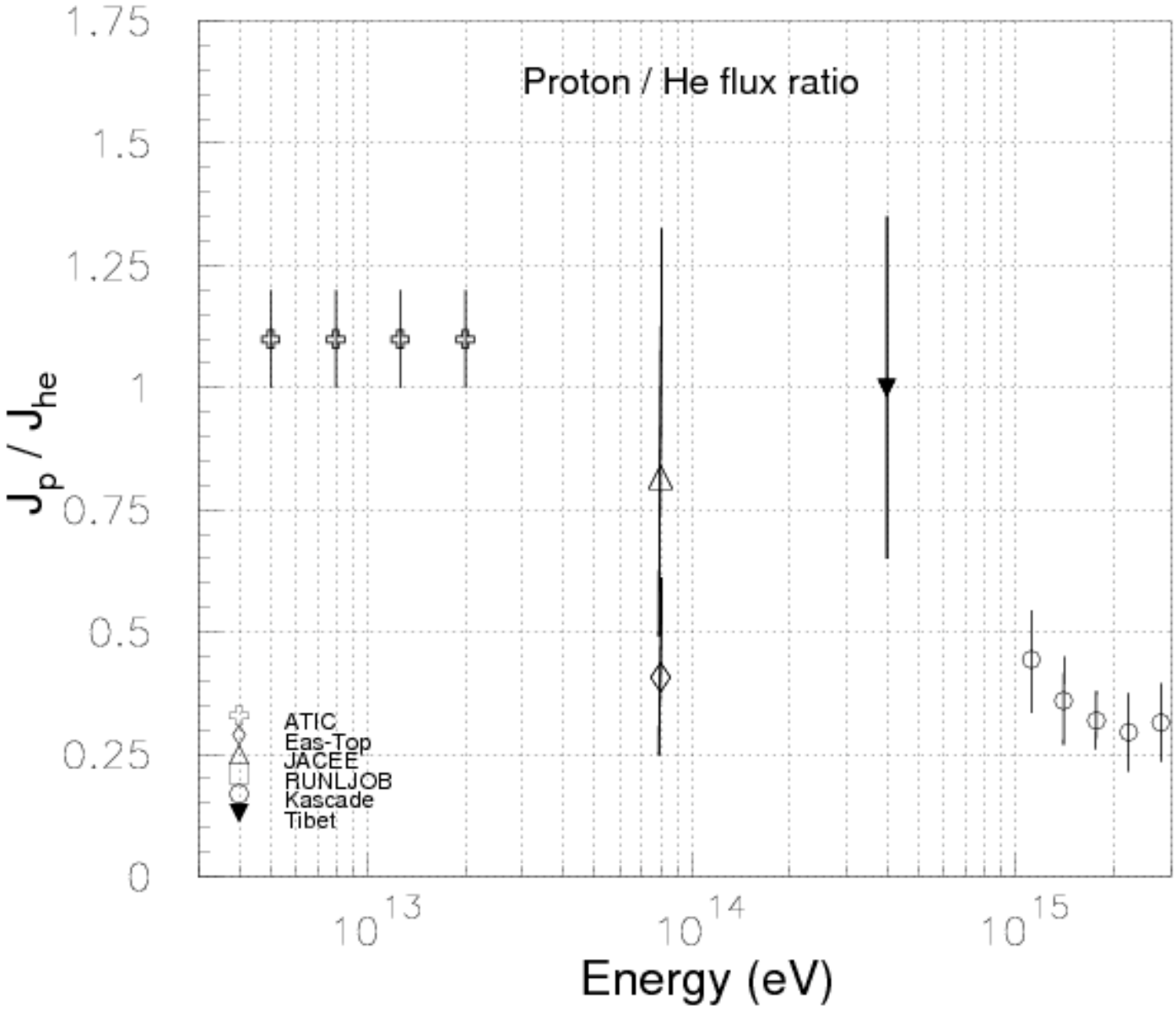
Proton / He flux ratio
J_p / J_{he}
1.75
1.5
1.25
1
0.75
0.5
0.25
0
ATIC
Eas-Top
JACEE
RUNLJOB
Kascade
Tibet
10^{13}
10^{14}
10^{15}
Energy (eV)

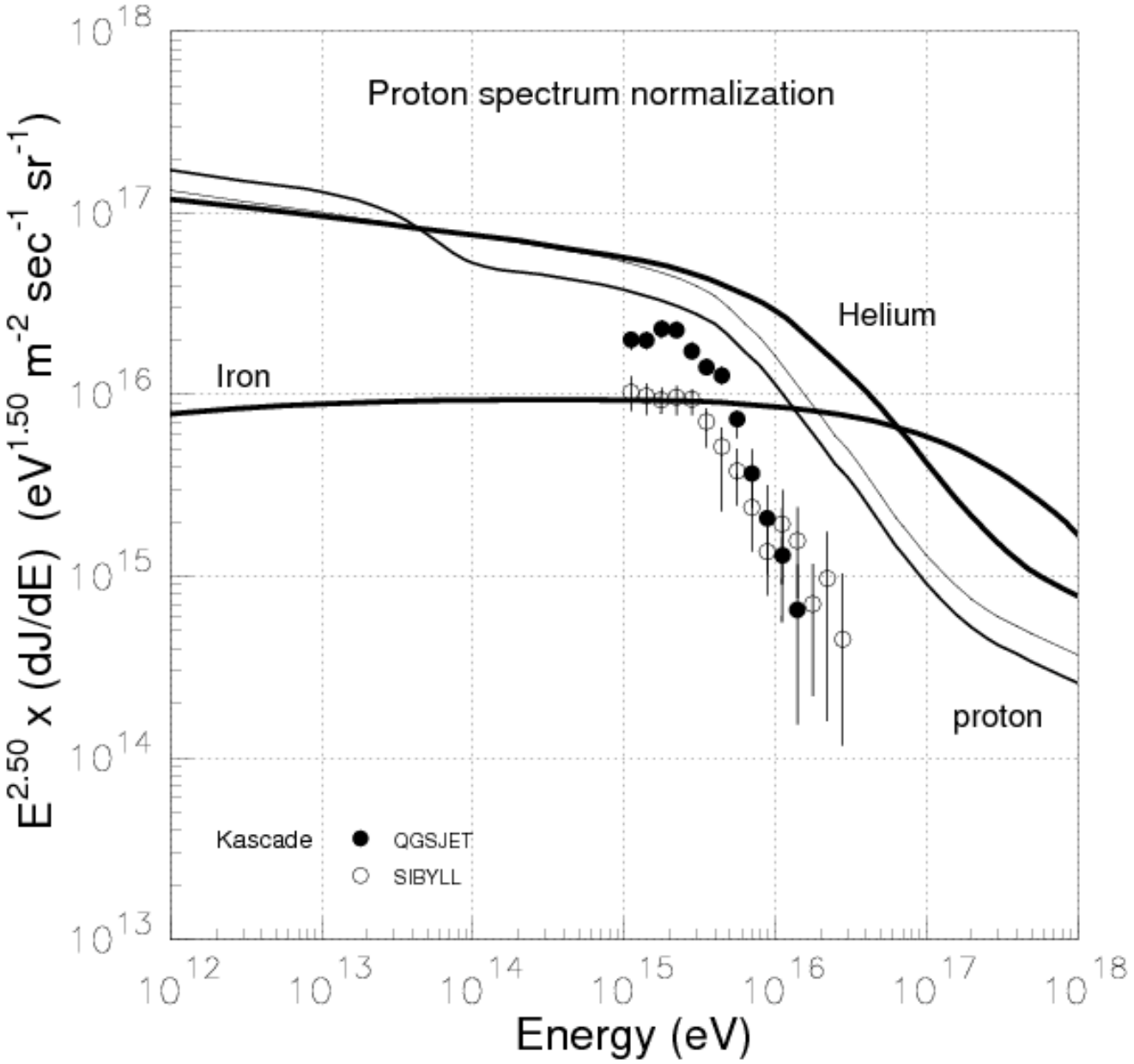
Proton spectrum normalization
Helium
Iron
proton
Kascade
QGSJET
SIBYLL
$E^{2.50}$ x (dJ/dE) ($eV^{1.50}$ m^{-2} sec^{-1} sr^{-1})
Energy (eV)
10^{18}
10^{17}
10^{16}
10^{15}
10^{14}
10^{13}
10^{12}
10^{13}
10^{14}
10^{15}
10^{16}
10^{17}
10^{18}

On the origin of the ankles

- Why the ankles of individual ions exist
- The positions of the ankles along the energy axis.
  - The slope of the cosmic ray spectrum between 10^{15} and $5\ 10^{18}$ eV and the the position of the ankle.

The bump in the complete spectrum, around $5\ 10^{19}$ eV.

- Evidence that the knee and ankle are produced by the same mechanism.

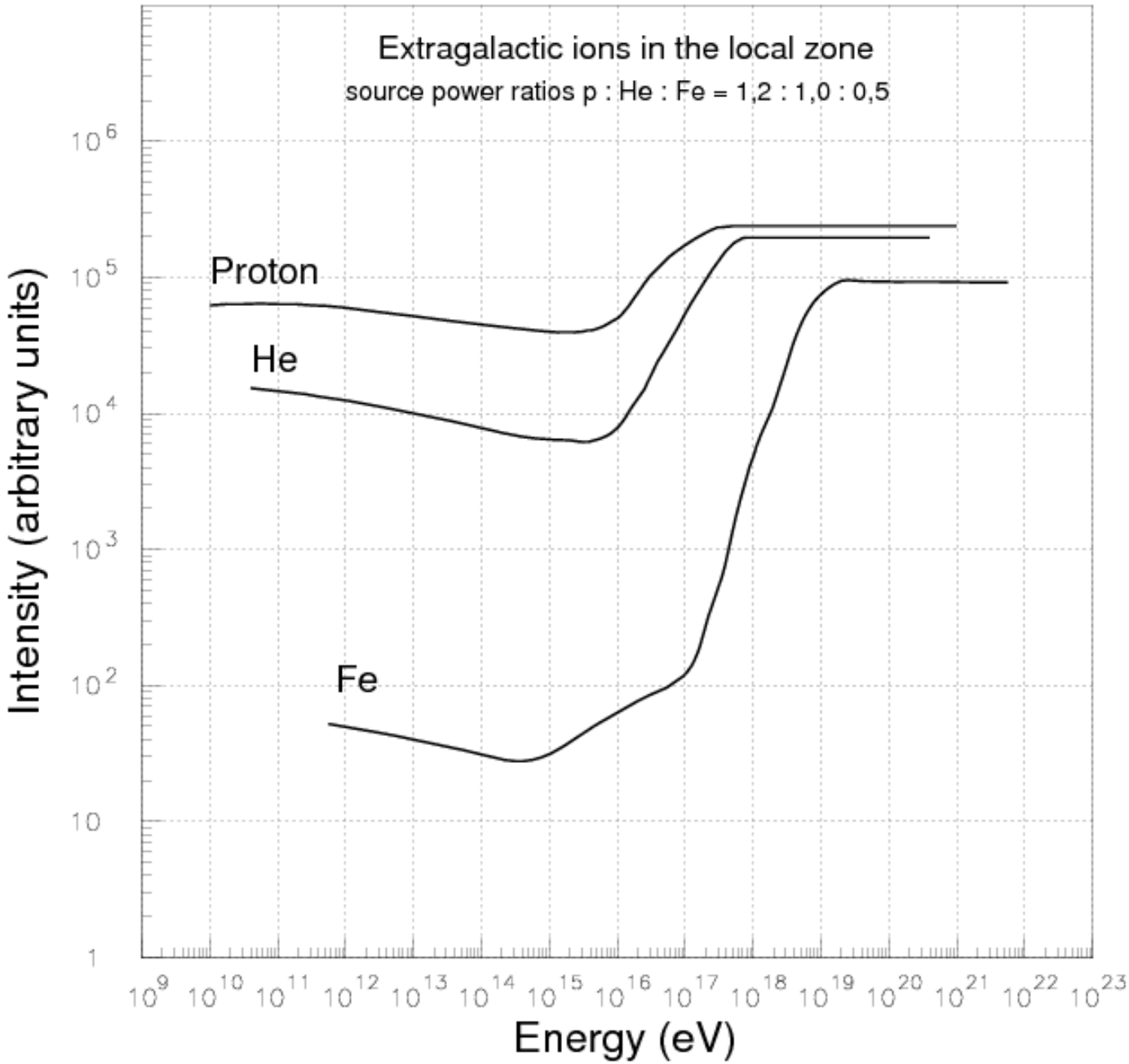
Extragalactic ions in the local zone
source power ratios p : He : Fe = 1,2 : 1,0 : 0,5
Proton
He
Fe
Intensity (arbitrary units)
Energy (eV)
10^6
10^5
10^4
10^3
10^2
10
1
10^9 10^10 10^11 10^12 10^13 10^14 10^15 10^16 10^17 10^18 10^19 10^20 10^21 10^22 10^23

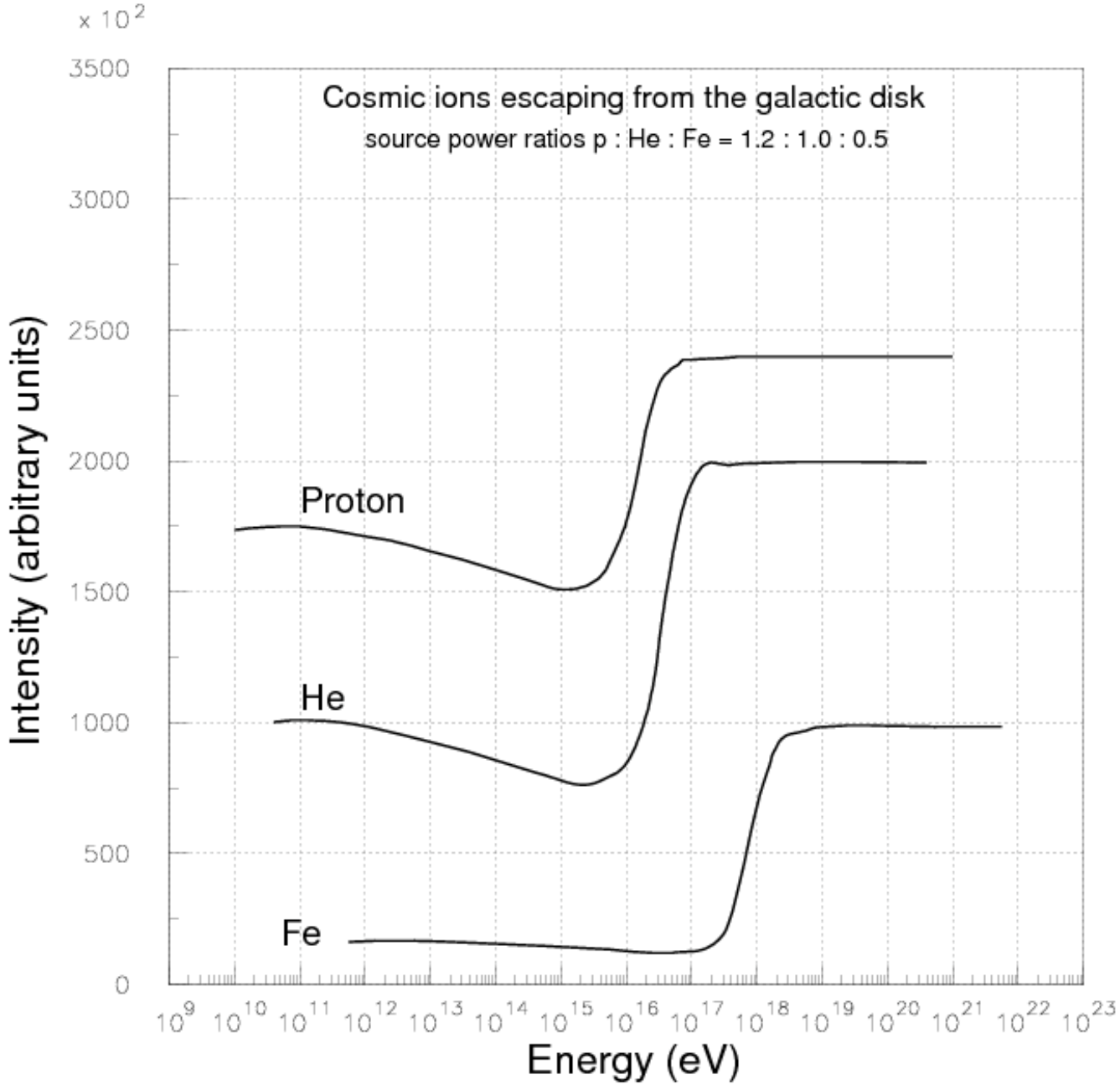
x 10^2
3500
3000
2500
2000
1500
1000
500
0
Cosmic ions escaping from the galactic disk
source power ratios p : He : Fe = 1.2 : 1.0 : 0.5
Proton
He
Fe
Intensity (arbitrary units)
10^9 10^10 10^11 10^12 10^13 10^14 10^15 10^16 10^17 10^18 10^19 10^20 10^21 10^22 10^23
Energy (eV)

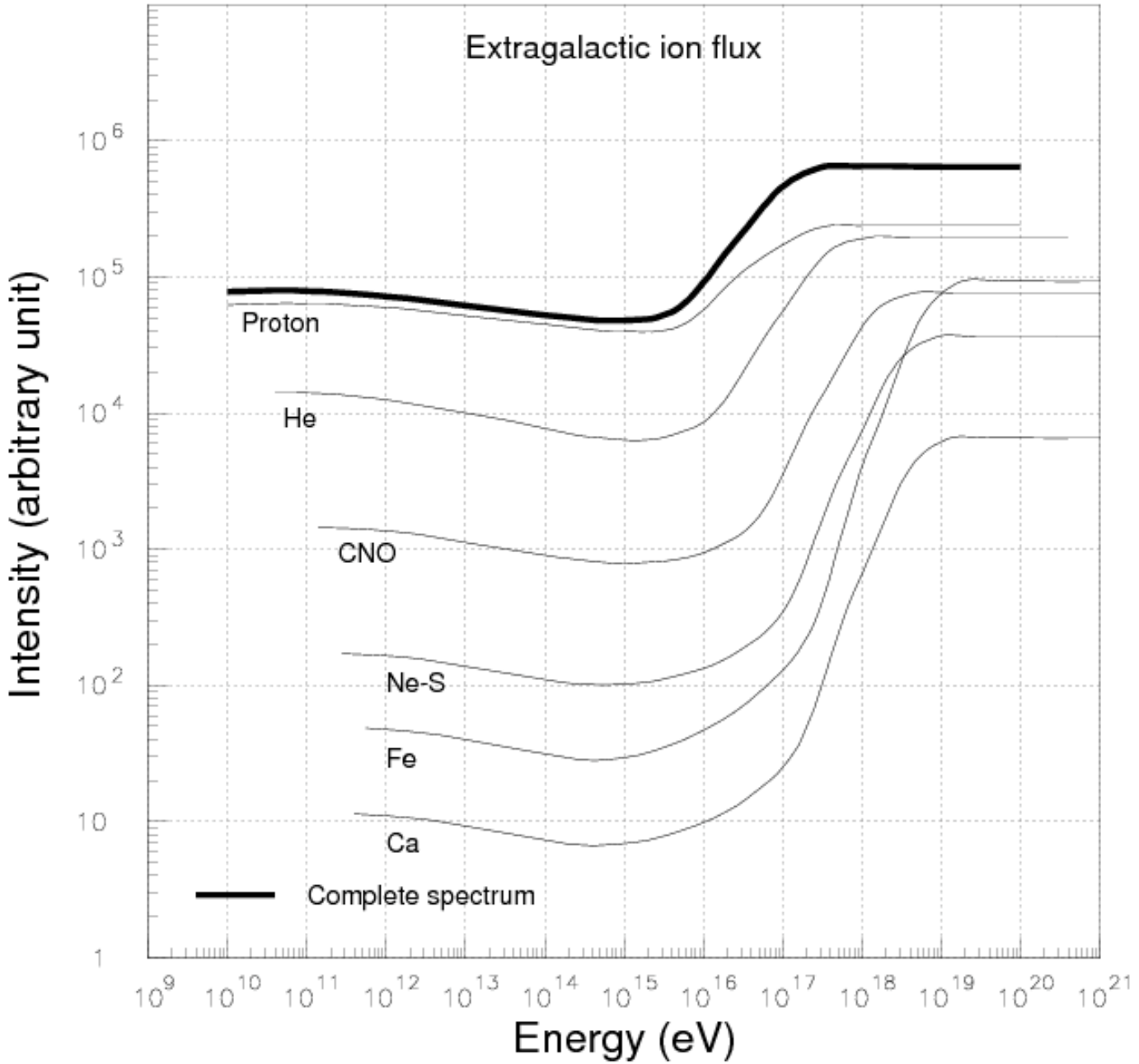
Extragalactic ion flux
Intensity (arbitrary unit)
Energy (eV)
Proton
He
CNO
Ne-S
Fe
Ca
Complete spectrum
10^6
10^5
10^4
10^3
10^2
10
1
10^9 10^{10} 10^{11} 10^{12} 10^{13} 10^{14} 10^{15} 10^{16} 10^{17} 10^{18} 10^{19} 10^{20} 10^{21}

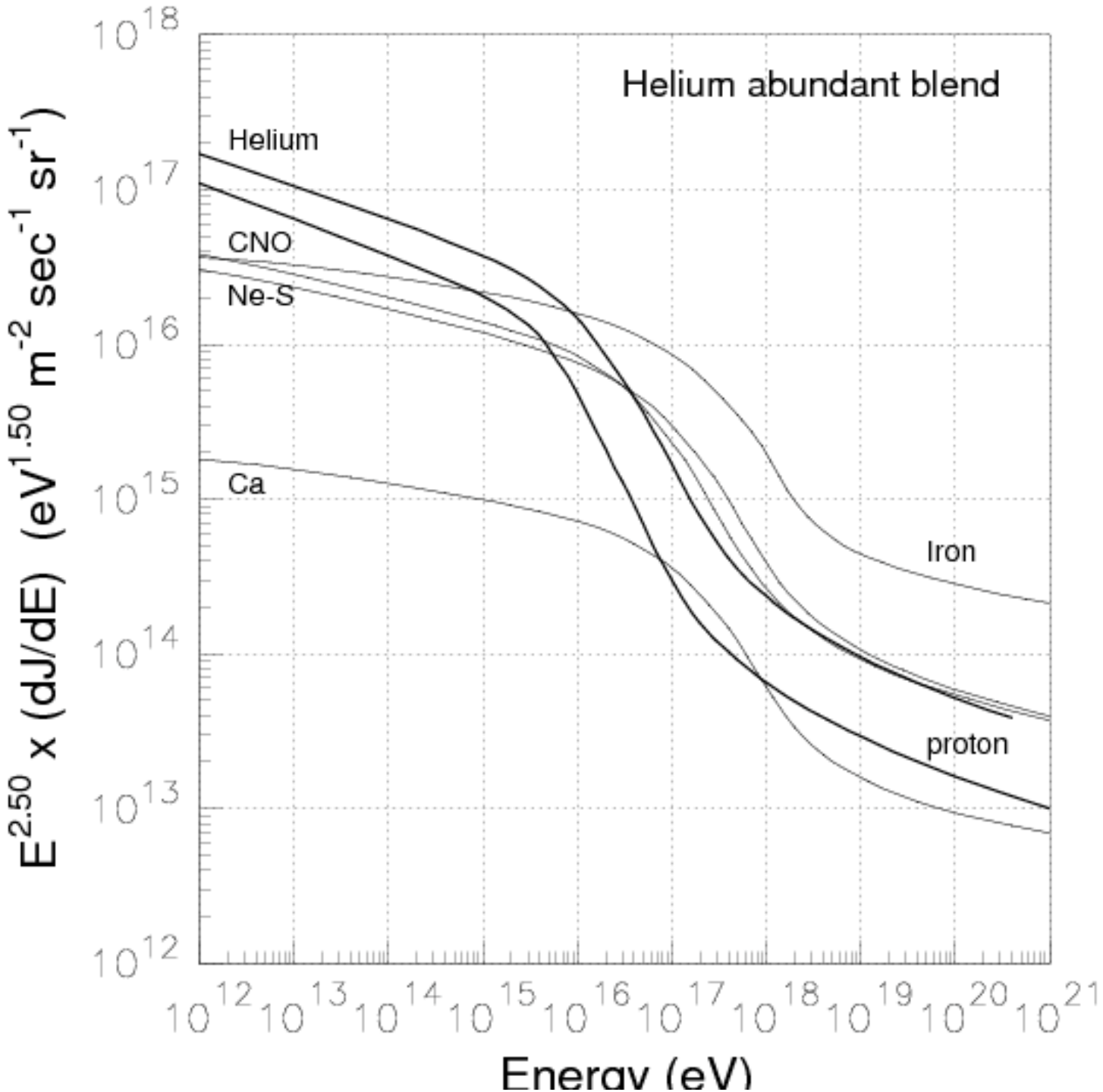
Helium abundant blend
Helium
CNO
Ne-S
Ca
Iron
proton
$E^{2.50}$ x (dJ/dE) ($eV^{1.50}$ m^{-2} sec^{-1} sr^{-1})
Energy (eV)
10^{18}
10^{17}
10^{16}
10^{15}
10^{14}
10^{13}
10^{12}
10^{12} 10^{13} 10^{14} 10^{15} 10^{16} 10^{17} 10^{18} 10^{19} 10^{20} 10^{21}

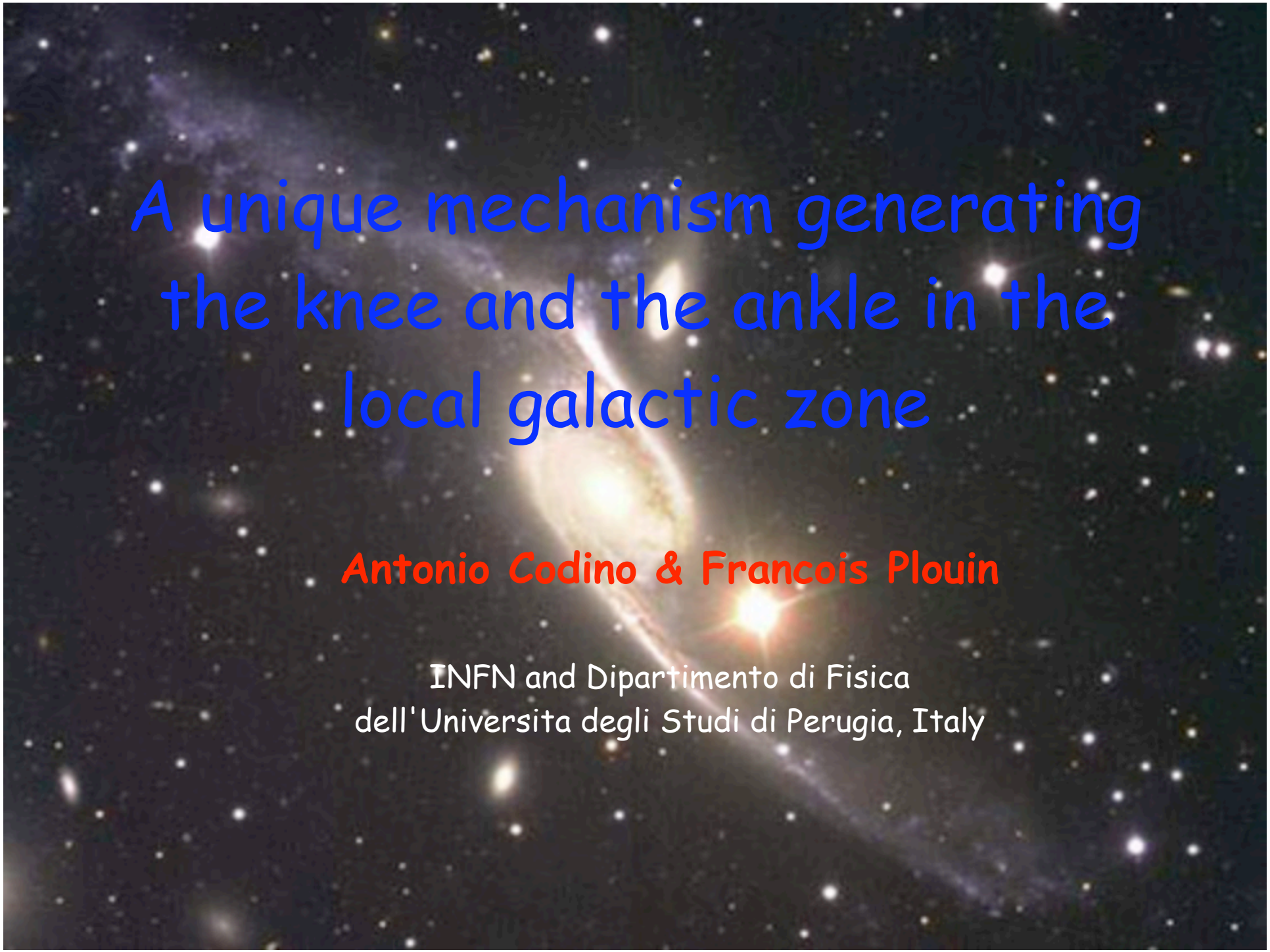

A unique mechanism generating the knee and the ankle in the local galactic zone

Antonio Codino & Francois Plouin

INFN and Dipartimento di Fisica
dell'Universita degli Studi di Perugia, Italy